jul.-21

TITULO

PARAMETRIC ANALYSIS AND OPTIMIZATION BY MEANS OF DoE TECHNIQUES OF A BUILDING INSULATION COATING FOR FAÇADE RENOVATION

PROYECTO

presentado para optar

al Título de Ingeniería Industrial por

Nerea Gargallo Ayastuy

bajo la supervisión de

Juan Carlos Ramos González

Donostia-San Sebastián, julio 2021

Alumno

tecnun
Universidad de Navarra

tecnun Universidad de Navarra

Proyecto Fin de Grado

INGENIERIA INDUSTRIAL

PARAMETRIC ANALYSIS AND OPTIMIZATION BY MEANS OF DoE TECHNIQUES OF A BUILDING INSULATION COATING FOR FAÇADE RENOVATION

Nerea Gargallo Ayastuy

San Sebastián, julio de 2021

Pº Manuel Lardizabal, 13. 20018 Donostia-San Sebastián, Gipuzkoa

Tel. 943 219 877 · Fax 943 311 442 · www.tecnun.es

Abstract

The energetic performance of a building insulation coating is assessed by means of simulations of a dynamic RC model and by carrying out a parametric analysis based on Design of Experiment techniques. The external insulation coating is characterized by three parameters: the thermal conductive resistance, the shortwave solar absorptivity, and the longwave emissivity. The façade of the building is modelled with two lumped thermal capacitances on the internal and the external surfaces, and two thermal resistances representing the conduction through the wall and the internal convective and radiative phenomena. The external insulation is modelled by two more thermal resistances, which simulate the external convective exchanges and the conduction through the insulation, and one thermal capacitance in the insulation external surface. The inputs to the model are the external ambient temperature, the internal temperature, and the weather conditions (the wind convective heat transfer coefficient and the incident shortwave and the longwave radiative heat fluxes). The analyzed output parameters of the model are the internal surface heat flux and the solar collection at the external surface of the wall, which have a direct impact on the heating and cooling loads. After trying different DoE methods, the Box-Behnken Design has been used to select the optimal values of the parameters of the insulation coating that result in a maximized internal heat flux during winter months and a minimized flux during summer months. The analysis has been carried out for three different types of walls under the weather conditions of Bilbao (North of Spain). The use of the Box-Behnken Design permits to assess the combined effect of the input parameters on the output parameter and the formulation of a simplified compact model to predict the latter as a function of the formers.

CONTENT

INDEX OF FIGURES

INDEX OF TABLES

1. INTRODUCTION

1.1. Generalities

Energy efficient buildings have become an increasingly common issue, due to the growing demand to satisfy not only economic and social but also more ambitious environmental requirements.

Until very recently, the only aim of the building envelope was to provide shelter and protection to the habitants. The buildings used to be constructed according to the specific climatic conditions where they were located. A good example of it is the vernacular architecture [*1*], what has led to find diverse designs in construction depending on the locations, taking advantage of the available conditions of the exterior environment.

As technology and materials evolved, the possibility of deciding how the building would look emerged, giving more importance to the design than to guarantee human comfort with the construction itself. Nowadays the required human comfort (such as thermal comfort, illumination, or air quality) is mainly provided using mechanical heat, ventilation, and air conditioning systems [*1*].

Over these past few years, the topic of energy efficiency has become a priority in our society. A building that makes the most of its climate conditions, taking advantage of them, is desired. A new generation of buildings is emerging: buildings that integrate various degrees of high technology with an intelligent use of functionally adaptive ecological materials and constructions, being able to react to changes in their surroundings and adjust themselves to suit.

Two alternative directions have been taken during these years to design low-energy consuming buildings: active and passive technologies [*2*].

The active strategies are focussed in providing, for instance, renewable energy, so that a cleaner consumption is favoured.

The passive alternatives, on the other hand, are related with the design and shape of the building itself. These techniques have an important role on capturing, storing, and distributing solar energy and wind.

In the past, building envelopes used to be homogeneous structures, constructed with one or two materials that acted together as thermal insulators and load carrying elements. Nowadays, conventional static building façades combine different materials or layers in the best way to maximize or minimize heat fluxes from the interior to the exterior of the building. Each layer fulfils a specific function. A common effective solution in passive technologies for building renovation is the application of an outer layer on the external wall of the building. This skin is known as “building insulation coating”. However, this technique can be limited if a real reduction of energy is desired. Meteorological conditions change throughout the year, and so they do the occupancy and thermal comfort requirements. In this context, the adaptive building layers have emerged. These building shells offer the opportunity to adapt the envelope to an optimal position or configuration to reach energy efficiency in the building at each specific moment.

A wide range of adaptive layers has been recently developed [*3*]. Two mechanisms can be marked out when it comes to adaptivity: micro and macro-level mechanisms [*2*]. Micro-level changes occur in small scales, as the variation occurs in the material itself (in the ones called “smart materials”). Smart materials have changeable properties and can reversibly change their shape and colour in response to physical and chemical

influences, such as light or temperature. A disadvantage is that they are not controllable (intrinsic control), in contrast to the macro-level mechanisms (extrinsic control). In the intrinsic control the adaptive behaviour is self-adjusting, being environmental impacts directly transformed into actions without an external decision-making component. In macro-level mechanisms, combining the advances in material sciences with the technological ones (sensors, processors, and actuators) a completely personalized envelope can be designed, making these passive technologies work like active alternatives. The driving principle behind a macro-level adaptive mechanism is usually an electromotor, which receives the inputs from a sensor and uses an external energy input to generate a motion such as folding, sliding, or rolling.

The concept of adaptive building envelope has a strong relation with the intelligent buildings that have become so popular within the last two decades. However, this is a topic which goes far away from the mentioned adaptive building envelopes, as it monitors and integrates intelligent systems not only to optimize the interaction between the exterior and interior of the building but also to maximize the whole technical performance, investment, and operating cost savings of a building.

Building passive technologies, both building insulation coatings and adaptive envelopes, are playing an important role in new constructions but also in the renovation of façades [*4*[*5*]. It has been proved that the retrofit of the building envelope contributes to high energy savings. This project aims to assess the energetic performance of a building insulation coating for façade renovation. By means of a dynamic RC model, the thermal performance of a wall of a building has been simulated in *Section 2*. Three parameters have been used to characterize the external coat or envelope: the thermal conductive resistance, the shortwave solar absorptivity, and the longwave emissivity. In *Section 3,* by using Design of Experiment (DoE) techniques, a parametric analysis of these variables has been carried out to find out which are the optimum values for the variables that represent the insulation coating of the building in terms of energy efficiency. The key parameters used as indicators of this efficiency have been the internal surface heat flux and the solar collection at the external surface of the wall, which have a direct impact on the heating and cooling loads. The inputs of the model have been the external ambient temperature, the internal temperature, and the weather conditions. The analysis has been carried out for three different types of walls under the weather conditions of Bilbao (North of Spain).

The programming and numeric computing platform *Matlab* has been used for describing the dynamic RC model that characterises the wall. For doing the Design of Experiments, the statistical analysis software *Minitab* has been used.

1.2. State of the art

According to the IEA (International Energy Agency) the building (or residential) sector is responsible for over one-third of global final energy consumption (36% of final energy use by 2018) [*6*]. The impact that this sector has in different energetic fields can be graphically seen in Figure 1 [*7*], where the energy that different sectors consumed in 2018 is represented.

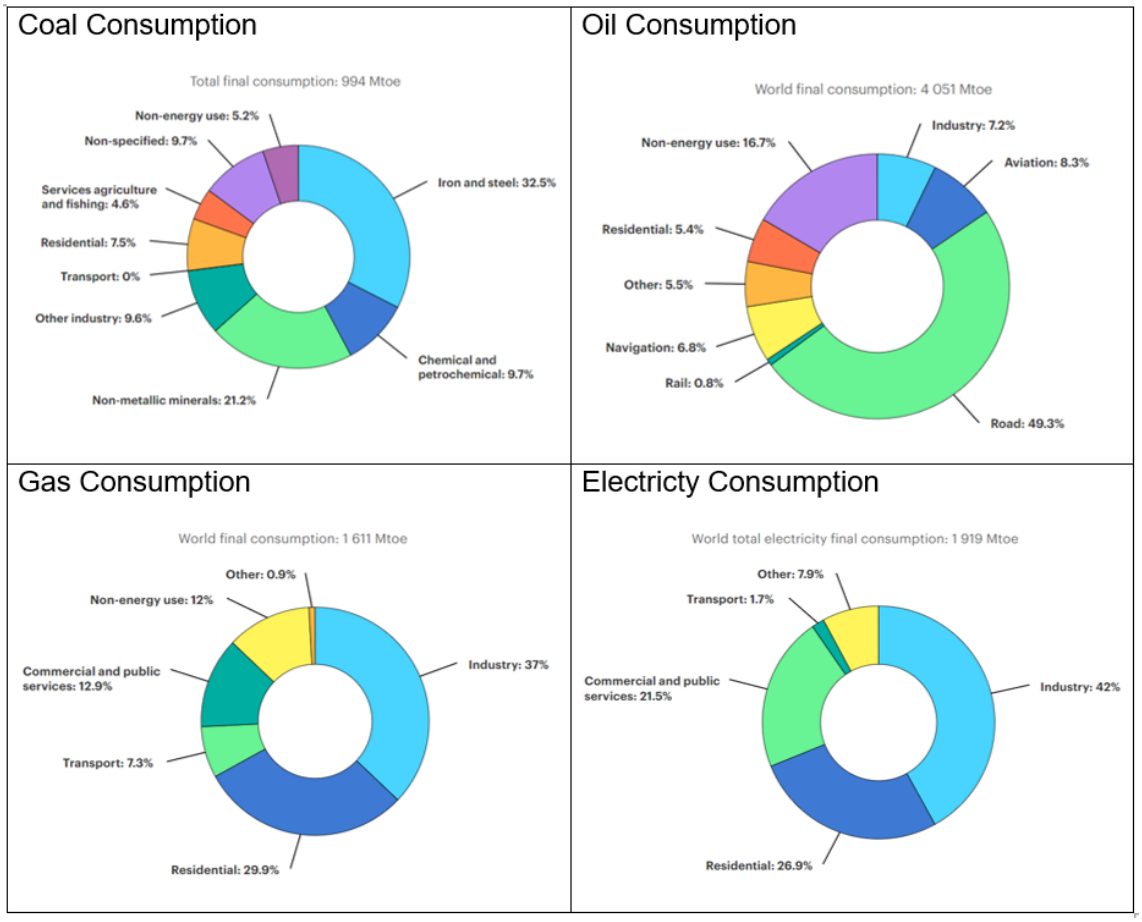

Figure 1. Energy consumed by different sectors (2018) [7].

In addition, contrary to visualizing a reduction in energy consumption in the buildings, the green curve in Figure 2 (derived from the World Energy Statistics and Balances, 2019) [*8*] shows an ascending trend during the years.

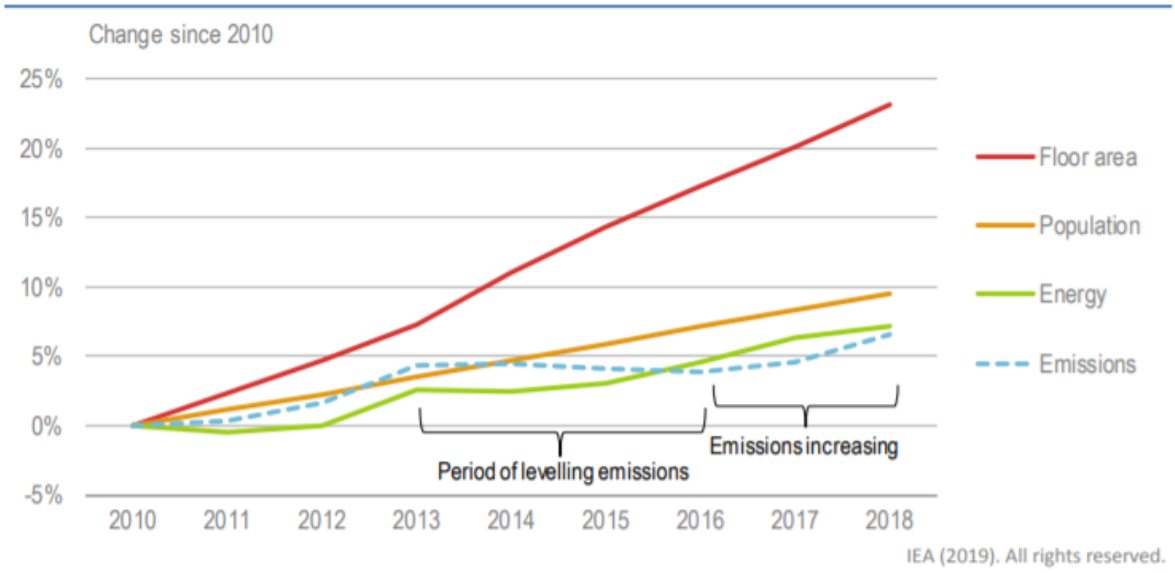

Figure 2. Changes in floor area, population, building sector energy use and energy-related emissions globally,2010-18 [8].

Figure 3 below represents the evolution of the energy demand inside buildings over the last years [*8*].

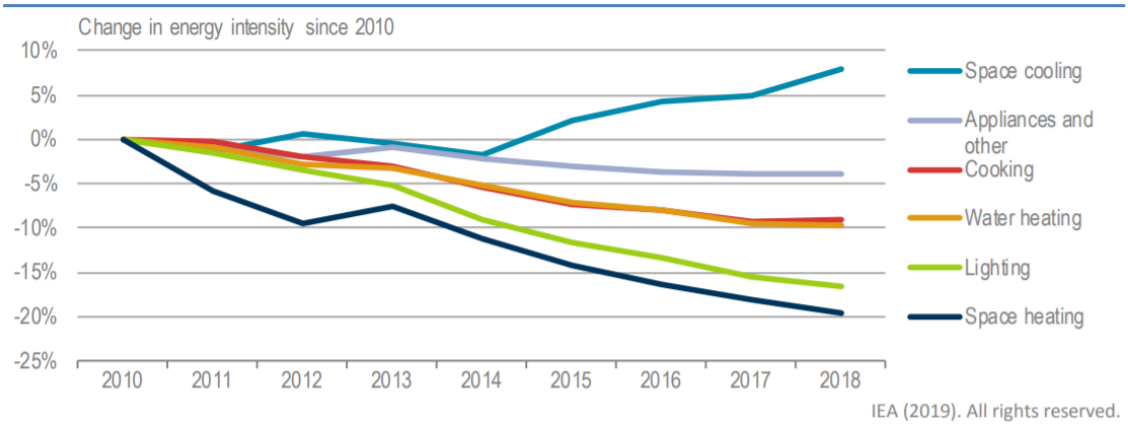

Figure 3. Global buildings sector final energy intensity changes, 2010-18 [8].

It can be seen that the greatest improvements have come from heating and lighting reductions. However, as the floor area has rapidly expand in hot countries, cooling demand has also increased.

All these graphs clearly show that some progresses need to be done in the building sector, as it has been proved how relevant it is when it comes to energy consumption. Being residential a sector that has noted a drastic decrease in new constructions, it is a fact that energy efficiency will not come from low-consuming new building designs but from the renovation of the existing façades. In addition, the OECC (Spanish Office of Climate Change) claims that the building sector constitutes the 7% of the total greenhouse gas emissions [*9*]. The concern on this topic is huge, and several goals and measures have been taken to reduce the existing emissions, such as the Horizon 2050 plan, proposed in 2018 by the European Commission [*10*], which states that by 2050 between the 80% and 95% of the emissions will be reduced. In this context the renovation of buildings seems to be the best solution to reach both, energy efficiency and reduction of greenhouse gas emissions.

Nowadays the majority of the countries in the world (almost two-thirds by 2019 [*8*]) lack mandatory building energy codes. Being aware of how important these building codes along with technology efficiency improvents are, some policies have been introduced recently, which promote a sustainable attitude, such as the Eco-Niwas Samhita energy conservation code (2018) [*11*], in India, or the Green Building Minimum Compliance System in Rwanda (November 2016) [*12*]. To stimulate improvements in both, the new and the existing building stock, Argentina's federal government launched in 2018 the national Energy Efficiency and Renewable Energy in Social Housing habitability [*13*], being the first national standard for building energy performance. Some more recent projects that support and accelerate building renovation plans are the European Performance of Building Directive (revised in June 2018 to accelerate renovation of existing buildings) [*14*] and the European World Green Building Council network's Build Upon project (launched in December 2019) [*15*]. Additionally, the project iBROAD (Individual Building Renovation Roadmaps) has just been funded by the Horizon 2020 European programme [*16*], which is developing a tool to outline building renovation plans at the individual building level. As it has previously been mentioned, due to the increasing concern on the topics of energy efficiency and greenhouse gas emissions, the European Union has launched a program called Horizon 2050 which has just been approved by

the Spanish government (June 2021) [*10*]. The objective of this Climate Change and Energy Transition law is, among others, to improve energy efficiency by reducing the primary energy consumption by 39.5% [*17*]. To accomplish that, a Housing Rehabilitation and Urban Renewal Plan has been approved [*18*]. A total of 1,000 million euros per year will be invested in housing renovation. The forecast is to reach 120,000 annual rehabilitations, in contrast with the nowadays existing 30,000 renovations. This plan is mainly focused on the renovation of buildings with a minimum of 25 years of lifetime. The priority is to reduce the energy consumption of the building by 40%, with façade renovations that will provide the old buildings with a new external envelope that reduces and regulates the consumption in the interior.

All these policies and financing programmes aim to increase the nowadays existing building energy renovation rates, which are about 1-2% of the building stock per year [*19*].

It has been mentioned that building envelopes have an important role on energy reduction inside the building. Late statistics show that heating and air conditioning (HVAC) systems constitute the main part of the building energy consumption [*20*]. Thermal comfort requirements can be fulfilled by optimizing the building thermal design, especially the envelopes [*21*[*22*]. It is reported that the main indoor cooling loads derive from the heat gains through building external envelopes, caused by indoor and outdoor temperature difference [*23*].

In this context, many researchers are dedicated to building passive systems to reduce heat transfer through envelopes [*24*]. Whereas building insulation coatings have become an effective and common way to reach energy efficiency in buildings, adaptive layers are still an area which is being developed and where much more knowledge is required. A summary of the most important accomplishments that have occurred in the just mentioned two passive technologies will be held below.

Over the years adaptive skins have been evolving, from the Mike Davis' Polyvalent Wall (in 1981) [*25*], which consisted on a multi-layered wall that could dynamically respond to changes in environmental conditions (Figure 4 and Figure 5) [*25*[*26*], to more modern and technologically advanced external structures.

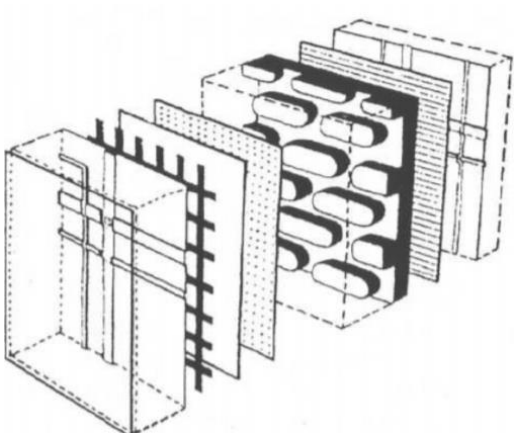

Figure 4. Polyvalent wall by Mike Davis [25].

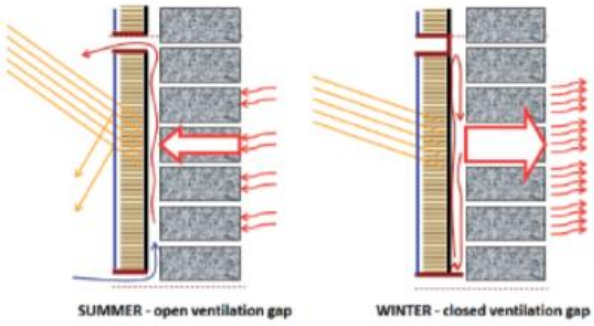

Figure 5. Cooperation of the layers. Summer and winter configurations [26].

Another early example of an adaptive envelope project is the US Pavilion for the World Expo in Montreal in 1967, designed by Richard Buckminster Fuller (Figure 6) [*29*]. It was constructed from a lattice steel structure with transparent acrylic sheets that kept the interior comfort within reasonable levels by a computer controlled shading system that was adapted to the direction of the incoming solar radiation (Figure 7) [*28*].

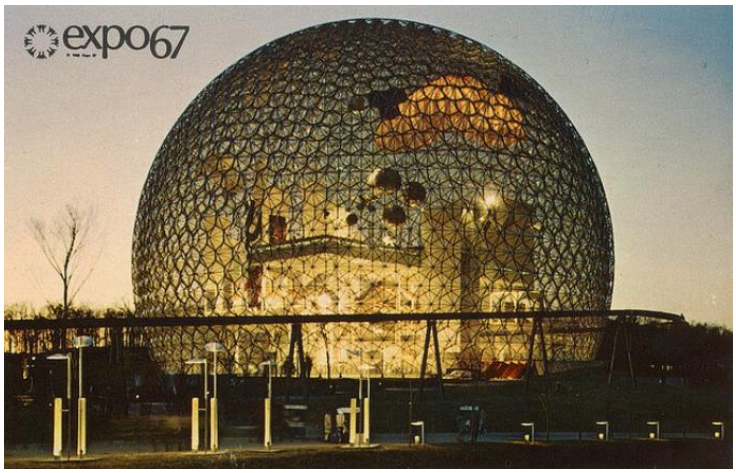

Figure 6. US Pavilion for the World expo in Montreal in 1967 [29].

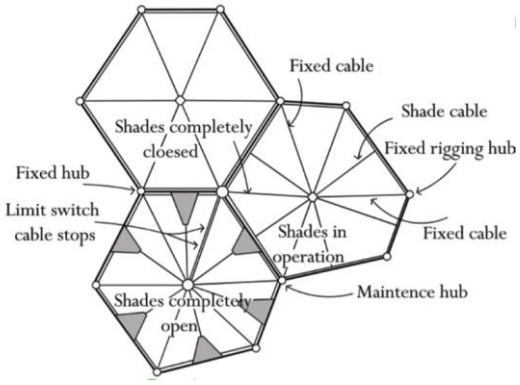

Figure 7. The canvas sunshades of American Pavillion by Buckminster Fuller [28].

Some more recent examples are the well-known Institute du monde Arab, in Paris (1989), with an adaptive envelope consisting of 240 photosensitive shutters that work as a sun-shading device (Figure 8 and Figure 9). These shutters' positions are regulated by some actuators that receive the information of the radiation level collected in a certain part of the façade. It is a highly mechanical solution which has caused a lot of problems with the fatigue in the moving elements [*30*].

Figure 8. Institute du monde Arab, in Paris (1989) [30].

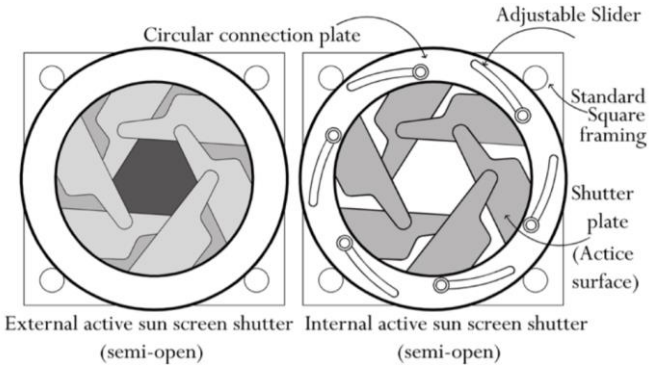

Figure 9. The six Kinetic Shutters panel of Institute Monde de Arabe which are used to create an open and close performance [30].

A similar project was later carried out in the Al Bahar towers in Abu Dhabi (2012), which incorporated a macro-system of programmed panels that moved according to the Sun (Figure 10 and Figure 11) [*31*].

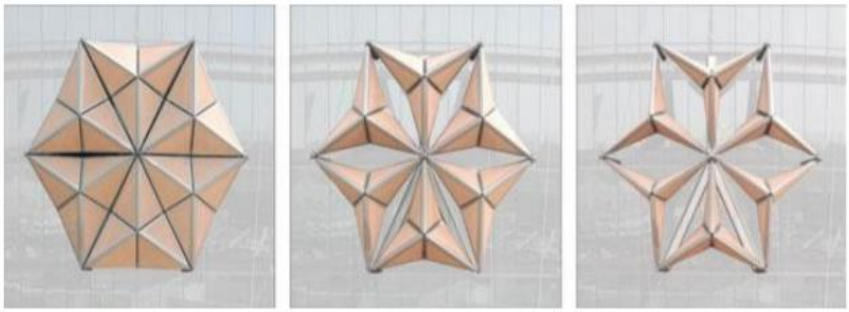

Figure 10. Thye Mashrabia system of operation [31].

Figure 11. Al Bahar towers in Abu Dhabi (2012) [31].

Some smart materials that have lately become popular for building envelopes are the ETFE (a transparent envelope filled with nitrogen gas) and the GLASSX (a multi-layer wall combining PCM with prismatic polycarbonate layers) [*31*]. An example of an adaptive envelope integrating ETFE is the Media ICT building, inaugurated in 2010 in Barcelona and awarded World building of the year (Figure 12 and Figure 13). The nitrogen inside the ETFE sticks with a vegetable oil when the oil melts due to the increased heat from the Sun. A fog is then created which works as a solar shading system on the south façade [*32*].

Figure 12. Media ICT building, Barcelona [32].

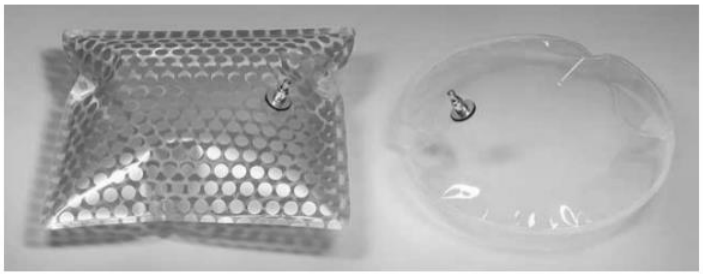

Figure 13. EFTE cushions from Media ICT building [32].

The diverse innovative designs and ideas that are currrently being developed for adaptive building envelopes are uncountable. A few remarcable examples will be presented below. The first one is the Homeostatic façade, which places dielectric elastometers (flexible elements that can transform electric energy in mechanical work) into a double skin façade. Depending on the environmental conditions of the surrounding, the elastometers (acting as capacitors), wrapped over a flexible polymer core (actuator), expand or contract, causing the flexible core to bend. The result would be similar to opening and closing wings (Figure 14) [*33*].

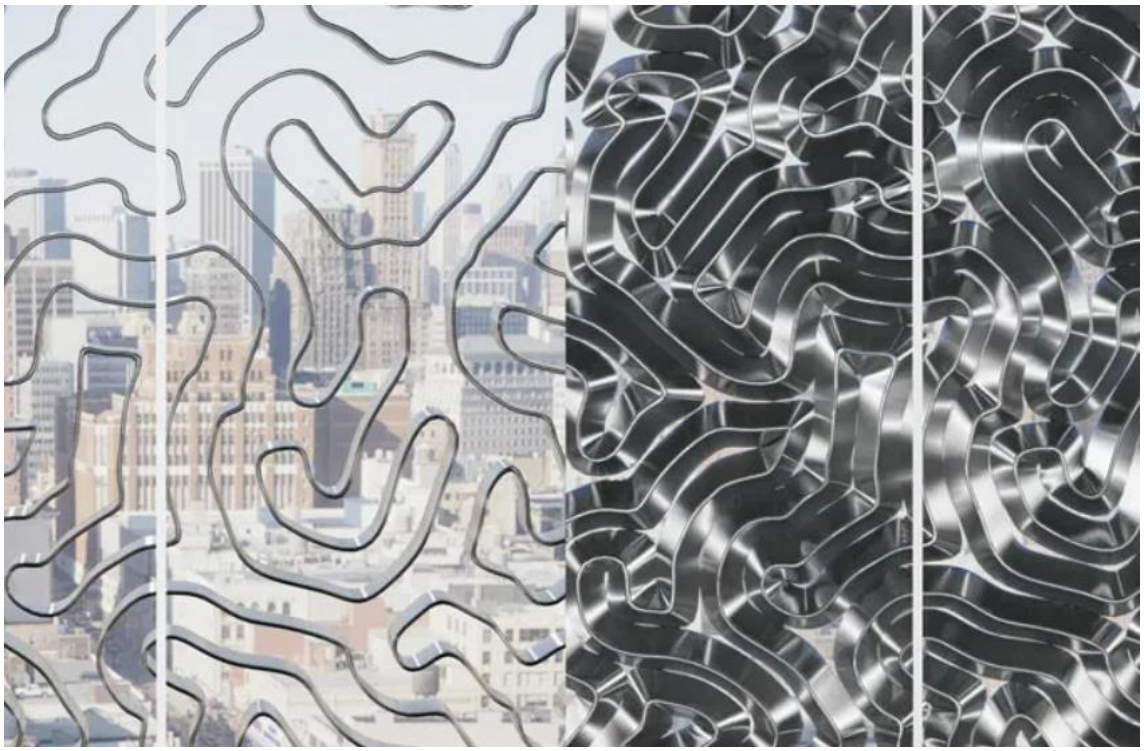

Figure 14. Example of pattern for homeostatic façade, in open and closed configurations. (Decker Yeadon Architects, 2013) [33].

The second example is the one called Smart Energy-Generating window. It is a pilot project that is currently being tested in the Netherlands. The idea is to be able to alter the g-value of the window (related with the transparency) by introducing small electric currents. Modifying the g-value, the solar radiation that enters the building can be regulated [*34*].

When talking about passive technologies, the above mentioned adaptive layers field is still under research. It has many positive aspects, but it is also more complicated and much more expensive than applying an external non-adaptable insulation layer to the outer wall. It has been remarked how crucial building envelopes are in building energy consumption. Therefore, improving building insulation properties is an urgent problem in the construction industry.

Reflective building insulation coatings have lately been proved to be an effective way to reach energy efficiency and they are being applied all over the world. By increasing reflectivity these walls can cut off most of the heat radiation decreasing the wall surface heat gain, what results in air conditioning reductions during summer months.

When talking about building insulation coatings, there are a few terms which must be explained:

On the one hand, a building coating is the surface finish that is applied to the external layer. It does not modify the thermal resistance of the façade in which it is applied (as painting a wall does not really add thickness) but it does have an effect on the reflection coefficient, which results in reduced absorbed solar radiation and surface temperature. The same way as it happened with the adaptive layers, there is a wide variety of building coatings in the market. Depending on the location and climatic conditions of the studied area, the characteristics that the ideal outer skin the building would require differ. Several researches have been carried out during the last years to analyse different characteristics attribued to these coatings. Givoni and Hoffman [*35*] demonstrated that the temperature inside the building changes depending on the colour in which the building is painted. Taha et al. [*35*] measured the reflectivity and surface temperatures of various materials used in urban surfaces and found that white coatings with a reflectivity over 0.72 could be as high as 45 °C cooler than black coatings with a reflectivity of 0.08. Synnefa et al. [*36*] investigated the thermal performance of 14 types of reflective coatings, deducing that their use could reduce the surface temperature of a white concrete tile under hot summer conditions. These and much more performed experiments clearly show how indoor temperatures are influenced by the external envelope's colour and reflectivity.

On the second hand, when talking about insulations, in contrast to the coating, it does add thickness to the existing wall. Thermal insulation retards the heat flow that enters or goes out of a building due to its high thermal resistance. It is a fact that it produces energy savings, but the magnitude of those reductions depends on several factors such as the building type, climatic conditions or the insulating material used. Thermal resistance (*R*-value) is the opposition that the heat flow faces during conduction, convection and radiation. It is a function of the material's thermal conductivity, thickness and density, and it is expressed in $m^2 \cdot K/W$. Typically, air-based insulation materials cannot exceed the *R*-value of still air. However, plastic foam insulations use fluorocarbon gas (heavier than air) instead of air within the insulation cells, which gives higher *R*-value.

There exists a wide variety of thermal insulator in the market, but the most common materials are shown in Figure 15, with their respective thermal resistances per 5 cm thickness [*37*].

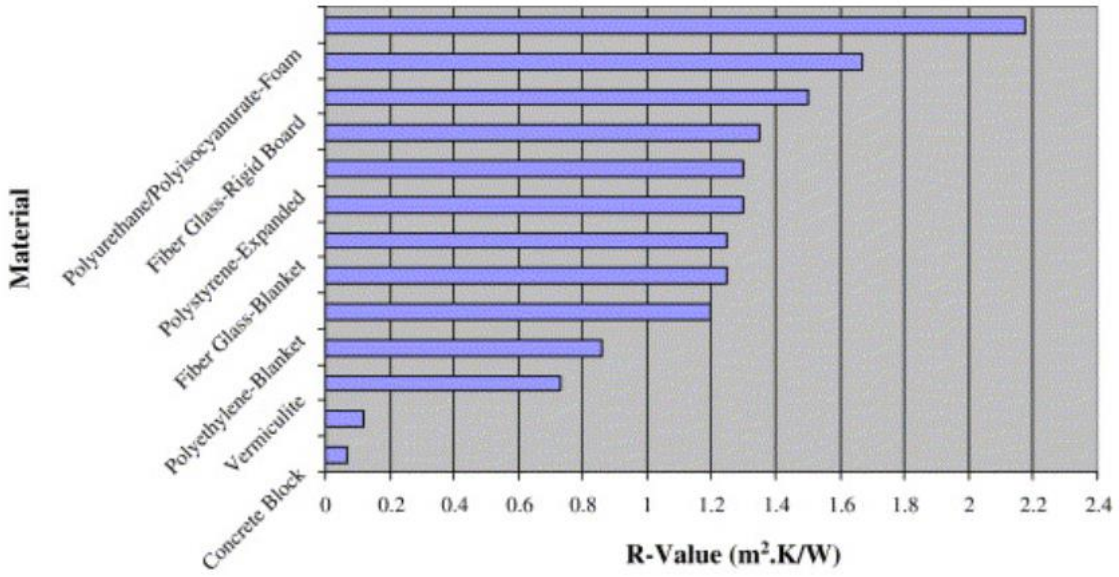

Figure 15. Thermal resistance (per 5 cm thickness) of common building insulation materials (Concrete block is added in the figure as a reference for comparison purposes) [37].

When selecting thermal insulation several parameters must be considered, such as the durability and cost. However, thermal resistance is the most important property. The more insulation does not necessarily mean the better. The optimum thickness is achieved when the added increment of insulation is balanced by the increased energy savings.

It is also important to mention that insulation can be located in the inside, in the outside or even in the middle of the building wall. In this project, the analyzed insulation will be attached to the exterior face of the façade (Figure 16).

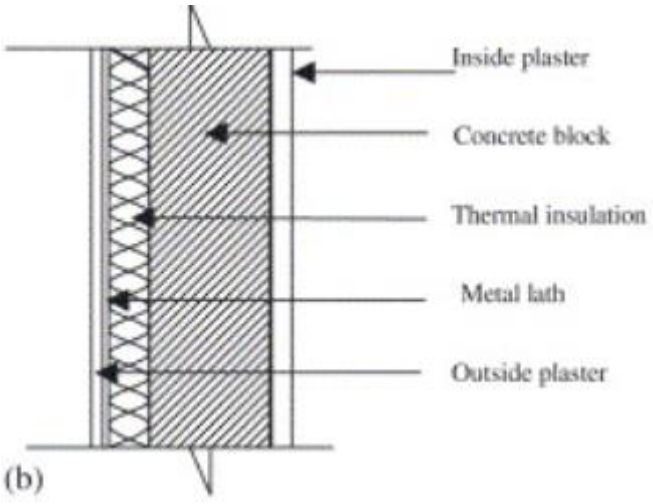

Figure 16. Insulation placement outside the building wall [37].

The present study fits in this context in which energy efficiency is gaining so much strength, with the building renovation sector playing an important role on it (supported by the numerous policies that have recently emerged which contribute on existing building rehabilitations). This project uses a model previously developed by Tecnalia to determine how a building insulation coating affects on the thermal performance of the building. The envelope that will be analysed consists of an external layer (in which the building

insulation coating is applied) that is incorporated in the outer part of an existing façade. It is intended to be applied in renovation of existing buildings.

1.3. Objectives

The main objective of the project is to find the best configuration of the varibles that constitute the external building insulation coating that covers a building so that its energy efficiency is increased. By optimizing those parameters that have an effect on energy consumption inside the building, the energy used for heating and cooling could be reduced.

The principal goals of the project are the ones listed below:

- Program a generic algorithm that represents and calculates the heat interaction between the interior and the exterioir of a building, by introducing some input arguments and data files, for the specific location and envelope characteristics of the building analysed. The programming and numeric computing platform *Matlab* will be used for this purpose.
- Estimate a mathematical model of the heat interaction to be able to make future predictions, using Design of Experiment (DoE) techniques.
- Determine the best combination of the parameters that represent the external insulation coating that will result in a energy consumption reduction of the building. In other words, find the optimally adapted insulation building coating for a certain façade and weather conditions, so that the internal heat flux is maximized during winter months and minimized during summer months.

1.4. Methodology

The first step in the realization of the project has been to analyse and study the existing model provided by Tecnalia. This model has been adapted from the computing platform *R* to *Matlab*. Even if some of the code has been directly used with little change, most of it has been obtained from different equations taken from the book by José Mª de Juana "*Energías renovables para el Desarrollo*" [*38*]. Almost the same results have been observed using both programs, the new code programmed in the project using *Matlab* and the model given by Tecnalia implemented in R.

Once the system had been correctly designed in *Matlab*, the second part of the project started. In this part, different parameters taking part in the heat flux through the wall have been studied with the Desing of Experiment (DoE) tecniques. Two DoE methods have been tried to finally select the Box-Behnken design as the most appropriate one. With this method, the optimal values of the parameters of the external building coating (building envelope) have been selected, with the objective of maximizing the internal heat flux during winter months and minimizing it during summer months.

Three different types of walls have been studied under the weather conditions of Bilbao (north of Spain) to obtain results for several real situations. The first case that has been studied is the heat flux trough a wall of a building provided by Tecnalia, which is part of a previous study they had already done, consisting of a solid concrete wall installed in the Kubik building of Tecnalia (located in Bilbao). This work can be found in the Eco-Binder proyect [*39*]. The remaining two walls which have been modeled are a brick wall with chamber and with or without thermal insulation. The location characteristics, as well as the orientation and other needed data have been given by Tecnalia and have been introduced as input parameters in the model constructed in *Matlab*. The specific climatic

characteristics of the studied location (climatic dataset of Bilbao) that change every second, have been obtained from the software *Meteonorm* [40], which is a tool that provides access to typical years and historical time series for any place on Earth. Some other parameters have been introduced as constant variables (such as the latitude, longitude and the time zone of the location or the vision factors of the façade).

2. DESCRIPTION OF THE MODEL

As it has already been said, the first part of the project consists of modelling the performance of a wall whose external building will be covered with an insulation coating. To analyse the heat interaction between the exterior and the interior of the building, a system that models this interaction has been constructed. The information given by Tecnalia has been used for developing the model.

The wall of the building can be represented as an RC model shown in Figure 17. It can be characterized by two capacitances (C_{me} and C_{mi}) and two resistances (R_m and R_{mi}), which will be explained below. The external insulation coating (or external envelope) of the façade is modeled by a capacitance (C_{mout}) and a thermal resistance (R_{out}), which represents the thickness of the layer that is being attached in the exterior. The resistance in the left (R_{se}) (see Figure 17) is related to convective phenomena.

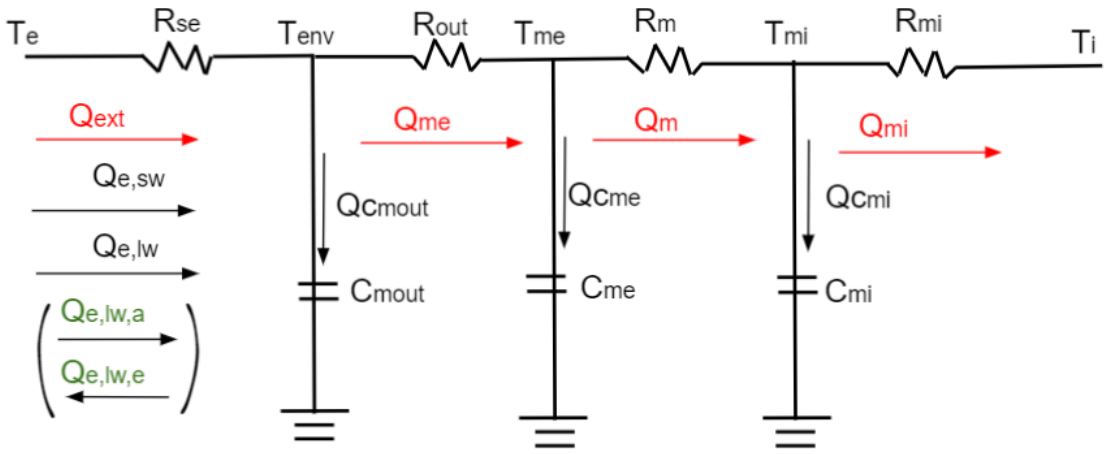

Figure 17. RC model of the heat transfer interaction through the wall and the insulation coating.

2.1. Input parameters

2.1.1. Boundary conditions

The external and internal air temperatures (T_e and T_i), as well as the short and long wave incident radiations ($Q_{e,sw}$ and $Q_{e,lw}$) are considered as boundary conditions, and they are values obtained and calculated from the climatic dataset of Bilbao.

2.1.2. Characteristics of the façade

The capacitors and resistances that are shown in Figure 17 and are needed to model the system are obtained from the climatic dataset of Bilbao and from the dataset of the thermophysical properties of the different materials of the façades.

2.2. Capacitors

The capacitors represent the external and internal capacitance of the wall (thermal capacitance lumped to the external surface of the wall, C_{me}, thermal capacitance lumped to the internal surface of the wall, C_{mi}, and the one lumped to the external coating of the façade, C_{mout} [J/m^2·K]). The values of C_{me} and C_{mi} change depending on the façade which is being analysed (a solid concrete wall in this first part of the project).

The next assumption will be made during the calculations: the value of C_{mout} will be omitted from the model ($C_{mout} = 0\ [\mathrm{J/m^2 \cdot K}]$) as it is insignificant compared to the values of C_{me} and C_{mi}.

In Figure 17 the capacitors are drawn grounded from one side while connected to the external and internal superficial temperatures (T_{me} and T_{mi}), as well as to the envelope's superficial temperature (T_{env}), from the other side.

2.3. Resistances

R_m [m^2·K/W] represents the thermal resistance of the wall, which also changes depending on the façade studied.
For describing the model in this first part of the project, a solid concrete façade will be analysed, with the $C_{me}, C_{mi}\ and\ R_m$ values obtained from the façade's dataset. In the second part of the project, when doing the energy optimization of the building, different façades will be studied, analysing how these three variables are obtained and how do they change for the different walls selected.

The external thermal resistance, R_{se}, is related to convective phenomena, with a variable value that depends on the wind velocity and the wind direction.

R_{out} is the thermal resistance of the external insulation of the wall. It models the effect of covering the building with an external skin (building envelope).

The internal superficial resistance, $R_{mi,}$ encompasses not only convective phenomena, but radiant. An estimation of its value, 0.125 [m^2·K/W], can be taken from *WUFI Pro* [41] a software which determines the hygrothermal performance of building components under real climate conditions).

2.4. States

The superficial exterior and interior temperatures of the wall (T_{me} and T_{mi}), as well as the envelope's superficial temperature (T_{env}), are obtained from the model for each time step. They are the unknowns that will be calculated.

2.5. Outputs of interest

From *Equation (1)* the model allows to calculate the value of the heat flux (Q_{mi}) [W/m^2] from the inside surface of the wall. This heat flux can be used as an indicator of the thermal influence of the wall (heat interaction between the façade and the climatized space) per surface unity. A positive value means heat gain to the inside while a negative sign represents heat loss. In the second part of the project, *Section 3*, this variable will be used as an energy optimization parameter of the building.

$$Q_{mi} = \frac{T_{mi} - T_i}{R_{mi}} \quad (1)$$

In addition, the solar collection at the external surface (Q_{col}), which is the heat captured at the external surface, is obtained with *Equation (2)*.

$$Q_{col} = Q_{Cme} + Q_m \quad (2)$$

This variable is a key parameter for controlling the heat demand of the building, as it responds immediately to the external changes. Along with Q_{mi}, this variable will be later used in *Section 3* as an estimator for optimizing the energy efficiency of the building.

2.6. Equations of the model

From the RC model of the system presented in Figure 17 the following three differential equations (*Equations (3*)*, (4*) *and (5))* characterizing the heat transfer in the system can be deduced:

$$C_{mout}\frac{dT_{env}}{dt} = \frac{T_e - T_{env}}{R_{se}} + \frac{T_{me} - T_{env}}{R_{out}} + Q_{e,sw} + Q_{e,lw} \quad (3)$$

$$C_{me}\frac{dT_{me}}{dt} = \frac{T_{env} - T_{me}}{R_{out}} + \frac{T_{mi} - T_{me}}{R_m} \quad (4)$$

$$C_{mi}\frac{dT_{mi}}{dt} = \frac{T_{me} - T_{mi}}{R_m} + \frac{T_i - T_{mi}}{R_{mi}} \quad (5)$$

To integrate these differential equations numerically, a temporal discretization has been done, where the temperatures in two consecutive time steps have been considered, resulting in the following three algebraic equations, *Equations (6*)*, (7*) *and (8*)*:*

$$C_{mout}\frac{T_{env} - T_{env,prev}}{\Delta t} = \frac{T_e - T_{env}}{R_{se}} + \frac{T_{me} - T_{env}}{R_{out}} + Q_{e,sw} + Q_{e,lw} \quad (6)$$

$$C_{me}\frac{T_{me} - T_{me,prev}}{\Delta t} = \frac{T_{env} - T_{me}}{R_{out}} + \frac{T_{mi} - T_{me}}{R_m} \quad (7)$$

$$C_{mi}\frac{T_{mi} - T_{mi,prev}}{\Delta t} = \frac{T_{me} - T_{mi}}{R_m} + \frac{T_i - T_{mi}}{R_{mi}} \quad (8)$$

To solve these equations (in which the only unknowns are T_{env}, T_{me} and T_{mi}) numerical calculations are needed. In this project, the programming and numeric computing platform *Matlab* has been used. The code implemented in the software (which will be explained in this section) can be found in *Section 9 (Annex 2)*.

Before proceeding with the explanation of how the model is solved in *Matlab*, it is necessary to analyze and understand each of the terms from *Equations (6*)*, (7*) *and (8*) that have not been mentioned yet.

First of all, Δt (the time step), corresponds to one hour. Therefore, the non-constant terms of the equations will vary each 60 minutes.

It has been said previously that C_{mout} will be omitted from the numerical calculations, so even if it is written in *Equation (6),* it will take a value of zero.

The superficial exterior resistance, R_{se}, is a function of the wind velocity and direction. It can be obtained as the inverse of the convection coefficient, from *Equation (9)* [*38*].

$$R_{se} = \frac{1}{4{,}5 + f_{wind} \cdot v_{wind}} \quad (9)$$

where v_{wind} is the wind speed (scalar average) [m/s] (which is an input value taken from the data provided in the climate file and it is different for each time step) and f_{wind} [-] is the wind direction (which can have two different values; f_{wind} = 1.6 if the wind blows face to the façade, forward, or f_{wind} = 0.33 if it blows leeward).

R_{out}, the thermal resistance of the outer insulation layer, is a characteristic of the exterior insulation coating which will be covering the building. In the second part of the project, *Section 3*, when the optimization is done, different values of R_{out} will be considered for

different insulations. R_{out} will always take values higher than zero in this project, as a null value would mean no insulation is applied to the external wall. To model the system in this section, a value of $R_{out} = 2.5$ [m²·K/W] has been considered.

The short-wave solar incident radiation ($Q_{e,sw}$) [W/m²] is a function of the global incident Sun irradiation on the façade (I_{sun}) [W/m²], the vision factor (f_{vis}) [-] and the short-wave absorptivity of the external surface of the wall (α_{se}) [-], and changes its value for each time step (see *Equation (10))* [*38*].

$$Q_{e,sw} = I_{sun} \cdot f_{vis} \cdot \alpha_{se} \qquad (10)$$

Without the existance of shading elements, the vision factor (f_{vis}) can be assumed as f_{vis} = 1. The absorptivity of the external surface of the coating (α_{se}) can be considered as a controllable variable with a determined value in systems that allow a change in colour or material of the external surface of the wall. In this project, a value of α_{se} = 0.2 is considered for white surfaces and α_{se} = 0.8 for black ones [*38*]. For this first part of the project, a value of α_{se} = 0.6 has been taken, whereas for the optimization part in *Section 3* different options will be analysed. The global incident Sun irradiation on the façade (I_{sun}) changes each value at each time step. The input data necessary for its calculation are the solar position (known from the latitude, longitude, and time zone) and the direct and diffuse irradiance. Therefore, the value of $Q_{e,sw}$ for each time step is independent from the temperatures or the different states of the wall.

I_{sun} can be calculated as the sum of three terms [*38*]: the diffuse sun irradiation (I_{dif}), the reflected irradiation (I_{ref}) and the direct sun irradiation (I_{dir}), as shown in *Equation* (11).

$$I_{sun} = I_{dif} + I_{ref} + I_{dir} \qquad (11)$$

I_{dif} is the irradiation received from the atmosphere due to the dispersion that the solar irradiation suffers. It depends on the cloudiness of the sky, taking higher values when the sky is cloudy. It can be obtained as a function of the diffuse solar irradiance (ISD) [W/m²] (assumed isotropic), which is a value taken from the climate file that changes every time step, and the vision factor of the diffuse component of the radiation ($f_{vis,dif}$) (see *Equation (12))* [*38*].

$$I_{dif} = f_{vis,dif} \cdot ISD \qquad (12)$$

This vision factor, in contrast with the one in *Equation (10)*, f_{vis}, takes a value of $f_{vis,dif}$ = 0.5 when working with vertical walls [*38*], *Equation (13).*

$$f_{vis,dif} = \frac{1 + cos\ (s)}{2} \qquad (13)$$

where *s* is the inclination of the wall with respect to the floor (90° in this project).

I_{ref} is the radiation reflected from the ground. The steeper the inclination angle *s*, the higher its value, reaching its maximum in perpendicular walls. I_{ref} is a function of three variables; the global solar irradiance on horizontal plane (ISGH) [W/m²], which is a value taken from the climate file that changes every time step, the reflectivity of the ground (ρ_{ground}) [-], with a value of ρ_{ground} = 0.2 assumed as default value, and the view factor of the ground (f_{ground}) [-] which as well as $f_{vis,dif}$ depends on the inclination angle *s* (in this project *s* = 90°) [*38*], *Equation (14).*

$$f_{ground} = \frac{1 - cos\,(s)}{2} \quad (14)$$

Therefore, I_{ref} is obtained from *Equation (15)* [*38*].

$$I_{ref} = f_{ground} \cdot ISGH \cdot \rho_{ground} \quad (15)$$

The direct sun irradiation, I_{dir}, is the one that comes directly from the Sun. It is the product of two terms, as observed in *Equation* (16) [*38*], the beam solar irradiance (I_{beam}) [W/m^2] and a correction called R_b, which is the quotient between the radiation that hits an inclined surface and an horizontal one, *Equation* (18) [*38*].

I_{beam} can easily be obtained by *Equation (17)* [*38*] (where ISGH and ISD have both been mentioned previously), but R_b requires futher explanation as it depends on many variables not mentioned yet.

$$I_{dir} = I_{beam} \cdot R_b \quad (16)$$

$$I_{beam} = ISGH - ISD \quad (17)$$

$$R_b = \frac{cos\,(i)}{sin(\alpha)} \quad (18)$$

The numerator in *Equation* (18) can be obtained from the source by José Mª de Juana et al [*38*] (see *Equation* (19)).

$$\begin{aligned} cos(i) = {} & sin(s) \cdot sin(azimuth) \cdot cos(\delta) \cdot sin(\omega) + sin(\delta) \\ & \cdot [cos(s) \cdot sin(latitude) - sin(s) \cdot cos(azimuth) \cdot cos(latitude)] + cos(\delta) \\ & \cdot cos(\omega) \\ & \cdot [(cos(s) \cdot cos(latitude)) \\ & + (sin(s) \cdot cos(azimuth) \cdot sin(latitude))] \end{aligned} \quad (19)$$

where *i* is the incident angle and *s* is the inclination of the wall with respect to the floor (90° in this project).

There exist three coordinate systems: the Geographical Coordinates, Sun Equatorial Coordinates and Sun Horizontal Coordinates (Figure 18) that permit to relate the relative position between the Sun and the Earth. Each of the system provides different coordinates that are included in *Equation* (19).

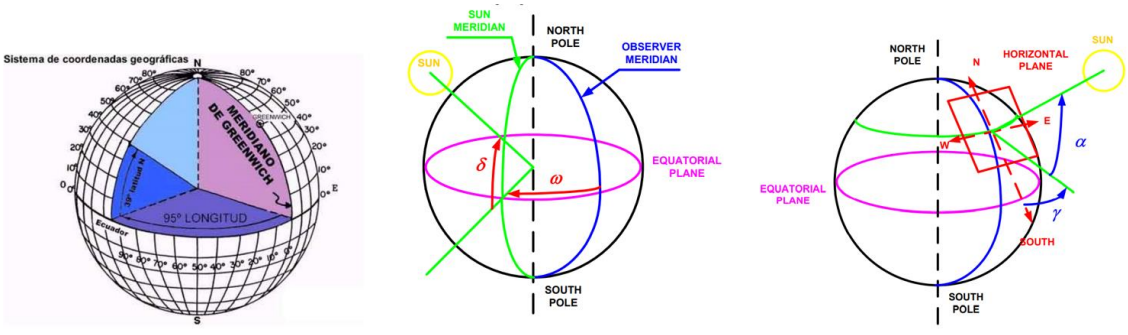

Figure 18. Geographical Coordinates (left), Sun Equatorial Coordinates (centre), Sun Horizontal Coordinates (right).

The azimuth angle (azimuth), expressed in the Sun Horizontal Coordinates (see *γ* in Figure 18 right), is the angle formed by the projection of the Sun-Earth line on the horizontal plane of the place and the line North-South of the horizontal plane of the place. The deviation from North (clockwise) is known as orientation, and it has a value of 180°

for South orientations (as it is the case in this project). Therefore, the azimuth angle can be obtained from Equation (20) [°], with a value of azimuth = 0° in this project.

$$azimuth = orientation - 180° \quad (20)$$

Delta (δ) [°], *Equation* (21) is the angle of the solar declination (angle formed by the line between Sun and Earth centres with its projection on the equatorial plane), expressed in the Sun Equatorial Coordinates (Figure 18 centre). It takes a different value every 24 hours, as it is a funtion of the day (n) [38].

$$\delta = 23.45° \cdot sin\frac{360°}{365°} \cdot (284 + n) \quad (21)$$

Omega (ω) is the solar hour angle, expressed in the Sun Equatorial Coordinates as well (Figure 18 centre). It is an expression of time, in angular measurement [°] from solar noon. At solar noon, the hour angle is 0 degrees, with the time before solar noon expressed as negative degrees and the time after expressed as positives. Note that one hour of time equals 15°. That way, the *Equation* (22) can be obtained, where the local time (that changes every time step, every hour) and the time zone (with a value of 1 h for Bilbao) are expressed in hours:

$$\omega = ((local\ time - timezone) - 12) \cdot 15° \quad (22)$$

The solar latitude (latitude), expressed in the Geographical Coordinates (see Figure 18 left), is the angle formed between the equatorial plane's projection and the radio of a certain point. In this project, a value of 43.3 degrees is taken for the latitude (considering North as positive).

Therefore, all the terms appearing in *Equation* (19) have been explained.

The denominator in *Equation (18*) can also be obtained from the source by José Mª de Juana et al [38], Equation (23), where alpha (α), Figure 18 right, is the angle that corresponds to the Sun height (angle formed by the Sun-Earth line with its projection on the horizontal plane).

$$sin(\alpha) = sin(\delta) \cdot sin(latitude) + cos(\delta) \cdot cos(latitude) \cdot cos(\omega) \quad (23)$$

In this project, the next two approximations have been made for the calculation of R_b.

When the value of $sin(\alpha)$ (the denominator in *Equation (18))* gets smaller than 0.1, it has been assumed that R_b = 0 (to avoid R_b tending to infinity).

On the other hand, all the negative values of R_b have been considered as R_b = 0.

With R_b explained I_{dir} in *Equation* (16) can be calculated, and so, I_{sun} in *Equation* (11), which results in a different value for $Q_{e,sw}$ in every time step (see *Equation* (10)).

Going back to the terms from *Equation* (6), it is now time to explain the long-wave incident radiation ($Q_{e,lw}$), which is the net gain of the outer surface of the wall. It can be obtained from *Equation* (24) [38] where $Q_{e,lw,a}$ is the absorbed radiation and $Q_{e,lw,e}$ is the emitted radiation.

$$Q_{e,lw} = Q_{e,lw,a} - Q_{e,lw,e} \quad (24)$$

$Q_{e,lw,a}$ can be calculated by *Equation* (25) [38].

$$Q_{e,lw,a} = I_{lw,a} \cdot \varepsilon_{lw} \quad (25)$$

ε_{lw} (Long-wave emissivity of external surface) [-] represents how effective a material is emitting energy thermal radiation. Black bodies will always have ε_{lw} = 1, while every other real object will have ε_{lw}<1. In this project, the material that is being analysed is the external envelope (coating) that is covering the building. The range of emissivity values that has been selected as possible is from 0.4 (supposing a reflective material) to 0.9 (typical value in many materials) [*42*]. For this first part of the project, a value of $\varepsilon_{lw} = 0.5$ has been taken, whereas in *Section 3* (optimization part) different options will be analysed.

$I_{lw,a}$ is the total long-wave counter radiation on assessed plane [W/m^2], which is the sum of three radiation components (*Equation* (26)) [*38*].

$$I_{lw,a} = I_{lw,a,sky} + I_{lw,a,ground} + I_{lw,a,ref} \qquad (26)$$

The atmospheric counter radiation on assessed plane [W/m^2] ($I_{lw,a,sky}$) can be calculated with *Equation* (28), where the atmospheric counter radiation on horizontal plane (ILAH) is a value taken from the climate file that changes every time step and the view factor of the sky (f_{sky}) [-] has a value of f_{sky} = 0.5 for unshaded walls (vertical walls *s* = 90º), obtained from *Equation* (27), similarly to what happened to f_{ground} in *Equation (14*).

$$f_{sky} = \frac{1 + cos\,(s)}{2} \qquad (27)$$

$$I_{lw,a,sky} = ILAH \cdot f_{sky} \qquad (28)$$

The terrestrial counter radiation on assessed plane [W/m^2] ($I_{lw,a,ground}$) can be obtained from *Equation (29).*

$$I_{lw,a,ground} = \varepsilon_{ground} \cdot \sigma \cdot T_e^4 \cdot f_{ground} \qquad (29)$$

Emissivity of ground (ε_{ground}) [-] is assumed as default value ε_{ground} = 0.9. The Stefan-Boltzmann constant (*σ)* has a value of *σ* = 5.67·10^{-8} [W/m^2·K^4]. The external air temperature (T_e) is an input taken from the climate file that changes every time step. Finally, the view factor of the ground (f_{ground}) [-] is the one calculated with *Equation (14*).

The reflected atmospheric counter radiation on assessed plane ($I_{lw,a,ref}$) [W/m^2] is calculated with *Equation (30).*

$$I_{lw,a,ref} = (1 - \varepsilon_{ground}) \cdot ILAH \cdot f_{ground} \qquad (30)$$

The same way it has been done with R_{out} and α_{se}, a value for ε_{lw} has been selected for this first part of the project ($\varepsilon_{lw} = 0.5$) but different values along the range will be analysed in the optimization of the second part, *Section* 3.

The long wave emitted radiation ($Q_{e,lw,e}$) from *Equation* (24) is dependent on the fourth power of the exterior coating temperature (T_{env}) what results in non-lineal energy-balance equations. A lineal approximation has been done using a Taylor series expansion, from the value of the exterior surface temperature in the previous time step ($T_{env,prev}$) which is known for the first time-step ($T_{env,prev} = 20$ ℃). That way, $Q_{e,lw,e}$ becomes lineally dependent on T_{env} (see *Equation (31)).*

$$Q_{e,lw,e} = f_{lw,e} \cdot \varepsilon_{lw} \cdot \sigma \cdot T_{env}^4$$
$$\approx f_{lw,e} \cdot \varepsilon_{lw} \cdot \sigma \cdot \left[T_{env,prev}^4 + 4\,T_{env,prev}^3\left(T_{env} - T_{env,prev}\right)\right] \qquad (31)$$

The long wave emission factor of the wall ($f_{lw,e}$) can be considered as $f_{lw,e} = 1$ for a vertical wall (as it is the case of this project) [*42*]. However, for a more detailed calculation of $f_{lw,e}$ the sum of three terms (as it happened with the long wave irradiation in *Equation* (11) must be considered, see *Equation* (32). This equation should be used if the wall is covered with an adaptive multi-layer building envelope (which would mean a reflectance obstacle and would end up in values of $f_{lw,e} < 1$ as part of the emitted LW radiation would be reflected). This is the case of the studied model.

$$f_{lw,e} = f_{lw,e,sky} + f_{lw,e,ground} + f_{lw,e,sky,ground} \qquad (32)$$

The atmospheric LW emission factor ($f_{lw,e,sky}$) can be obtained from *Equation (33).*

$$f_{lw,e,sky} = \varepsilon_{sky} \cdot f_{sky} \qquad (33)$$

f_{sky} was calculated with *Equation (27*), while the sky emissivity (ε_{sky}) can be obtained as the ratio of the sky radiance (ILAH) to $\sigma \cdot T_a^4$, where T_a is the absolute air temperature near the ground (which equals the exterior temperature, T_e) (see *Equation*)*(34)* [*38*].

$$\varepsilon_{sky} = \frac{ILAH}{\sigma \cdot T_e^4} \qquad (34)$$

Similarly, the terrestrial LW emission factor, $f_{lw,e,ground}$, and $f_{lw,e,sky,ground}$ can be obtained from *Equations (35) and (36)* [*38*].

$$f_{lw,e,ground} = \varepsilon_{ground} \cdot f_{ground} \qquad (35)$$

$$f_{lw,e,sky,ground} = \varepsilon_{sky} \cdot \left(1 - \varepsilon_{ground}\right) \cdot f_{ground} \qquad (36)$$

The envelope's surface temperature (T_{env}) in *Equation (31*) is the variable which is obtained from the program implemented in *Matlab*.

Before explaining how to solve *Equations (6*), *(7*) *and (8*) there is one more variable (in *Equation* (8), the internal air temperature (T_i), that must be mentioned.

The internal air temperature of the building is not an input value as it is the external air temperature (T_e). However, it can be estimated from the average external temperature ($T_{e,aver}$) by using the EN 15026 method *(from the source British Standard BS Hydrothermal performance of building components and building elements [43]).* This method takes for granted that mechanical conditioning systems will be applied to assure thermal comfort inside the building. As can be seen in Figure 19, the internal temperature range is limited between 20 ºC and 30 ºC, which fits with the thermal comfort standards [*44*].

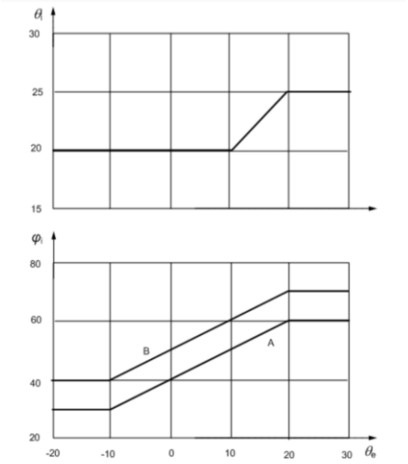

Key	
θ_i internal temperature, °C	φ_i internal relative humidity, %
θ_e external temperature, °C	A : normal occupancy
	B : high occupancy

Figure 19. Daily mean internal air temperature and humidity in dwellings and office buildings depending on the daily mean external air temperature [43].

Θ_e in Figure 19 is the one called $T_{e,aver}$ in this project and it has been obtained as the moving average of 24 hours centred in the external temperature T_e taken from the climate file. With $T_{e,aver}$ the lineal internal temperature ($T_{i,lin}$) has been calculated (Θ_i between 20 °C and 25 °C in Figure 19). The equation of the curve $T_{i,lin}$ would be the one presented in *Equation (37).*

$$T_{i,lin} = 15°C + \frac{T_{e,aver}}{2} \qquad (37)$$

From Figure 19, *Equations (38), (39) and (40)* are obtained:

$$T_i = 20°C, \quad if \ T_{i,lin} < 20°C \qquad (38)$$

$$T_i = T_{i,lin}, \ if \ 20°C < T_{i,lin} < 25°C \qquad (39)$$

$$T_i = 25°C, \quad if \ T_{i,lin} > 25°C \qquad (40)$$

Now all the variables have been explained, it is time to analyse how the *Equations (6*), *(7*) *and (8*) have been adapted to implement them in *Matlab* and obtain T_{env}, T_{me} and T_{mi} for each time step.

2.7. Resolution of the model

First, the *Equation (6*) is converted by expressing $Q_{e,lw,e}$ (variable that depends on T_{me}) by using *Equations (24*) *and (31*). That way, the corresponding *Equation (41) is* obtained:

$$C_{mout}\frac{T_{env} - T_{env,prev}}{\Delta t} = \frac{T_e - T_{env}}{R_{se}} + \frac{T_{me} - T_{env}}{R_{out}} + Q_{e,sw} + Q_{e,lw,a} - f_{lw,e} \cdot \varepsilon_{se} \cdot \sigma \cdot \left[\left(T_{env,prev}\right)^4 + 4\left(T_{env,prev}\right)^3 \left(T_{env} - T_{env,prev}\right)\right] \qquad (41)$$

Regrouping *Equations (7*), *(8*) *and (41),* the following *Equations (42-44)* are obtained:

$$\frac{C_{mout}}{\Delta t}T_{env} + \frac{1}{R_{se}}T_{env} + \frac{1}{R_{out}}T_{env} + 4f_{lw,e}\varepsilon_{se}\sigma\left(T_{env,prev}\right)^3 T_{env} - \frac{1}{R_{out}}T_{me} = \frac{C_{mout}}{\Delta t}T_{env,prev} + \frac{T_e}{R_{se}} + Q_{e,sw} + Q_{e,lw,a} - f_{lw,e}\varepsilon_{se}\sigma\left(T_{env,prev}\right)^4 + 4f_{lw,e}\varepsilon_{se}\sigma\left(T_{env,prev}\right)^3 T_{env,prev} \quad (42)$$

$$-\frac{1}{R_{out}}T_{env} + \frac{C_{me}}{\Delta t}T_{me} + \frac{1}{R_{out}}T_{me} + \frac{1}{R_m}T_{me} - \frac{1}{R_m}T_{mi} = \frac{C_{me}}{\Delta t}T_{me,prev} \quad (43)$$

$$-\frac{1}{R_m}T_{me} + \frac{C_{mi}}{\Delta t}T_{mi} + \frac{1}{R_m}T_{mi} + \frac{1}{R_{mi}}T_{mi} = \frac{C_{mi}}{\Delta t}T_{mi,prev} + \frac{T_i}{R_{mi}} \quad (44)$$

Finally, *Equations (45), (46) and (47)* are obtained, which can be represented in a matricial way in *Equation* (48) and from which T_{env}, T_{me} and T_{mi} can be easily calculated with the function “linsolve” in *Matlab (see Section 8,* ANNEX 2*)*:

$$A_1T_{env} + B_1T_{me} + C_1T_{mi} = D_1 \quad (45)$$

$$A_2T_{env} + B_2T_{me} + C_2T_{mi} = D_2 \quad (46)$$

$$A_3T_{env} + B_3T_{me} + C_3T_{mi} = D_3 \quad (47)$$

$$\begin{bmatrix} A_1 & B_1 & C_1 \\ A_2 & B_2 & C_2 \\ A_3 & B_3 & C_3 \end{bmatrix}\begin{bmatrix} T_{env} \\ T_{me} \\ T_{mi} \end{bmatrix} = \begin{bmatrix} D_1 \\ D_2 \\ D_3 \end{bmatrix} \quad (48)$$

The coefficents from the just mentioned equations are expressed below, *Equations (49-60):*

$$A_1 = \frac{C_{mout}}{\Delta t} + \frac{1}{R_{se}} + \frac{1}{R_{out}} + 4f_{lw,e}\varepsilon_{se}\sigma\left(T_{env,prev}\right)^3 \quad (49)$$

$$B_1 = -\frac{1}{R_{out}} \quad (50)$$

$$C_1 = 0 \quad (51)$$

$$D_1 = \frac{C_{mout}}{\Delta t}T_{env,prev} + \frac{T_e}{R_{se}} + Q_{e,sw} + Q_{lw,a,k} - f_{lw,e}\varepsilon_{se}\sigma\left(T_{env,prev}\right)^4 + 4f_{lw,e}\varepsilon_{se}\sigma\left(T_{env,prev}\right)^3 T_{env,prev} \quad (52)$$

$$A_2 = -\frac{1}{R_{out}} \quad (53)$$

$$B_2 = \frac{C_{me}}{\Delta t} + \frac{1}{R_{out}} + \frac{1}{R_m} \quad (54)$$

$$C_2 = -\frac{1}{R_m} \quad (55)$$

$$D_2 = \frac{C_{me}}{\Delta t} T_{me,prev} \qquad (56)$$

$$A_3 = 0 \qquad (57)$$

$$B_3 = -\frac{1}{R_m} \qquad (58)$$

$$C_3 = \frac{C_{mi}}{\Delta t} + \frac{1}{R_m} + \frac{1}{R_{mi}} \qquad (59)$$

$$D_3 = \frac{C_{mi}}{\Delta t} T_{mi,prev} + \frac{T_i}{R_{mi}} \qquad (60)$$

To obtain T_{env}, T_{me} and T_{mi} for the first time-step, $T_{env,prev}$, $T_{me,prev}$ and $T_{mi,prev}$ are needed. They are introduced as input data, with a value of $T_{env,prev} = T_{me,prev} = T_{mi,prev}$ = 20 ºC. For the following time steps, these previous temperatures are the values obtained in T_{env}, T_{me} and T_{mi}, respectively.

In the former equations, all the temperatures must be in Kelvin [K].

Matlab gives the values of T_{env}, T_{me} and T_{mi} for each time step. With these temperatures, all the data needed for the calculation of the different heat fluxes in Figure 17 is arranged.

The value of the heat flux through the inside surface of the wall (Q_{mi}) can be calculated from *Equation (1*).

Equally, the heat flux in the external coating (Q_{ext}) the heat flux in the external surface of the wall (Q_{me}) and the heat flux through the wall core (Q_m) are obtained from *Equations* (61), (62) and (63), respectively.

$$Q_{ext} = \frac{T_e - T_{env}}{R_{se}} \qquad (61)$$

$$Q_{me} = \frac{T_{env} - T_{me}}{R_{out}} \qquad (62)$$

$$Q_m = \frac{T_{me} - T_{mi}}{R_m} \qquad (63)$$

The short-wave solar incident radiative heat ($Q_{e,sw}$), as well as the long wave emitted ($Q_{e,lw,e}$) and absorbed ($Q_{e,lw,a}$) radiative heat outputs from external surfaces have been already calculated in *Equations (10*), *(31*) *and (25*), respectively.

The heat flux towards C_{mout}, C_{me} and C_{mi} (heat flux stored in each of the capacitors) are values obtained from *Equations (64), (65) and (66):*

$$Q_{Cmout} = \frac{C_{mout} \cdot (T_{env} - T_{env,prev})}{t_{step}} \qquad (64)$$

$$Q_{Cme} = \frac{C_{me} \cdot (T_{me} - T_{me,prev})}{t_{step}} \qquad (65)$$

$$Q_{Cmi} = \frac{C_{mi} \cdot (T_{mi} - T_{mi,prev})}{t_{step}} \qquad (66)$$

Once all the heat fluxes involved in the process are obtained, the next energy balances can be done (*Equations (67), (68) and (69)):*

$$Q_{ext} + Q_{e,lw} + Q_{e,sw} = Q_{me} + Q_{Cmout} \qquad (67)$$

$$Q_{me} = Q_{Cme} + Q_m \qquad (68)$$

$$Q_m = Q_{Cmi} + Q_{mi} \qquad (69)$$

In addition, the solar collection at the external surface (Q_{col}), which is the heat captured at the external surface, is obtained from *Equation* (2).

Figure 20 shows the results obtained for the heat flux through the inside surface of the wall for this first example that has been used to model the system (R_{out} = 2.5 [m²·K/W], ε_{lw} = 0.5 and α_{se} = 0.6):

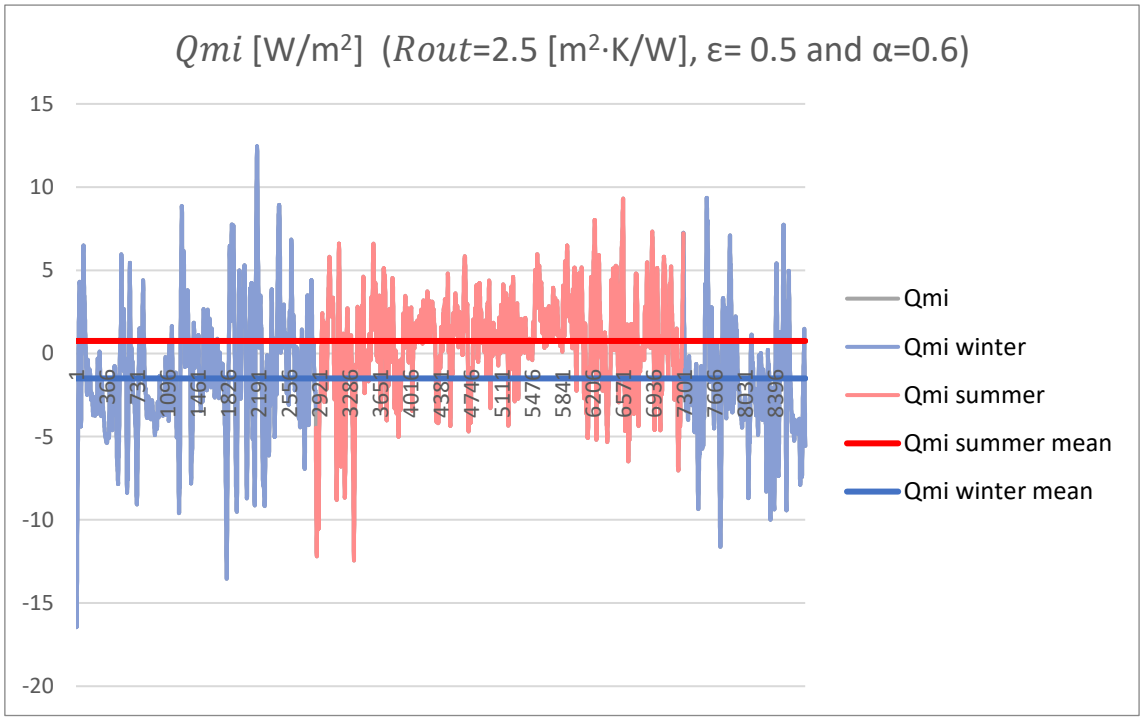

Figure 20. Heat flux through the inside surface of the wall (Q_{mi} [W/m2]) for Rout = 2.5 [m²·K/W], ε = 0.5 and α = 0.6.

Figure 20 shows the distribution of the internal heat flux (Q_{mi}) all over a year. The whole year has been divided into two periods (summer and winter) to study the mean value of the internal flux in the cooler and warmest months. The summer period considered has been from May to October and the winter period from November to April (with the months mentioned included, respectively).

In addition, with this model, a prediction of the heating and cooling demand inside the building can be done, analysing the external air temperatures (T_e). The average of the predicted next 24 hours (24 time-steps) external temperatures are compared with the HDD and CDD (which are the reference external temperatures for heating and cooling demand, respectively). These values depend on the insulation level of the building and on the internal heat gains (which can change from one building to another). Latest

Eurostat updates propose a value of HDD around 15.5 °C and a value of around 22 °C for CDD [*45*]. To simplify, in this project a value of HDD = 15 °C and CDD = 20 °C have been considered.

Therefore, if the predicted external temperature is higher than 20 °C, cooling demand is foreseen, while if it is lower than 15 °C, heating is foreseen. For predicted external temperatures between 15 °C and 20 °C no demand is foreseen. This criterion has been used to analyse the response Q_{col} in *Section 3*.

3. DESIGN OF EXPERIMENTS (DoE)

3.1. Introduction

In a building, there are several parameters that do affect the heat interaction between the exterior and the interior. To analyse how these variables can have an effect on the energy efficiency of the building, a parametric analysis and an optimization have been carried out by means of Design of Experiments (DoE) [46] techniques.

The Design of Experiments (DoE) is a statistics method used not only to improve or optimize products or processes, but also to find out which are the factors (and quantify them) that have an influence in other variables that have been selected as the interesting ones.

By doing several experiments, these techniques study the response that a certain process has when it is subjected to changes in its regular conditions. Therefore, its aim is to identify the significant changes in the response so that a more accurate knowledge of the process is reached. In other words, the DoE techniques try to control the variability of a random process that can have different origins.

These techniques are usually used to identify the reasons why the responses of a certain process change, find out the conditions that give extreme values of a certain parameter, contrasts different solutions when changing variables or even to estimate a mathematical model of a random process to be able to make future predictions.

In this project, the process which is going to be evaluated is the heat transfer through the wall of the building studied in *Section 2* and modelled in *Matlab* (a wall to which an external insulation layer with a coating has been applied). To evaluate the energy efficiency of the building, the following input and output variables have been selected (which have been already mentioned in *Section 2* when describing the model implemented in *Matlab*):

The three input parameters that model the attached external insulation coating:

- R_{out} (Thermal resistance of the outer coating) [m^2·K/W]. It is the resistance that models the effect of covering the building with a skin (building insulation) of a certain thickness. In this project, the values that this resistance will take are limited: (0.01 - 5) [m^2·K/W]. The reason of not letting R_{out} take a value of zero is that certain coefficients in *Equations (43*) *and (44*) would tend to infinite. To avoid this, a minimum value of 0.01 is permitted. A maximum value of 5 m^2·K/W has been chosen.

- Epsilon (***ε*** or ε_{lw}*)* (long-wave emissivity of external surface), [-]. The emissivity of the surface of a material, ε, represents how effective the material is emitting energy as thermal radiation. It is a non-dimensional number that relates the capacity that a material has to irradiate thermal energy with the one it would have if it was a black body (a black body is a theorical, idealized, object that absorbs all the light and energy irradiance that hits the object).

  ε = radiation emitted by a surface/emitted radiation if it was a black body.

That way, black bodies will always have ***ε*** = 1, while every other real object will have ***ε*** < 1. In this project, the material that is being analysed is the building coating. The range of

emissivity values that have been selected as possible is from 0.4 (supposing a reflective material) to 0.9 (typical value in many materials) [*42*].

- Alpha (α or α_{se}) (short-wave absorptivity of external surface), [-]. It represents the fraction of the incident radiative energy absorbed by the material. Similar to what happens with the emissivity, alpha takes a value of $\alpha = 1$ for ideal black bodies while $\alpha < 1$ for the rest of the objects. In this case a range of alpha between 0.2 (considering that the coating can have a high reflectance) and 0.8 (dark surface) have been selected [*42*].

With these three input parameters the external layer (building coating) that is covering the building is modelled.

To analyse the energy efficiency of the building, two representative outputs have been studied: Q_{mi} and Q_{col}. The model has been first studied considering Q_{mi} as the output. Later, once the correct DoE method has been selected, the response Q_{col} will be also analysed.

The objective of this analysis, therefore, is to find out which are the optimum characteristics of the insulation coating that will end up in a decreasing energy consumption of the building. These solutions will vary for the different weather conditions corresponding to the place the studied building is located, as well as for different materials used in the façade of the building.

As it has been said, in this project, the location, orientation and other needed characteristics are obtained from the weather file of Bilbao. When it comes to the façade of the building, the first case which is studied is the one analysed until now, the solid concrete façade. Two more façades will be observed to contrast how the solutions vary.

3.2. Response 1: $Q_{mi,summer,mean}$ and $Q_{mi,winter,mean}$

Q_{mi} (heat flux through the inside surface of the wall) (*Equation (1)*) [W/m^2] is one of the output variables that can be obtained from the model constructed in *Matlab* in *Section 2.* By analysing the Q_{mi} obtained during summer ($Q_{mi,summer}$) and the one obtained during winter ($Q_{mi,winter}$) independently, the following two output parameters have been selected:

- $Q_{mi,summer.mean}$: mean value of the values of $Q_{mi,summer}$ during the hours (time steps) that constitute the summer period [W/m^2].

- $Q_{mi,winter.mean}$: mean value of the values of $Q_{mi,winter}$ during the hours that constitute the winter period [W/m^2].

The summer and winter periods considered are the ones expressed above in *Section 2* (Figure 20): summer period from May to October and winter period from November to April (with the months mentioned included, respectively).

Once the input and output variables have been selected, the next step is to apply different Design of Experiment techniques in order to perform a parametric analysis and an optimization. Before identifying the method that best fits this concrete problem, two designs have been tried: Faced-Centred Central Composite Design (CCF) and Box-Behnken Design. In each of these experiments, some statistic aspects have been analysed: Response Surface Regression (Pareto Chart of the Effects, Regression Equation, Analysis of Variance, P-values, R^2 and Residual Plots), Factorial Plots and finally the Response Optimization. A Fractional Factorial ½ method has also been tried

but it has been discarded as this method is just valid to estimate first-rate models (not curvatures), and it will be seen when analysing the other two methods that the studied model does present curvature. Therefore, the Factorial DoE method will not be presented in this work.

For doing the Design of Experiments, the statistical analysis software *Minitab* [47] has been used.

3.2.1. Faced-Centred Central Composite Design (CCF)

The first Design of Experiments (DoE) method that has been tried (once the Fractional Factorial was discarded) is a Central Composite Design (CCD) [*46*].

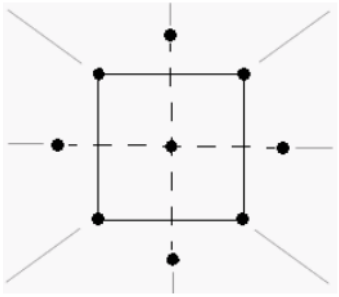

Figure 21. Central Composite Design (CCD) [46].

The Central Composite design is a Response Surface design with several centre points analysed. It is a Factorial, or Fractional Factorial, design that does not focus only on centre points but also considers some axial points (at a distance α from the centre point) that allow estimating curvature. Therefore, the mentioned Factorial design is now enlarged. For this concrete project, a special type of Central Composite Design has been selected: Faced-Centred Central Composite design (CCF), with face-centred axial points (α=1). The reason of choosing CCF (Figure 22 left) and no other Central Composite Design is that the input variables of the model have a maximum and a minimum value which cannot be exceeded because it would not make physical sense.

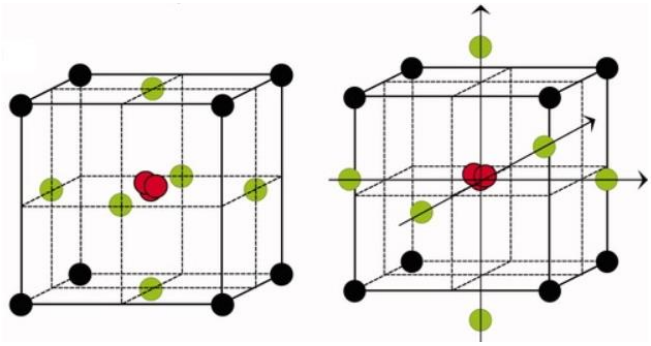

Figure 22. Central Composite Design, CCD, (left) and Central Composite Circumscribed, CCC, (right) designs [46].

The black dots in the corners in Figure 22 represent the Factorial points, while the red points are the central points. The green dots (axial dots) are the ones that differentiate the CCF from other CCD methods. In CCF the axial points are displaced inside the space (α = 1) (Figure 22 left), while in other methods are not, as can be seen in Figure 22 right (example of a Central Composite Circumscribed design, CCC).

As it has been said, values outside the range of each of the input variables are not considered in this model, as they do not make sense.

The procedure followed will be now presented. First, the Response Surface Design (Central Composite) has been created *(Stat→DoE→Response Surface→Create Response Surface Design)* for three continuous factors (Rout, Epsilon and Alpha). A value of α = 1 has been given to make it face-centred. A total of twenty experiments have been proposed by Minitab. Next to each of the proposed input parameter combinations, the respective outputs have been calculated with *Matlab* and introduced in *Minitab* (Figure 23).

	C1	C2	C3	C4	C5	C6	C7	C8	C9
	StdOrder	RunOrder	PtType	Blocks	Rout	Epsilon	Alpha	Qmi,winter,mean	Qmi,summer,mean
1	1	1	1	1	0.010	0.40	0.2	-21.4452	-6.3518
2	17	2	0	1	2.505	0.65	0.5	-1.9469	0.1718
3	14	3	-1	1	2.505	0.65	0.8	-1.0729	1.2769
4	5	4	1	1	0.010	0.40	0.8	-5.8040	13.6485
5	11	5	-1	1	2.505	0.40	0.5	-1.7143	0.4915
6	12	6	-1	1	2.505	0.90	0.5	-2.1248	-0.0658
7	18	7	0	1	2.505	0.65	0.5	-1.9469	0.1718
8	4	8	1	1	5.000	0.90	0.2	-1.5614	-0.5836
9	2	9	1	1	5.000	0.40	0.2	-1.4701	-0.4606
10	20	10	0	1	2.505	0.65	0.5	-1.9469	0.1718
11	6	11	1	1	5.000	0.40	0.8	-0.3813	0.9392
12	10	12	-1	1	5.000	0.65	0.5	-1.0402	0.0775
13	9	13	-1	1	0.010	0.65	0.5	-15.7415	1.4816
14	8	14	1	1	5.000	0.90	0.8	-0.7198	0.4670
15	13	15	-1	1	2.505	0.65	0.2	-2.8495	-0.9686
16	16	16	0	1	2.505	0.65	0.5	-1.9469	0.1718
17	15	17	0	1	2.505	0.65	0.5	-1.9469	0.1718
18	7	18	1	1	0.010	0.90	0.8	-11.0397	7.8005
19	19	19	0	1	2.505	0.65	0.5	-1.9469	0.1718
20	3	20	1	1	0.010	0.90	0.2	-24.1126	-8.5526

Figure 23. The 20 experiments proposed by Minitab for the Response Surface Design method: in columns C5-C7 the values of the input parameters provided by the design and in columns C8 and C9 the values of the outputs obtained from the model implemented in Matlab.

From the twenty possible combinations that Minitab offers, six of them are the same (Rout = 2.505 [m^2·K/W], Epsilon = 0.65 and Alpha = 0.5). This makes sense with what has been said and showed in Figure 22. These six experiments correspond to the red dots in the figure (centre points).

Once the table is completed, the Response Surface analysis can be done.

Response Surface Regression

A Response Surface Design analysis has been done to model curvature in the data and identify factor settings that optimize the response. It is specially used to find out which are the factors that have statistical significance in the response, and that way, estimate the response surface curvature.

Pareto Chart of the Standardized Effects

The Pareto Chart of the Standardized Effects is used to compare the relative magnitude and the statistical significance of the terms (main value, square, and interaction of them).

Minitab plots the terms in decreasing order of their absolute values. The reference line on the chart (red line in Figure 24) indicates which terms are significant. By default, *Minitab* uses a significance level of 0.05 to draw the reference line.

To be statistically significant the blue bar must extend past the red line. The farthest the bar extends, the largest its effect is.

The following charts (obtained with *Minitab*) show the statistical significance between the outputs and the three input parameters, as well as with the interaction of them.

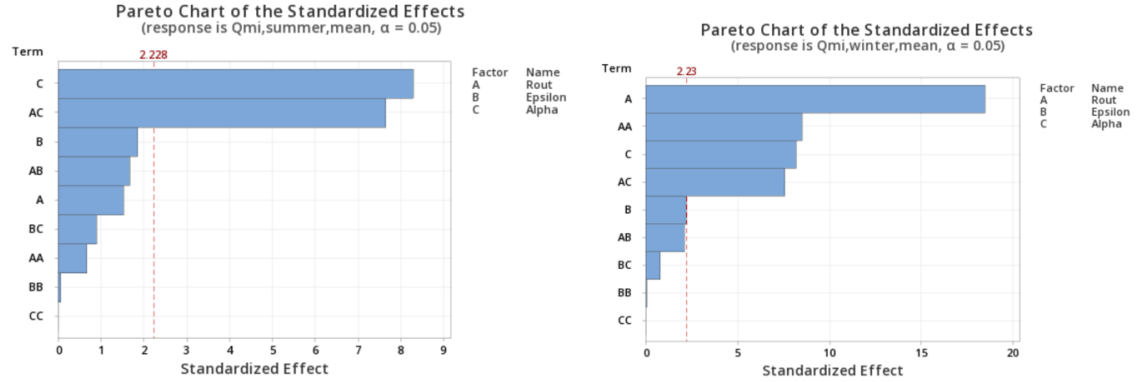

Figure 24. Pareto Charts of the Standardized Effects for both Q_{mi} responses.

The variable that has the biggest significance in the $Q_{mi,summer,mean}$ response is Alpha (A), followed by the interaction of Alpha with R_{out} (AC). In this response, Epsilon (B) appears to have no statistical significance (as the blue bar does not extend past the red line). When observing the other response ($Q_{mi,winter,mean}$) R_{out} seems to have a clear impact, followed by Alpha and finally by Epsilon in a less significant way. At a first sight, R_{out} seems to be the variable that has the biggest impact in the responses, and it is as well the term that makes the model be quadratic (as the interaction of A with C and its own (AA) is significant). These results have a physical meaning: during summer months, the absorptivity (Alpha), is the variable which has the biggest impact in the heat flux entering the building (what makes sense as during summer solar radiation is big). During winter months, on the other hand, Rout (the insulation), seems to be the variable that plays the most important role (as solar radiation is not that important during these months and the convection due to the wind has a bigger impact, which can be prevented by adding more insulation). When doing the response optimization, the physical meaning of the obtained results will be better explained. The interactions of BC, BB and CC are not significant for neither of the responses. It has been proved that omitting these terms from the analysis, Minitab is able to offer a more accurate response. Therefore, just the modified version (omitting these terms) will be shown and analysed below, which results in the following Pareto Charts:

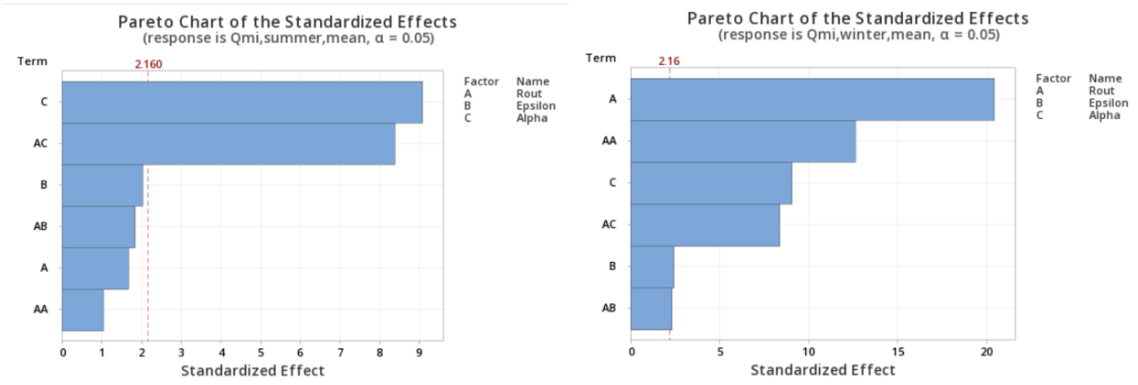

Figure 25. Modified Pareto Charts of the Standardized Effects for both Q_{mi} responses.

Regression Equation

The relation between input and outputs have been given by Minitab as follows:

$$Qmi,winter,mean = -22.00 + 9.328\ Rout - 7.25\ Epsilon + 22.01\ Alpha - 1.0261\ Rout*Rout + 1.498\ Rout*Epsilon - 4.473\ Rout*Alpha \quad (70)$$

$$Qmi,summer,mean = -7.49 + 1.017\ Rout - 7.42\ Epsilon + 27.87\ Alpha + 0.108\ Rout*Rout + 1.494\ Rout*Epsilon - 5.662\ Rout*Alpha \quad (71)$$

These equations are not valid until some conditions that will now be analysed are checked.

Analysis of Variance (ANOVA)

The analysis of variance is useful to determine if a parameter is statistically significant or not. The p-value is a clear indicator of it. The p-value of a term is used to determine whether the association between the response ($Q_{mi,summer,mean}$ and $Q_{mi,winter,mean}$) and each term is statistically significant. First, a null hypothesis has to be done: consider there is no association between the term and the response. The p-value of a term is then compared with a significance level (alpha, α) which usually is given a value of 0.05. A significance level of 0.05 indicates a 5% risk of concluding that an association exists when there is no actual association.

If the p-value is less than or equal to the significance level (0.05), it can be concluded that there is a statistically significant association between the response variable and the term. However, if the p-value is greater than 0.05 there is no statistically significant association between the response variable and the term. Therefore, the model might be refitted without the term.

To determine if the studied parameters are statistically significant or not, the p-values have been analysed (Figure 26).

$Q_{mi,summer,mean}$

Analysis of Variance

Source	DF	Adj SS	Adj MS	F-Value	P-Value
Model	6	335.593	55.932	27.29	0.000
Linear	3	182.727	60.909	29.72	0.000
Rout	1	5.756	5.756	2.81	0.118
Epsilon	1	8.466	8.466	4.13	0.063
Alpha	1	168.505	168.505	82.23	0.000
Square	1	2.245	2.245	1.10	0.314
Rout*Rout	1	2.245	2.245	1.10	0.314
2-Way Interaction	2	150.621	75.311	36.75	0.000
Rout*Epsilon	1	6.945	6.945	3.39	0.089
Rout*Alpha	1	143.677	143.677	70.11	0.000
Error	13	26.641	2.049		
Lack-of-Fit	8	26.641	3.330	*	*
Pure Error	5	0.000	0.000		
Total	19	362.235			

$Q_{mi,winter,mean}$

Analysis of Variance

Source	DF	Adj SS	Adj MS	F-Value	P-Value
Model	6	945.861	157.643	123.07	0.000
Linear	3	645.222	215.074	167.90	0.000
Rout	1	532.465	532.465	415.68	0.000
Epsilon	1	7.645	7.645	5.97	0.030
Alpha	1	105.113	105.113	82.06	0.000
Square	1	203.987	203.987	159.25	0.000
Rout*Rout	1	203.987	203.987	159.25	0.000
2-Way Interaction	2	96.651	48.326	37.73	0.000
Rout*Epsilon	1	6.981	6.981	5.45	0.036
Rout*Alpha	1	89.670	89.670	70.00	0.000
Error	13	16.652	1.281		
Lack-of-Fit	8	16.652	2.082	3.42994E+19	0.000
Pure Error	5	0.000	0.000		
Total	19	962.513			

Figure 26. Analysis of Variance for the response $Q_{mi,summer,mean}$ (left) and $Q_{mi,winter,mean}$ (right).

For the $Q_{mi,winter,mean}$ response the p-value of the three inputs is lower than the significance level 0.05, and so it is the p-value of all the combinations of these parameters. Therefore, statistical significance can be assured on those variables. In the

$Q_{mi,summer,mean}$ response, however, Alpha is the only parameter which presents statistical significance (as it could be seen in the Pareto Charts in Figure 25 left), and the only interaction of variables with a significant p-value is Rout*Alpha, the same as it has been shown in the Pareto Chart.

The asterisk (*) in the lack-of-fit of the error (Figure 26) is because *Minitab* has not sufficient information to return an answer to it.

From these answers, the Regression Equation proposed by Minitab for the winter response appears to be better modelled than the one given for the summer response. Some more things need to be checked before assuming the Regression Equation is valid, starting from R^2 and S and following with the residual plots.

R^2

To determine how well the model fits the data, the goodness-of-fit statistics in the Model Summary table must be examined.

- R-sq (R^2): The higher the R^2 value, the better the model fits the data. R^2 is always between 0% and 100%. R^2 increases if additional predictors are added to a model, even if there is no real improvement.
- R-sq (adj): Adjusted R^2 is used to compare models that have different numbers of predictors.
- R-sq (pred): The predicted R^2 is used to determine how well the model predicts the response for new observations. Models that have larger predicted R^2 values have better predictive ability.

$Q_{mi,summer,mean}$

Model Summary

S	R-sq	R-sq(adj)	R-sq(pred)
1.43154	92.65%	89.25%	73.91%

$Q_{mi,winter,mean}$

Model Summary

S	R-sq	R-sq(adj)	R-sq(pred)
1.13179	98.27%	97.47%	94.10%

Figure 27. Model Summary for the response $Q_{mi,summer,mean}$ (left) and $Q_{mi,winter,mean}$ (right).

It can be observed in Figure 27 that R^2 takes a high value for both responses, meaning that the model fits well the data (much better in the $Q_{mi,winter,mean}$ response). The response is well described by the model.

Residual Plots

Residual plots are used to determine whether the model meets the assumptions of the analysis. The following four graphs (Figure 28) give the information mentioned below.

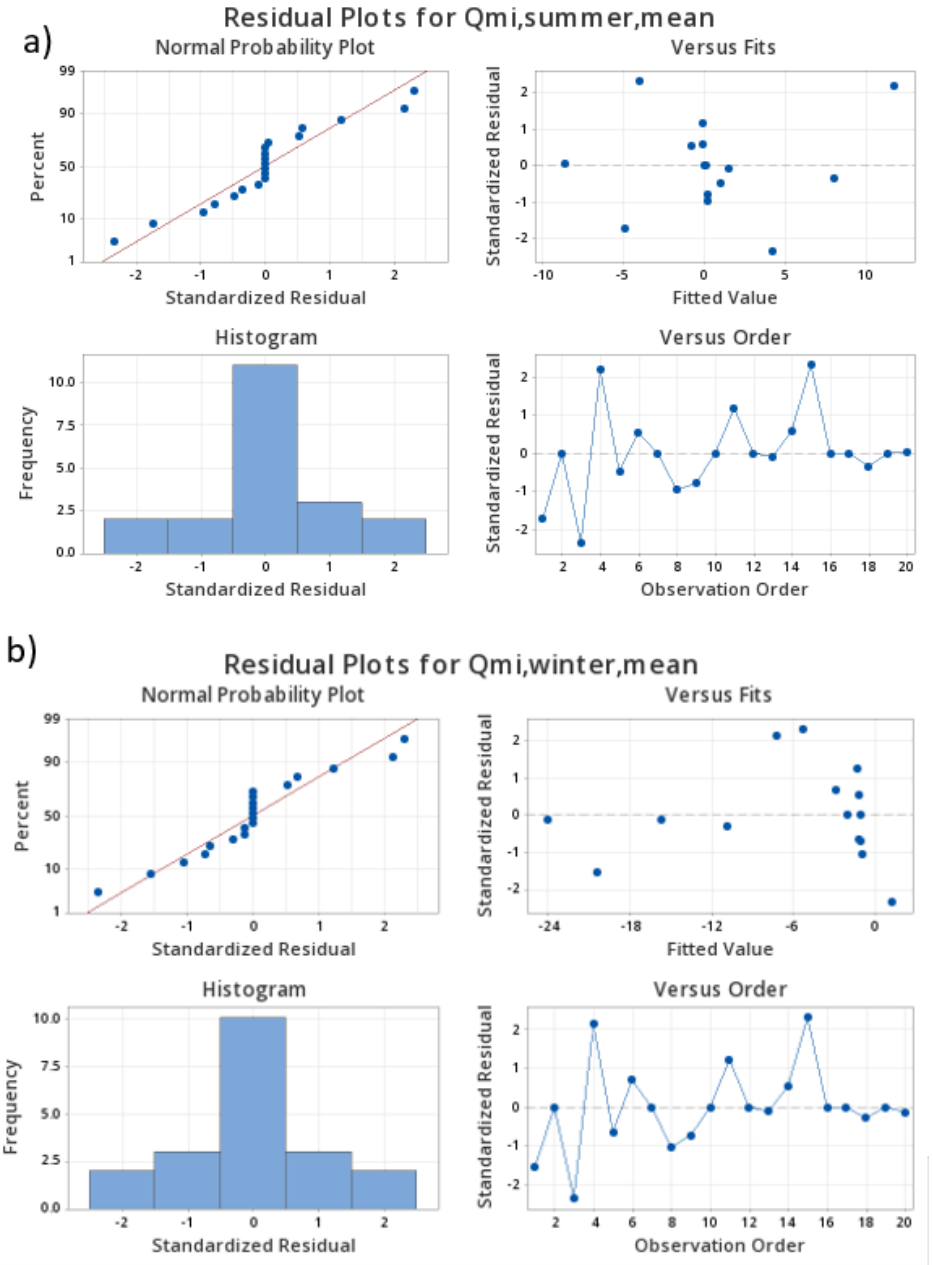

Figure 28. Residual Plots for $Q_{mi,summer,mean}$ (a) and $Q_{mi,winter,mean}$ (b).

- Residuals versus fits plot (graph in upper right corner): Used to verify the assumption that the residuals are randomly distributed and have constant variance. Ideally, the points should fall randomly on both sides of 0, with no recognizable patterns in the points.

  Furthermore, this plot gives information about the existence of outliers, which are standardized residuals with a value exceeding 2 and -2. They can cause trouble when estimating the response of the model.

  In this case, points fall randomly on both sides of 0 in both responses, even if there are several outliers.

- Residuals versus order plot (graph in lower right corner): Used to verify the assumption that the residuals are independent from one another. Independent residuals show no trends or patterns when displayed in time order. Patterns in

the points may indicate that residuals near each other may be correlated, and thus, not independent. Ideally, the residuals on the plot should fall randomly around the centre line.

In both responses, a random distribution is observed. In consequence, independence between residuals is guaranteed.

- Normal probability plot of the residuals (graph in upper left corner): Used to verify the assumption that the residuals are normally distributed. The normal probability plot of the residuals should approximately follow a straight line.

  In this case, the points follow the red line quite accurately.

Having checked the Residual Plots, the Regression of the Response Surface Design has been finally analysed. Therefore, enough information as to confirm that the given equations are valid has been collected. The next step is to optimize the response.

Response Optimization

The main objective of the DoE is to reach an estimation of the response of the model so that future predictions can be accurately made that allow optimizing processes.

In this project, the analysed responses have been the mean Q_{mi} during summer and during winter. It has been explained and it can be seen in Figure 17 that Q_{mi} is the heat flux entering the building.

To reach energy efficiency, the objective of the project is to find out the combination of the input parameters (R_{out}, Epsilon and Alpha) that result in the best solution that maximizes Q_{mi} during winter and minimizes it during summer.

The bigger Q_{mi} is during winter, the better, as less heating would be required inside the building. In contrast, during summer, the opposite effect is desired: the lower Q_{mi} gets (desiring negative values if possible, so that the heat flux goes from inside to the exterior) the better, as less cooling would be required.

In the factorial plots, the interaction of the variables can be graphically analysed (Figure 29 and Figure 30) (Stat>DoE>Response Surface>Factorial Plots).

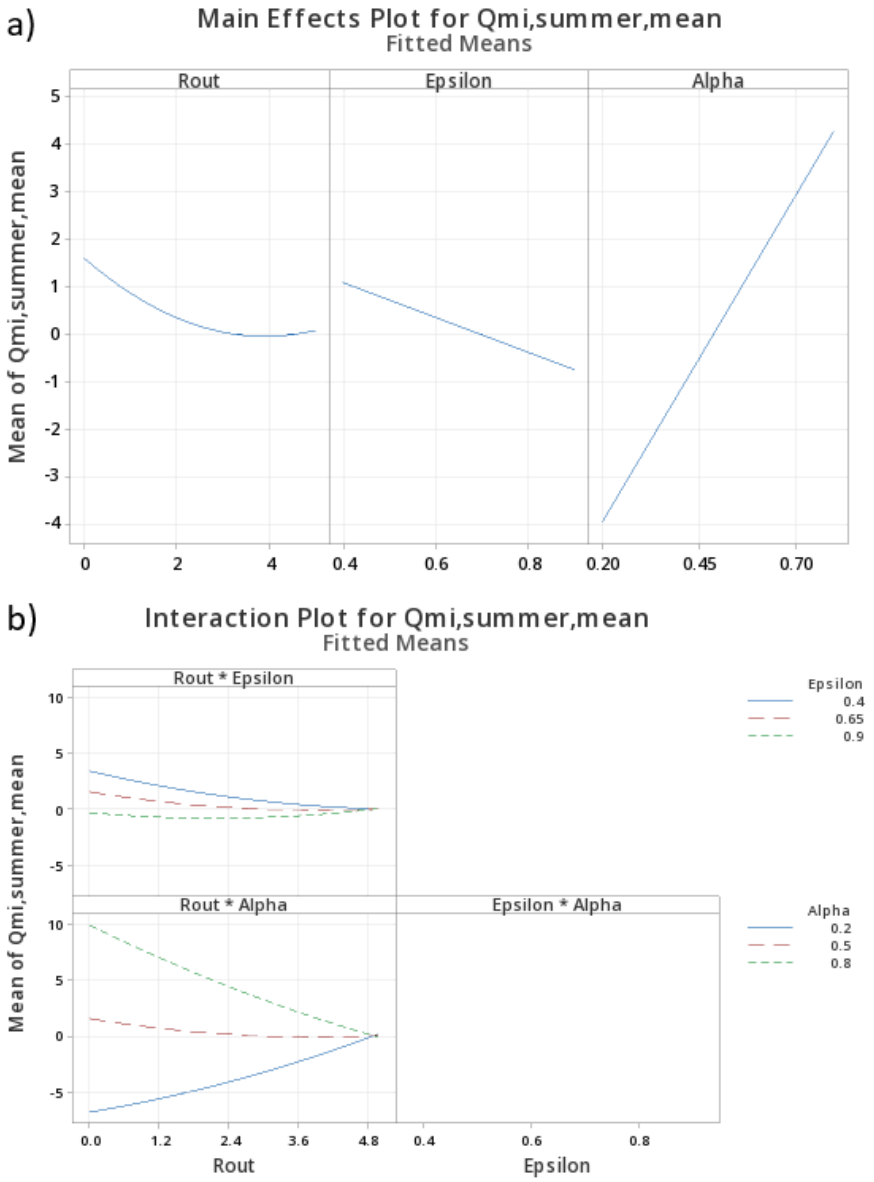

Figure 29. Factorial Plots for $Q_{mi,summer,mean}$ response: main Effects Plot (a) and Interaction Plot (b).

In the case of the response of the mean Q_{mi} during summer, the one which is desired to be minimized, it can be seen (Figure 29 a) that the lower Alpha gets, the better, and in contrast, the higher values Epsilon gets the better. The physical meaning of these answers is expalined two paragraphs below. When it comes to Rout, as its value gets higher, Q_{mi} gets lower. However, there is a point (close to Rout = 4 [m^2·K/W]) where opposite to decreasing, Q_{mi} gets higher values as Rout increases.The explanation to this strange shape of the curve Rout will be better understood when analyzing Figure 29 b.

Figure 29 b shows the interaction of the variables. For instance, looking at the graphs showing the interation of Rout with the other two inputs, lowest values of Q_{mi} during summer are obtained with low values of Alpha (blue curve) and high values of Epsilon (green curve). When it comes to Rout, when analysing the interaction with Epsilon, high values of Rout are preferible. However, when it comes to the interaction with Alpha, depending on the value Alpha gets, high or low values of Rout are preferible. It can be seen that if Alpha gets a value of 0.2, Rout should be low to minimize the mean Q_{mi} during summer, while in contrast, if Alpha has a value of 0.8, high values of Rout are

preferible. This can be the reason why in Figure 29 a the shape of Rout is not straight. Depending on the value Alpha gets, a higher or lower Rout is desired. The interaction of Alpha and Epsilon has been omitted as it was not significant.

It can be concluded, therefore, that Q_{mi} during summer is minimized with low values of Alpha and high values of Epsilon. If the physical meaning of the results is studied, a low value of Alpha means that a low fraction of energy is absorbed by the material, what is desirable if the heat entering the building is looking to be minimized. Therefore, a light material would be preferible for the coating. Finally, high values of Epsilon mean the capacity that the selected material has to irradiate thermal energy is high, emitting more infrared radiation. Therefore, a reflective coating is preferible. It is more difficult to conclude which Rout is the optimum, but the optimization carried out below gives the best result.

Similarly, the response Q_{mi} during winter can be analysed by means of Figure 30.

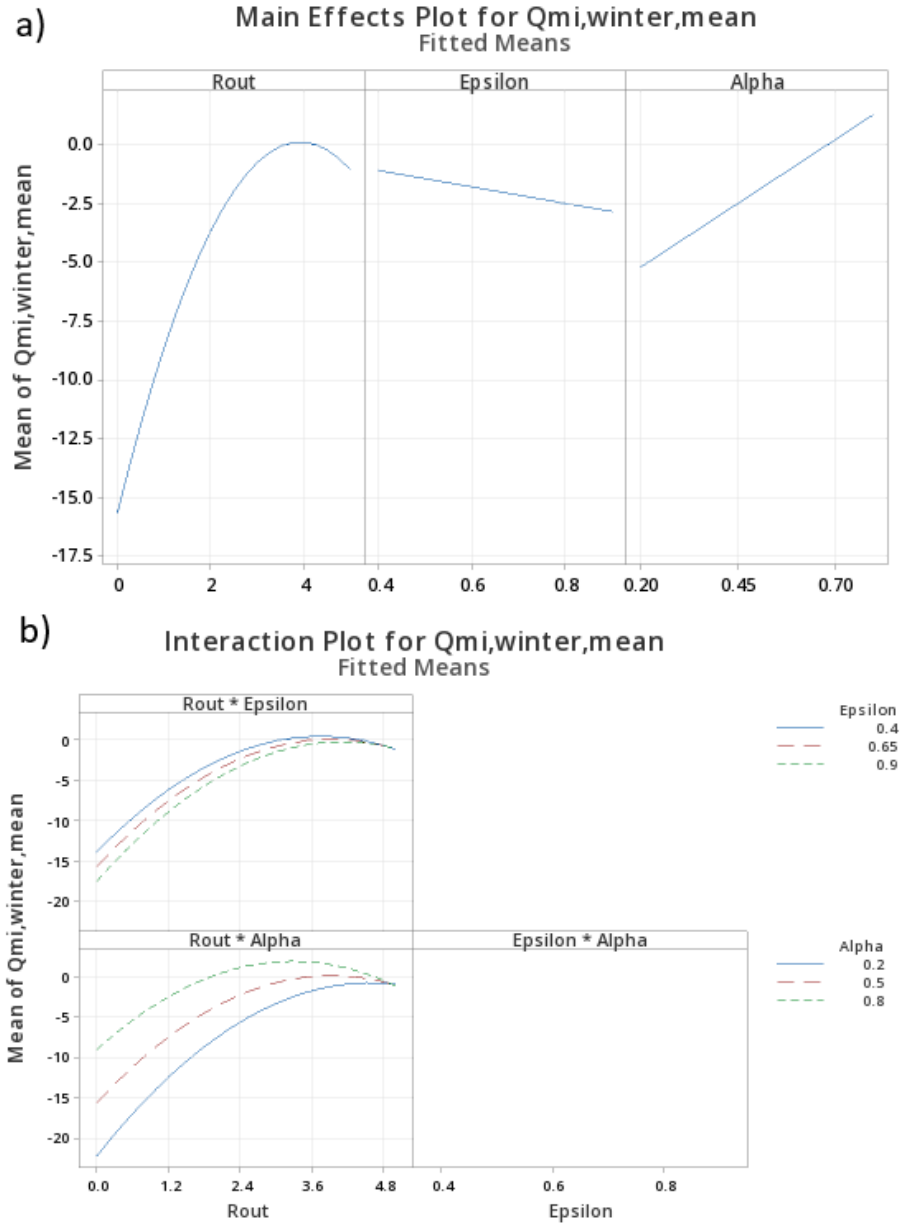

Figure 30. Factorial Plots for $Q_{mi,winter,mean}$ response. Main Effects Plot (a) and Interaction Plot (b).

Figure 30 a shows that Alpha and Epsilon follow the same trend as in the summer response. With high values of Alpha more solar radiation is absorbed (increasing the heat flux that gets into the interiour of the building). When it comes to Epsilon, as it happened with the summer response, the slope of the curve is almost flat, what means that the response is hardly influenced by its value. On the other hand, it seems that the higher Rout gets the higher Q_{mi} gets as well (contrary to what occurred during summer). This makes sense, as higher values of Rout mean more insulation, resulting in less heat flux getting out from the interiour of the building. There is also a value (close to Rout = 4 [m^2·K/W]) in which the opposite effect starts to occur, same as in the summer response.

The intercation plots do also differ from the previous response's ones. High Rout values are prerible for maximizing Q_{mi} (in both interactions), with low Epsilon and high Alpha values, respectively (opposite to what was desired in the summer response).

To analyse this optimality, the following steps have been taken in Minitab (Stat>DoE>Response Surface>Response Optimizer) to then select which response is desired to be maximized and which minimized.

Three optimality tests have been carried out: a combined optimization, and two individual optimizations (one to maximize Q_{mi} during winter months and the other one to minimize Q_{mi} during summer months). However, these last two situations are just a theoretical configuration. In real life the insulation and coating characteristics do not vary during winter and summer. Just a theoretical analysis is being carried out to find out which the best hypothetical configuration would be if the possibility of altering the insulation coating's properties from summer to winter existed.

Combined optimization

The first optimization consists of finding a unique configuration of the parameters that constitute the external insulation coating so that both objectives are reached at the same time: maximizing Q_{mi} during winter and minimizing it during summer. Therefore, a Combined Optimality test has been performed by *Minitab* (Figure 31).

Parameters

Response	Goal	Lower	Target	Upper	Weight	Importance
Qmi,summer,mean	Minimum		-8.55261	13.6485	1	1
Qmi,winter,mean	Maximum	-24.1126	-0.38129		1	1

Solution

Solution	Rout	Epsilon	Alpha	Qmi,summer,mean Fit	Qmi,winter,mean Fit	Composite Desirability
1	3.48788	0.9	0.2	-3.00695	-2.49050	0.826759

Multiple Response Prediction

Variable	Setting
Rout	3.48788
Epsilon	0.9
Alpha	0.2

Response	Fit	SE Fit	95% CI	95% PI
Qmi,summer,mean	-3.007	0.820	(-4.778, -1.235)	(-6.571, 0.557)
Qmi,winter,mean	-2.490	0.648	(-3.891, -1.090)	(-5.308, 0.327)

Figure 31. Combined Optimality Test by Minitab.

As can be seen in Figure 31, an optimal solution has been reached (Rout = 3.48788 m^2·K/W, Epsilon = 0.9 and Alpha = 0.2) which can also be observed in Figure 32.

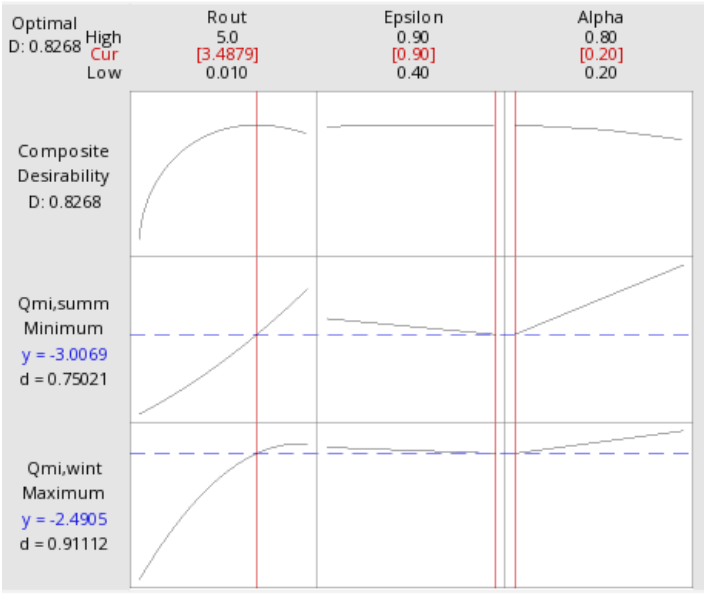

Figure 32. Optimal Solution for the Combined Optimization.

The optimization plot above (Figure 32) determines the optimal settings for the predictors (Q_{mi} winter and Q_{mi} summer) given the parameters previously specified (Rout, Epsilon and Alpha).

The composite desirability is 0.8268. This desirability is due to the fact that a combined objective is asked (conflicting goals). The first column of the graph shows the response values at each level of the variable settings which are Rout = 3.4879 m^2·K/W, Epsilon =

0.9 and Alpha = 0.2. The goal is to maximize Q_{mi} during winter, with a predicted value of -2.4905 W/m^2 and an individual desirability of 0.91112 and minimize Q_{mi} during summer, with a predicted value of -3.0069 W/m^2 and an individual desirability of 0.75021.

The prediction interval (PI) in Figure 31 is a range that is likely to contain a single future response value for a specified combination of variable settings. Narrower prediction intervals indicate a more precise prediction.

Once the optimality test has been performed the obtained result has been checked and contrasted in the model implemented in *Matlab*. This is the solution given by *Matlab* when the optimal combination of parameters is introduced (see *Table 1*), which can be compared to what it was expected by the model's prediction in Minitab, *Table 2*:

Optimal Combination of Parameters	
Rout [m^2·K/W]	3.4879
Epsilon	0.9
Alpha	0.2

Table 1. Optimal Combination of parameters in the Combined Optimization with the CCF method.

	MATLAB	MINITAB	Difference
$Q_{mi,summer,mean}$ [W/m^2]	-0.8023	-3.0069	2.2046
$Q_{mi,winter,mean}$ [W/m^2]	-2.1774	-2.4905	0.3131

Table 2. Minitab´s response predictions vs Matlab's responses for the optimal combination of parameters in CCF method in the Combined Optimization.

If the results given for the combined optimization are analysed, it can be concluded that the given Rout allows reaching both objectives: minimizing the heat flux entering the building during summer and minimizing the flux going out from the interior during winter. The resulting Epsilon (0.9) seems to be more appropriate for summer months, but it has been proved that this variable is not significant in the responses. Finally, the optimal value given for Alpha (0.2, low absorptivity) would contribute positively to the goal of minimizing the heat flux during summer.

The values given by *Minitab* for the optimal solution make sense with what has been said before and are in concordance with the significancy that each parameter has in the different responses (seen in Figure 24 and Figure 25).

Finally, it can be said that the Q_{mi} values given by Minitab are quite close to ones obtained from the physical model, especially during winter months.

Maximizing Q_{mi} during winter

The second optimization consists of finding the best combination of the input parameters considering just winter months (from November to April) in which Q_{mi} is desired to be maximized. The aim of this is to reduce heating loads in the interior of the building by making the most of the solar radiation. What is more, heat loses from the interior to the

exterior are desired to be minimized, not letting the heating loads scape. The optimality test performed in *Minitab (Figures 33 and 34)*:

Parameters

Response	Goal	Lower	Target	Upper	Weight	Importance
Qmi,winter,mean	Maximum	-24.1126	-0.381295		1	1

Solution

Solution	Rout	Epsilon	Alpha	Qmi,winter,mean Fit	Composite Desirability
1	3.08465	0.4	0.8	2.52785	1

Multiple Response Prediction

Variable	Setting
Rout	3.08465
Epsilon	0.4
Alpha	0.8

Response	Fit	SE Fit	95% CI	95% PI
Qmi,winter,mean	2.528	0.629	(1.169, 3.886)	(-0.269, 5.325)

Figure 33. Optimality Test for maximizing Q_{mi} during winter.

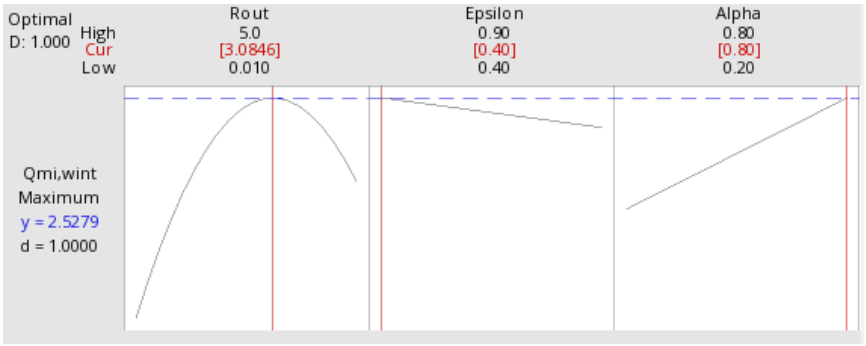

Figure 34. Optimal Solution for maximizing Q_{mi} during winter.

Optimal Combination of Parameters	
Rout [m^2·K/W]	3.0846
Epsilon	0.4
Alpha	0.8

Table 3. Optimal Combination of parameters for maximizing Q_{mi} during winter, with the CCF method.

	MATLAB	MINITAB	Difference
$Q_{mi,winter,mean}$(*maximum*) [W/m^2]	-0.59111	2.52785	3.11896

Table 4. Minitab´s response predictions vs Matlab's responses for the optimal combination of parameters in CCF method for maximizing Q_{mi} during winter.

When analysing the results (*Table 3*), it is concluded that Rout plays a significant role when preventing the heat flux scape from the interior of the building. A value of around 3 m^2·K/W has been given as the optimum, what means an insulation is desired. A high value of Alpha is also desired (high absorptivity) so that heat is collected, and higher temperatures are reached. Epsilon has been proved to make no real difference in the response, but the given value (0.4) makes sense with what is desired to reach: low emissivity and high absorptivity.

In this case, the Q_{mi} values given by Minitab fit also quite accurately to the ones obtained from the physical model, *Table 4*.

Minimizing $\boldsymbol{Q_{mi}}$ during summer

The last optimization consists of finding the best combination of the input parameters considering just summer months (from May to October) in which Q_{mi} is desired to be minimized. By minimizing the heat flux that enters the building, a cooling load reduction is desired to be reached. The optimality test performed in *Minitab (Figures 35-36)*:

Parameters

Response	Goal	Lower	Target	Upper	Weight	Importance
Qmi,summer,mean	Minimum		-8.55261	13.6485	1	1

Solution

Solution	Rout	Epsilon	Alpha	Qmi,summer,mean Fit	Composite Desirability
1	0.01	0.9	0.2	-8.58941	1

Multiple Response Prediction

Variable	Setting
Rout	0.01
Epsilon	0.9
Alpha	0.2

Response	Fit	SE Fit	95% CI	95% PI
Qmi,summer,mean	-8.59	1.15	(-11.08, -6.10)	(-12.56, -4.62)

Figure 35. Optimality Test for minimizing Q_{mi} during summer.

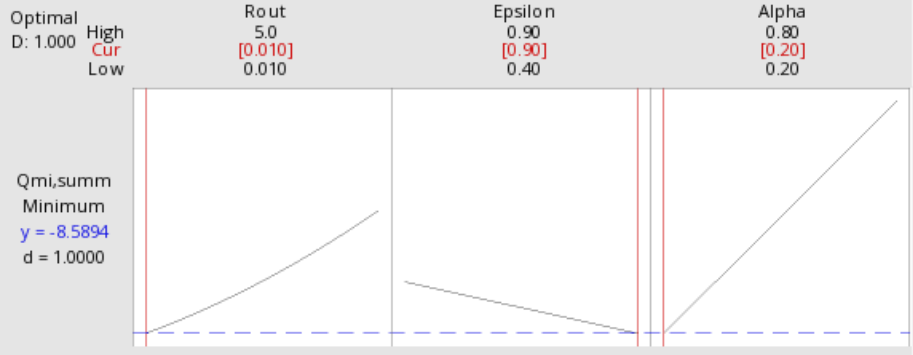

Figure 36. Optimal Solution for minimizing Q_{mi} during summer.

Optimal Combination of Parameters	
Rout [m²·K/W]	0.01
Epsilon	0.9
Alpha	0.2

Table 5. Optimal Combination of parameters for minimizing Q_{mi} during summer, with the CCF method.

	MATLAB	MINITAB	Difference
$Q_{mi,summer,mean}$(*minimum*) [W/m^2]	-8.55261	-8.58941	0.0368

Table 6. Minitab´s response predictions vs Matlab's responses for the optimal combination of parameters in CCF method for minimizing Q_{mi} during summer.

When analysing these results (*Table 5*), the obtained values of Alpha and Epsilon make sense with what has been said till now. During summer, when the heat flux entering the building is desired to be minimized, low absorptivity and high emissivity is preferable, to reflect the sun radiation and prevent the interior from reaching high temperatures. When it comes to Rout, however, no clear explanation has been found. A value of 0.01 is given by Minitab as the optimum, what would mean no insulation is desired, letting the heat enter the building (opposite to what is desired).

It can be seen (*Table 6*) that for this response the Q_{mi} values given by Minitab fit perfectly with the ones obtained from the physical model.

Conclusion

As the differences in the results given by *Minitab* and the ones obtained with *Matlab* are relatively small in all optimizations, this DoE method can be admitted as valid to predict future responses. However, one more DoE technique is studied in this project to find out if an equation that fits the model even better can be obtained.

3.2.2. Box-Behnken Design (BBD)

The results obtained with the CCF method clearly show that the studied model is not lineal. Therefore, the other DoE method studied has been the Box-Behnken Design (BBD), which does consider curvature [46].

BBD is an independent quadratic design containing no Factorial or Fractional Factorial design (in contrast with the previously studied Design Surface CCF). In this design the analysed points are the centre points and the midpoints of the edges (but not the edges itself, which are the factorial points). Figure 37 [*48*] shows a Box-Behnken design:

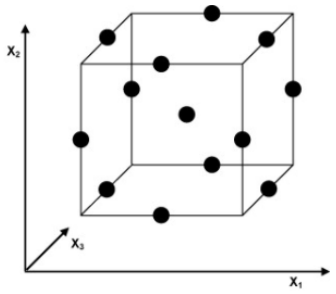

Figure 37. Box-Behnken Design [48*].*

It can be seen in Figure 37 that there are no dots in the corners.

The first step has been to create the Box-Behnken design (Stat>DoE>Response Surface>Create Response Surface Design>Box Behnken with three continuous factors).

A total of fifteen experiments have been given by Minitab, in which the centre point (Rout = 2.505 [m^2·K/W], Epsilon = 0.65 and Alpha = 0.5) is twice repeated.

The proposed experiments have been introduced in *Matlab*, giving the following responses (Figure 38).

	C1	C2	C3	C4	C5	C6	C7	C8	C9
	StdOrder	RunOrder	PtType	Blocks	Rout	Epsilon	Alpha	Qmi,winter,...	Qmi,summe...
1	5	1	2	1	0.010	0.65	0.2	-22.8970	-7.5602
2	9	2	2	1	2.505	0.40	0.2	-2.7466	-0.8350
3	11	3	2	1	2.505	0.40	0.8	-0.7097	1.7822
4	1	4	2	1	0.010	0.40	0.5	-13.5939	3.6897
5	3	5	2	1	0.010	0.90	0.5	-17.5339	-0.3229
6	8	6	2	1	5.000	0.65	0.8	-0.5745	0.6665
7	13	7	0	1	2.505	0.65	0.5	-1.9469	0.1718
8	10	8	2	1	2.505	0.90	0.2	-2.9292	-1.0690
9	2	9	2	1	5.000	0.40	0.5	-0.9180	0.2493
10	14	10	0	1	2.505	0.65	0.5	-1.9469	0.1718
11	6	11	2	1	5.000	0.65	0.2	-1.5217	-0.5310
12	12	12	2	1	2.505	0.90	0.8	-1.3477	0.9050
13	4	13	2	1	5.000	0.90	0.5	-1.1331	-0.0494
14	7	14	2	1	0.010	0.65	0.8	-8.6630	10.4235
15	15	15	0	1	2.505	0.65	0.5	-1.9469	0.1718

Figure 38. The 15 experiments proposed by Minitab for the Box-Behnken Design method, in columns C5-C7 the values of the input parameters provided by the design and in columns C8 and C9 the values of the outputs obtained from the model implemented in Matlab.

Once the table is completed, the same steps as in the CCF have been followed, starting with the Response Surface analysis.

Response Surface Regression

(Stat>DoE>Response Surface>Analyse Response Surface Design).

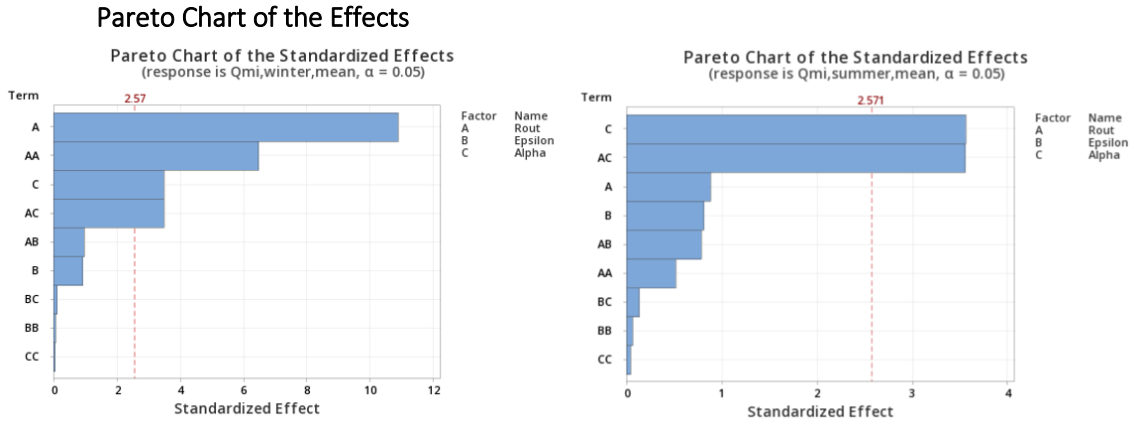

Figure 39. Pareto Chart of the Standardized Effects for response $Q_{mi,winter,mean}$ (left) and $Q_{mi,summer,mean}$ (right).

The input Epsilon (and its interactions) appears to be statistically insignificant in both responses. Therefore, it could be omitted from the analysis. However, in order to find out how this variable affects the model (even if its impact is insignificant compared to the impact of the remaining two inputs) the two possibilities have been analysed: the model with and without omitting Epsilon (the long-wave emissivity of external surface). In both cases, the interactions of the variables that are insignificant for both responses have been discarded (CC, BB, BC and AB), resulting in the Pareto Charts of Figure 40 and

Figure 41. The physical meaning of the variables affecting each response will be analysed when doing the Response Optimization.

Pareto Chart of the Effects omitting long-wave emissivity

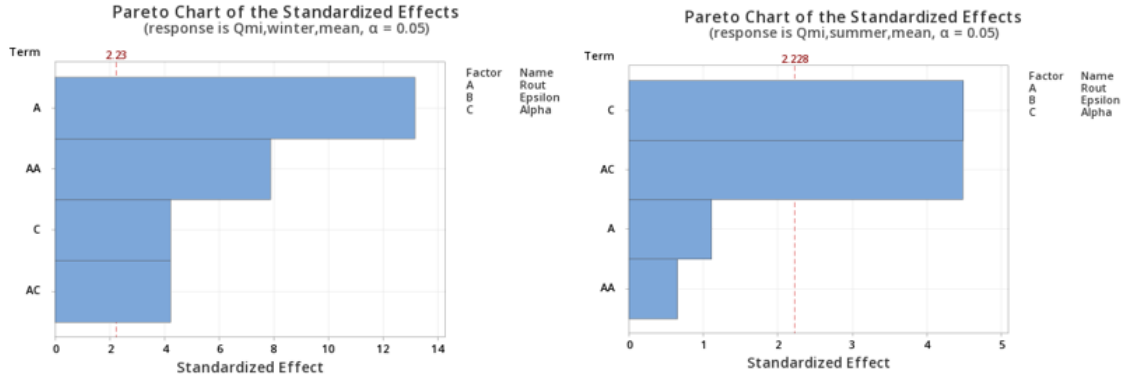

Figure 40. Pareto Chart of the Standardized Effects for response $Q_{mi,winter,mean}$ (left) and $Q_{mi,summer,mean}$ (right) omitting Epsilon.

Pareto Chart of the Effects considering long-wave emissivity

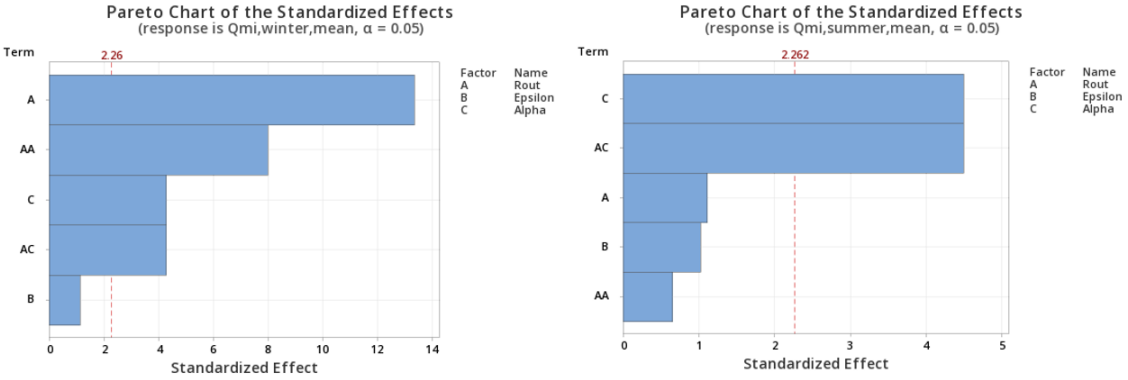

Figure 41. Pareto Chart of the Standardized Effects for response $Q_{mi,winter,mean}$ (left) and $Q_{mi,summer,mean}$ (right) considering Epsilon.

Regression Equation

The regression equations that relate the input parameters with the outputs, for both studied possibilities (*Equations 72-75*):

Regression Equation omitting long-wave emissivity

$$Qmi,winter,mean = -25.23 + 10.315\ Rout + 18.95\ Alpha - 1.031\ Rout*Rout - 4.44\ Rout*Alpha \quad (72)$$

$$Qmi,summer,mean = -10.41 + 2.00\ Rout + 23.95\ Alpha + 0.102\ Rout*Rout - 5.61\ Rout*Alpha \quad (73)$$

Regression Equation considering long-wave emissivity

$$Qmi,winter,mean = -23.61 + 10.315\ Rout - 2.49\ Epsilon + 18.95\ Alpha - 1.031\ Rout*Rout - 4.44\ Rout*Alpha \quad (74)$$

$$Qmi,summer,mean = -8.65 + 2.00\ Rout - 2.71\ Epsilon + 23.95\ Alpha + 0.102\ Rout*Rout - 5.61\ Rout*Alpha \quad (75)$$

As in the CCF method, in order to accept these equations, several things must be checked.

Analysis of Variance (ANOVA)

An analysis of variance has been carried out to determine whether a parameter is statistically significant or not. The p-values have been checked.

Analysis of Variance (ANOVA) omitting long-wave emissivity

The data obtained after the analysis of variance of both responses:

$Q_{mi,summer,mean}$

Analysis of Variance

Source	DF	Adj SS	Adj MS	F-Value	P-Value
Model	4	146.935	36.7339	10.44	0.001
Linear	2	74.985	37.4924	10.66	0.003
Rout	1	4.343	4.3434	1.23	0.293
Alpha	1	70.641	70.6414	20.08	0.001
Square	1	1.506	1.5062	0.43	0.528
Rout*Rout	1	1.506	1.5062	0.43	0.528
2-Way Interaction	1	70.444	70.4445	20.02	0.001
Rout*Alpha	1	70.444	70.4445	20.02	0.001
Error	10	35.181	3.5181		
Lack-of-Fit	8	35.181	4.3976	*	*
Pure Error	2	0.000	0.0000		
Total	14	182.117			

$Q_{mi,winter,mean}$

Analysis of Variance

Source	DF	Adj SS	Adj MS	F-Value	P-Value
Model	4	670.336	167.584	67.67	0.000
Linear	2	472.553	236.277	95.41	0.000
Rout	1	428.374	428.374	172.98	0.000
Alpha	1	44.179	44.179	17.84	0.002
Square	1	153.648	153.648	62.04	0.000
Rout*Rout	1	153.648	153.648	62.04	0.000
2-Way Interaction	1	44.135	44.135	17.82	0.002
Rout*Alpha	1	44.135	44.135	17.82	0.002
Error	10	24.765	2.476		
Lack-of-Fit	8	24.765	3.096	4.59080E+19	0.000
Pure Error	2	0.000	0.000		
Total	14	695.101			

Figure 42. Analysis of Variance for the response $Q_{mi,summer,mean}$ (left) and $Q_{mi,winter,mean}$ (right), omitting long-wave emissivity.

In the winter response, the p-value of the two inputs (Rout and Alpha) is lower than the significance level 0.05, and so it is the p-value of all their combinations. However, in the summer response, Rout seems to be not significant, neither Rout^2. This supports the results in the Pareto Charts.

Analysis of Variance (ANOVA) considering long-wave emissivity

$Q_{mi,summer,mean}$

Analysis of Variance

Source	DF	Adj SS	Adj MS	F-Value	P-Value
Model	5	150.611	30.1221	8.60	0.003
Linear	3	78.660	26.2200	7.49	0.008
Rout	1	4.343	4.3434	1.24	0.294
Epsilon	1	3.675	3.6753	1.05	0.332
Alpha	1	70.641	70.6414	20.18	0.002
Square	1	1.506	1.5062	0.43	0.528
Rout*Rout	1	1.506	1.5062	0.43	0.528
2-Way Interaction	1	70.444	70.4445	20.12	0.002
Rout*Alpha	1	70.444	70.4445	20.12	0.002
Error	9	31.506	3.5007		
Lack-of-Fit	7	31.506	4.5008	*	*
Pure Error	2	0.000	0.0000		
Total	14	182.117			

$Q_{mi,winter,mean}$

Analysis of Variance

Source	DF	Adj SS	Adj MS	F-Value	P-Value
Model	5	673.431	134.686	55.94	0.000
Linear	3	475.648	158.549	65.85	0.000
Rout	1	428.374	428.374	177.91	0.000
Epsilon	1	3.095	3.095	1.29	0.286
Alpha	1	44.179	44.179	18.35	0.002
Square	1	153.648	153.648	63.81	0.000
Rout*Rout	1	153.648	153.648	63.81	0.000
2-Way Interaction	1	44.135	44.135	18.33	0.002
Rout*Alpha	1	44.135	44.135	18.33	0.002
Error	9	21.670	2.408		
Lack-of-Fit	7	21.670	3.096	4.59100E+19	0.000
Pure Error	2	0.000	0.000		
Total	14	695.101			

Figure 43. Analysis of Variance for the response $Q_{mi,summer,mean}$ (left) and $Q_{mi,winter,mean}$ (right), considering long-wave emissivity.

In the winter response, Epsilon is the only variable with a p-value lower than 0.05. In the case of the winter response, Rout, Epsilon and Rout^2 seem to have no statistical significance.

Some more things need to be checked to accept the regression equations:

R^2

Looking at the goodness-of-fit statistics in the Model Summary it is possible to see how well the model fits the data.

Omitting long-wave emissivity

$Q_{mi,summer,mean}$

S	R-sq	R-sq(adj)	R-sq(pred)
1.87566	80.68%	72.95%	25.94%

$Q_{mi,winter,mean}$

S	R-sq	R-sq(adj)	R-sq(pred)
1.57369	96.44%	95.01%	87.13%

Figure 44. Model Summary for the response $Q_{mi,summer,mean}$ (left) and $Q_{mi,winter,mean}$ (right), omitting Epsilon.

Considering long-wave emissivity

$Q_{mi,summer,mean}$

S	R-sq	R-sq(adj)	R-sq(pred)
1.87100	82.70%	73.09%	21.21%

$Q_{mi,winter,mean}$

S	R-sq	R-sq(adj)	R-sq(pred)
1.55171	96.88%	95.15%	86.33%

Figure 45. Model Summary for the response $Q_{mi,summer,mean}$ (left) and $Q_{mi,winter,mean}$ (right), considering Epsilon.

In both cases (with and without omitting Epsilon from the analysis), the model fits better the data in the winter response, as high values of R^2 are obtained, approximately of a 97%. Even though the R^2 values obtained for the summer response are not that big, they are not a reason to discard the method. Residual Plots are checked to valorate how well the equations fit the model.

Residual Plots

Residual plots have been used to determine whether the model meets the assumptions of the analysis. The following information has been obtained from the graphs below:

Residual Plots omitting long-wave emissivity

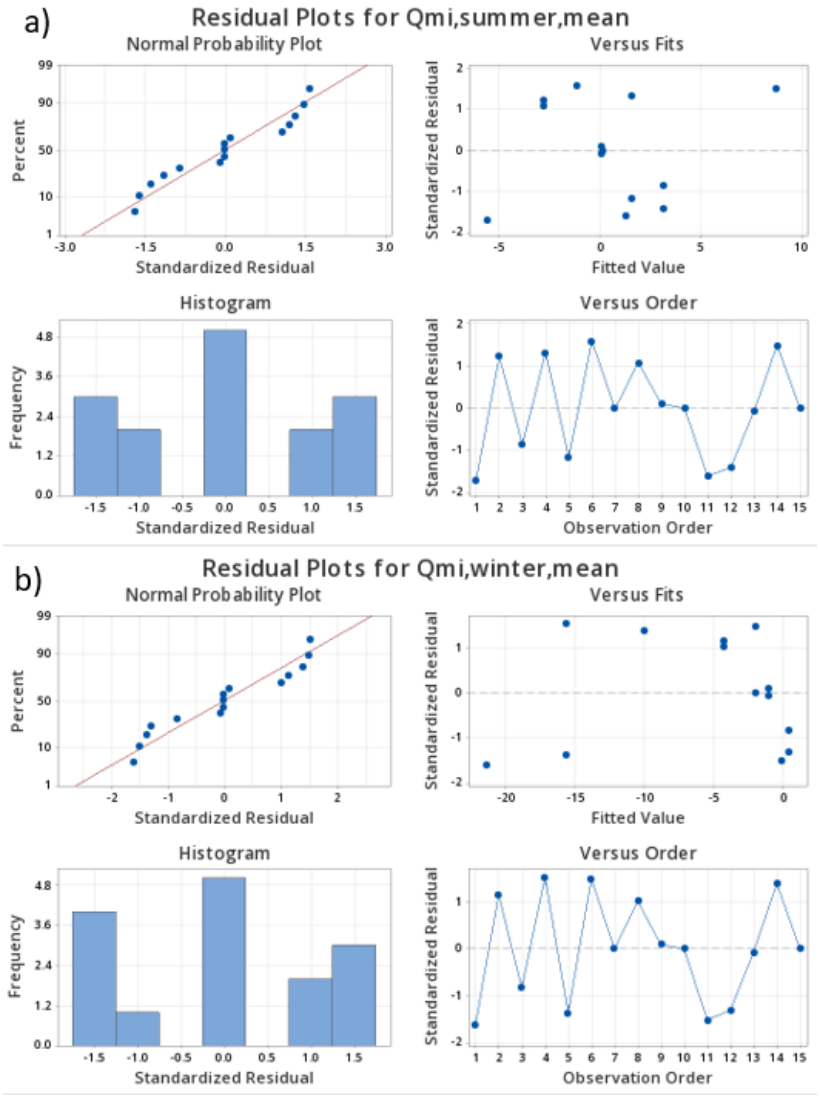

Figure 46. Residual Plots for response $Q_{mi,summer,mean}$ (a) and $Q_{mi,winter,mean}$ (b), omitting Epsilon.

In the residuals versus fits plots of both responses (graphs in the upper right corners of Figure 46 a and b) points fall randomly on both sides of 0. What is more, no outliers are detected (residuals outside the range +-2). Therefore, the initial assumption that the residuals are randomly distributed and have constant variance has been proved in both responses.

As it happened with the CCF method, the residuals versus order plots of both responses (graphs in the lower right corners of Figure 46 a and b) guarantee that independence between residuals exist, as points are randomly distributed with no outliers.

What is more, the normal probability plots of the residuals (graphs in the upper left corners of Figure 46 a and b) verify the assumption that the residuals are normally distributed, as the dots follow the red line quite accurately in both responses.

Residual Plots considering long-wave emissivity

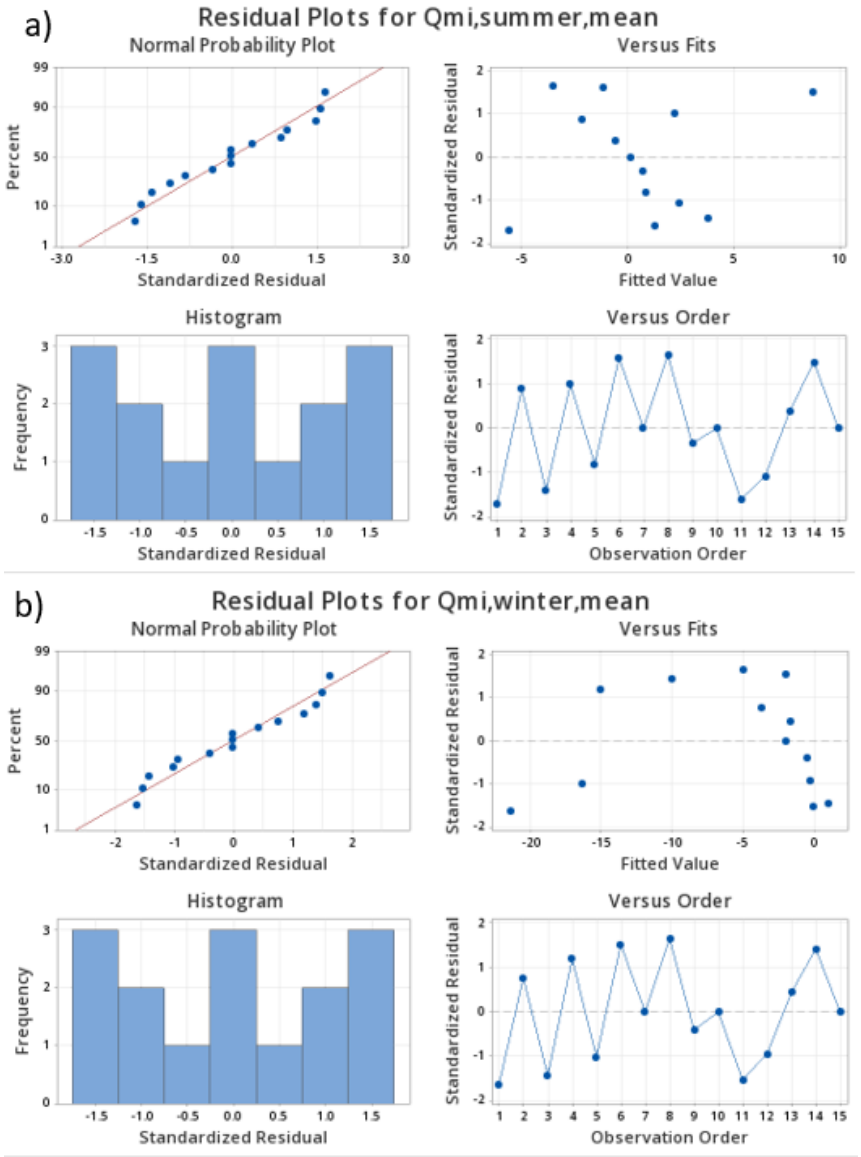

Figure 47. Residual Plots for response $Q_{mi,summer,mean}$ (a) and $Q_{mi,winter,mean}$ (b), considering Epsilon.

When Epsilon is considered in the analysis (see Figure 47), the same criteria as when analysing Figure 46 is used to visually confirm the initial assumptions of residuals being randomly distributed, with constant variance, independent and normally distributed.

Response Optimization

To reach energy efficiency, the same steps as in the CCF method have been followed.

In the factorial plots, the interaction of the variables can be graphically analysed:

Factorial Plots omitting long-wave emissivity

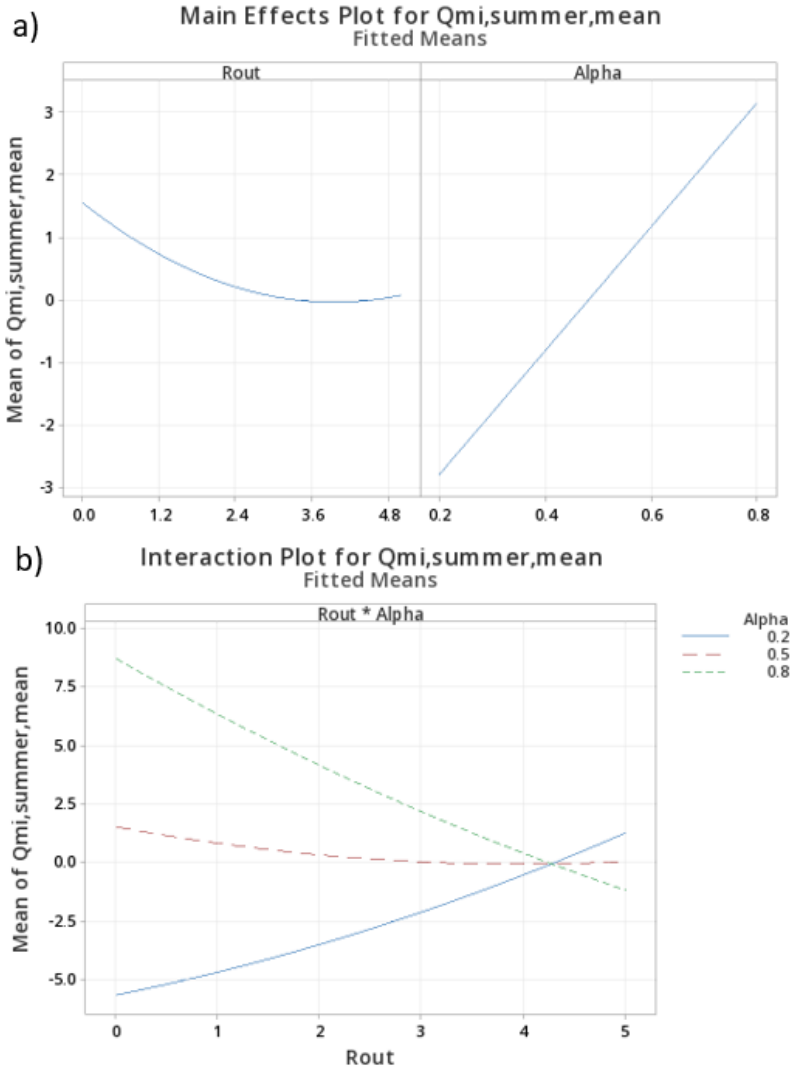

Figure 48. Factorial Plots for $Q_{mi,summer,mean}$ response. Main Effects Plot (a) and Interaction Plot (b), omitting Epsilon.

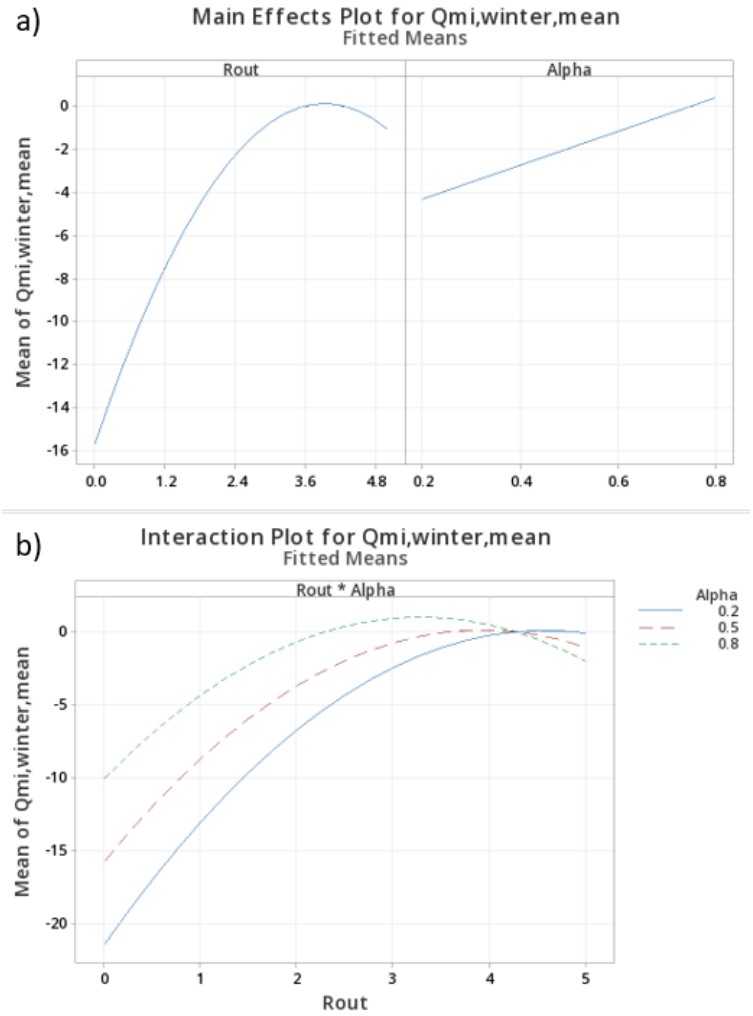

Figure 49. Factorial Plots for $Q_{mi,winter,mean}$ response. Main Effects Plot (a) and Interaction Plot (b), omitting Epsilon.

Whereas Alpha (see Figure 48 and Figure 49) follows the same shape for both responses (what makes it difficult to predict the optimal value for the combined optimization, as contrary effects are desired), Rout seems to reach the optimal value around 3.6 m^2·K/W, being the point in which $Q_{mi,summer,mean}$ gets minimized and $Q_{mi,winter,mean}$ maximized. The shape that the curve of Rout presents in Figure 48 a and Figure 49 a is due to the fact that in the interaction of Rout with Alpha (for the summer response, Figure 48 b) Rout is desired to get high values when the absorptivity is high, and low values for low Alpha values (in order to minimize Q_{mi} during summer months).

Factorial Plots considering long-wave emissivity

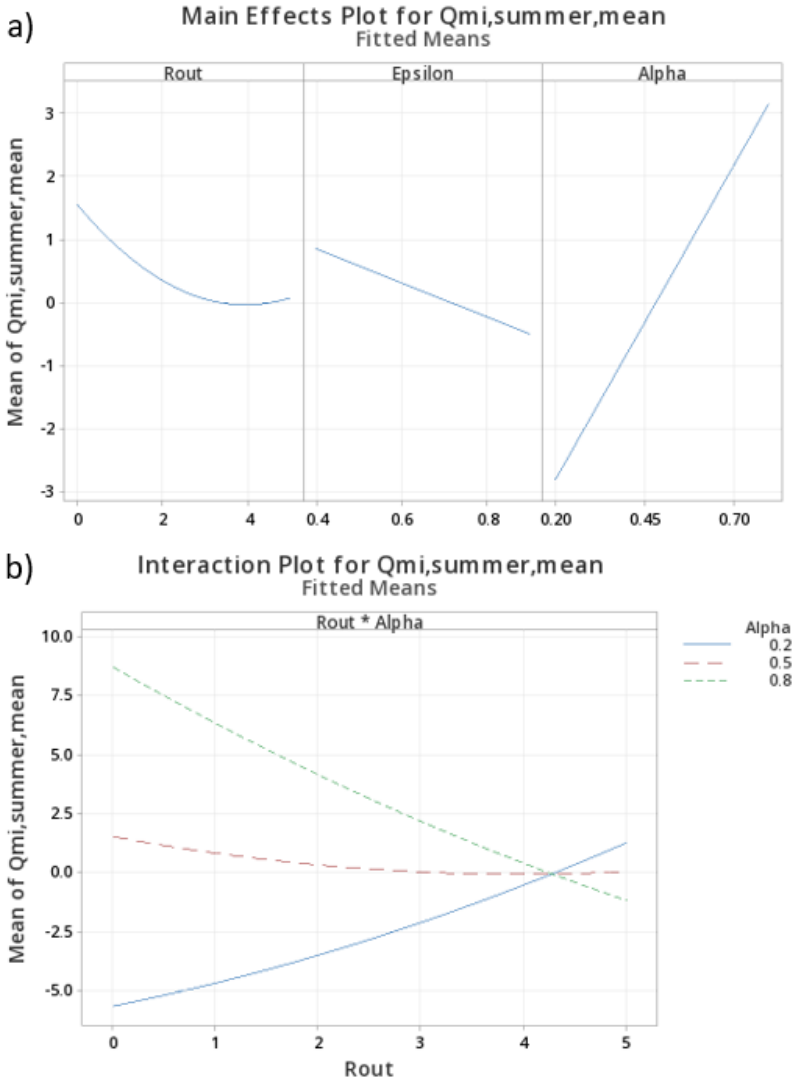

Figure 50. Factorial Plots for $Q_{mi,summer,mean}$ response. Main Effects Plot (a) and Interaction Plot (b), considering Epsilon.

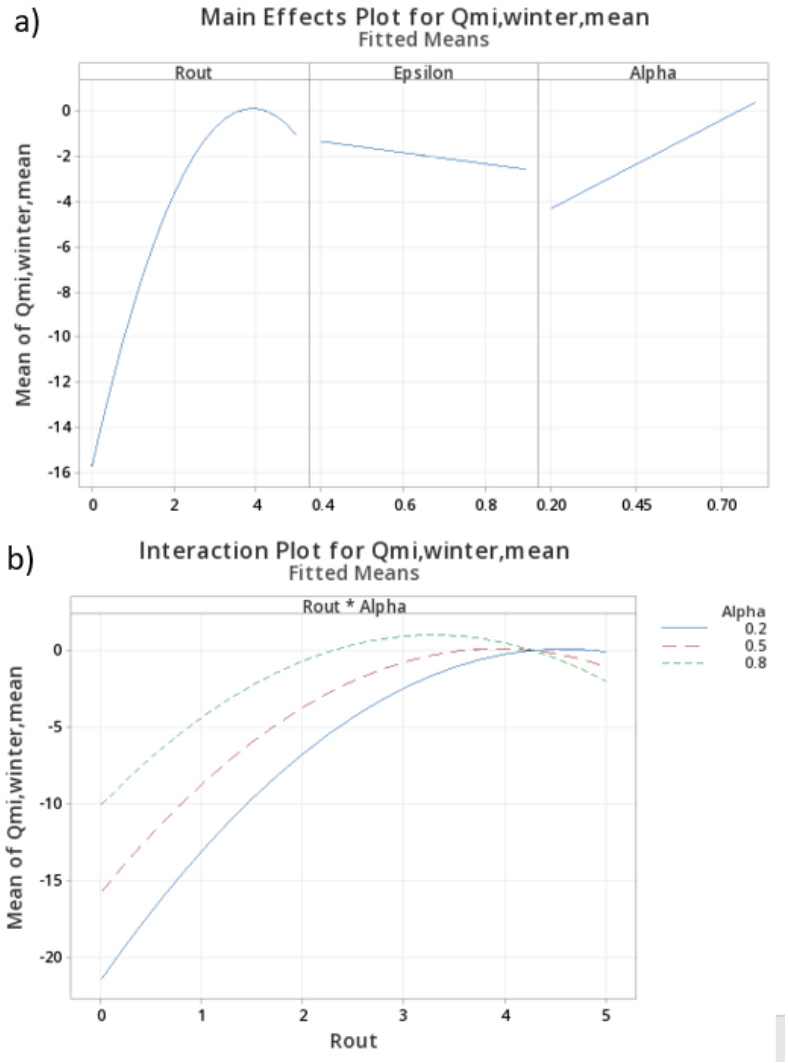

Figure 51. Factorial Plots for $Q_{mi,winter,mean}$ response. Main Effects Plot (a) and Interaction Plot (b), considering Epsilon.

Rout and Alpha (see Figure 50 and Figure 51) follow the same pattern as in the case when Epsilon was being omitted. The only novelty that this graphics bring is how does Q_{mi} vary with Epsilon. The slope of Epsilon in both responses is small compared to the other input's slopes. Therefore, once more, it is affirmed that Epsilon makes little change in the response Q_{mi}. Even if in small measure, high values of Epsilon contribute to lower values of Q_{mi}, what makes sense, as high emissivity is a property of reflective materials which will reject the radiation coming from the Sun (so less heat flux entering the building).

Combined Optimization omitting long-wave emissivity

The results given by Minitab when Epsilon is omitted and a unique configuration that reaches both objectives (maximizing Q_{mi} during winter and minimizing it during summer) is desired (Figure 52 and Figure 53):

Parameters

Response	Goal	Lower	Target	Upper	Weight	Importance
Qmi,summer,mean	Minimum		-7.56024	10.4235	1	1
Qmi,winter,mean	Maximum	-22.8970	-0.57448		1	1

Solution

Solution	Rout	Alpha	Qmi,summer,mean Fit	Qmi,winter,mean Fit	Composite Desirability
1	3.24553	0.2	-1.70322	-1.69644	0.800265

Multiple Response Prediction

Variable	Setting
Rout	3.24553
Alpha	0.2

Response	Fit	SE Fit	95% CI	95% PI
Qmi,summer,mean	-1.703	0.989	(-3.906, 0.500)	(-6.427, 3.021)
Qmi,winter,mean	-1.696	0.829	(-3.545, 0.152)	(-5.660, 2.267)

Figure 52. Combined Response Optimization omitting Epsilon.

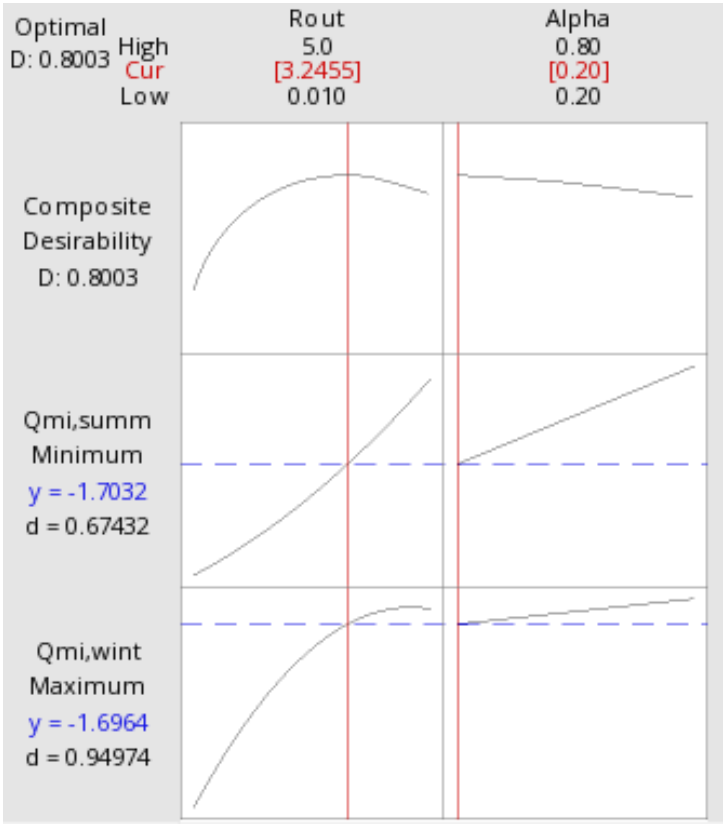

Figure 53. Optimal configuration of parameters for the Combined Optimization omitting Epsilon.

No comparison between what *Minitab* predicts and what *Matlab* gives for the optimal combination of parameters (Table 7) can be done, as no Epsilon has been proposed (not enough input data to introduce in *Matlab*).

Optimal Combination of Parameters	
Rout [m^2·K/W]	3.24553
Alpha	0.2

Table 7. Optimal Combination of parameters for the combined optimization, omitting Epsilon.

Combined Optimization considering long-wave emissivity

The same procedure as in the combined optimization not considering Epsilon has been followed (Figure 54 and Figure 55):

Parameters

Response	Goal	Lower	Target	Upper	Weight	Importance
Qmi,summer,mean	Minimum		-7.56024	10.4235	1	1
Qmi,winter,mean	Maximum	-22.8970	-0.57448		1	1

Solution

Solution	Rout	Epsilon	Alpha	Qmi,summer,mean Fit	Qmi,winter,mean Fit	Composite Desirability
1	3.33667	0.9	0.2	-2.24002	-2.07743	0.810404

Multiple Response Prediction

Variable	Setting
Rout	3.33667
Epsilon	0.9
Alpha	0.2

Response	Fit	SE Fit	95% CI	95% PI
Qmi,summer,mean	-2.24	1.19	(-4.94, 0.46)	(-7.26, 2.78)
Qmi,winter,mean	-2.077	0.989	(-4.314, 0.159)	(-6.240, 2.085)

Figure 54. Combined Response Optimization considering Epsilon.

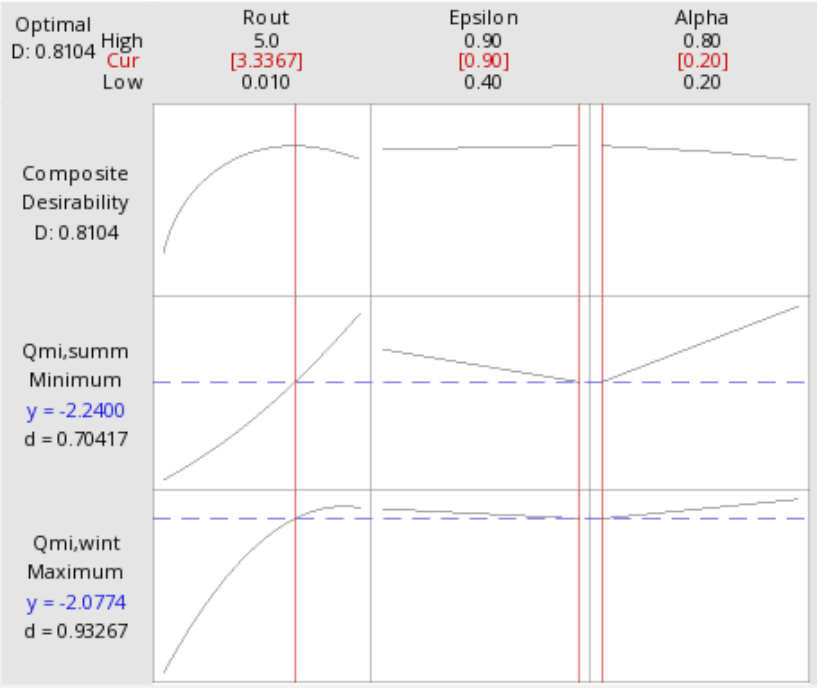

Figure 55. Optimal configuration of parameters for the Combined Optimization considering Epsilon.

If the optimal configuration given by *Minitab* (*Table 8*) is introduced in *Matlab*, the mean Q_{mi} values for summer and winter can be obtained and compared to what *Minitab* predicted (*Table 9)*:

Optimal Combination of Parameters	
Rout [m^2·K/W]	3.33667
Epsilon	0.9
Alpha	0.2

Table 8. Optimal Combination of parameters for the combined optimization, considering Epsilon

	MATLAB	MINITAB	Difference
$Q_{mi,summer,mean}$ [W/m^2]	-0.83401	-2.24002	1.40601
$Q_{mi,winter,mean}$ [W/m^2]	-2.26690	-2.07743	0.18947

Table 9. Minitab´s response predictions vs Matlab's responses for the optimal combination of parameters considering Epsilon.

The same way as it has been done with the CCF method, the results given for the combined optimization in the Box-Behnken Design (*Table 8*) will be analysed. It can be concluded that the given Rout allows reaching both objectives: minimizing the heat flux entering the building during summer and minimizing the flux going out from the interior during winter. The resulting Epsilon (0.9) is more appropriate for summer months, and the given value for Alpha (0.2, low absorptivity) contributes positively to the goal of minimizing the heat flux during summer.

The values given by *Minitab* are in concordance with the significancy that each parameter has in the different responses. In this method, the values of Q_{mi} given by *Minitab* are really close to the ones obtained from the physical model, even more than in the previous method, especially for winter months.

Maximizing $\boldsymbol{Q_{mi}}$ during winter

If the individual optimization is performed, just considering that Q_{mi} is desired to be maximized during winter months, these are the results observed in both studied cases:

Maximizing $\boldsymbol{Q_{mi}}$ during winter omitting long-wave emissivity

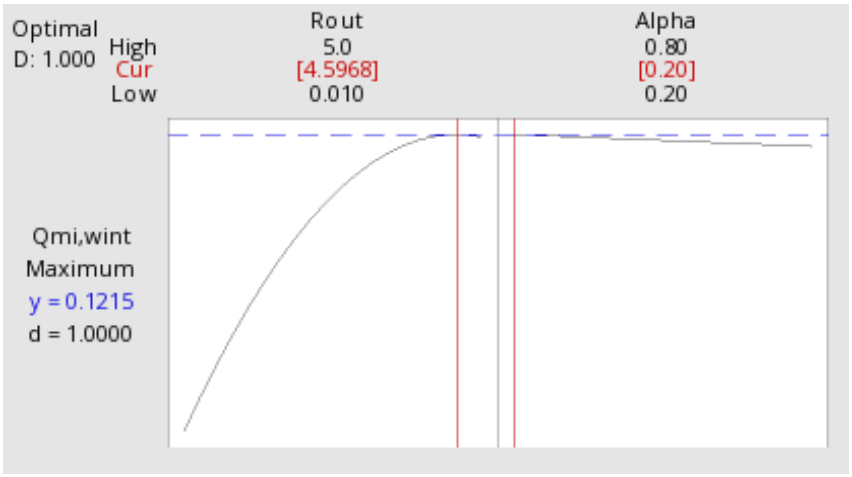

Figure 56. Optimal configuration of parameters for the winter optimization omitting Epsilon.

Maximizing $\boldsymbol{Q_{mi}}$ during winter considering long-wave emissivity

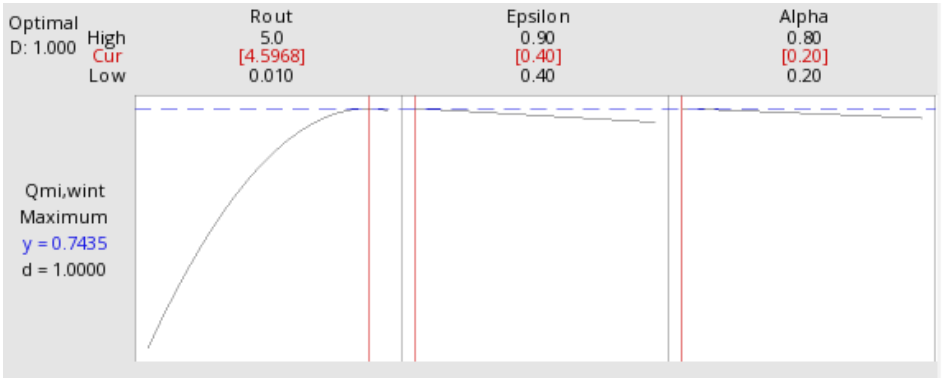

Figure 57. Optimal configuration of parameters for the winter optimization considering Epsilon.

Results show (Figure 56 and Figure 57) that if just winter months could be optimized, an insulation with a high thermal resistance would be preferable. Additionally, the coating would present low absorptivity and emissivity, being the slopes of these two variables almost flat, what means they are insignificant in the response.

Minimizing Q_{mi} during summer

Individual optimizations have been performed, considering Q_{mi} is desired to be minimized during summer months:

Minimizing Q_{mi} during summer (omitting long-wave emissivity)

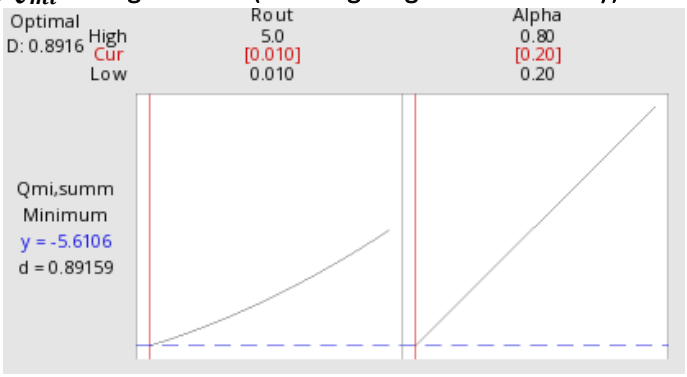

Figure 58. Optimal configuration of parameters for the summer optimization omitting Epsilon.

Minimizing Q_{mi} during summer (considering long-wave emissivity)

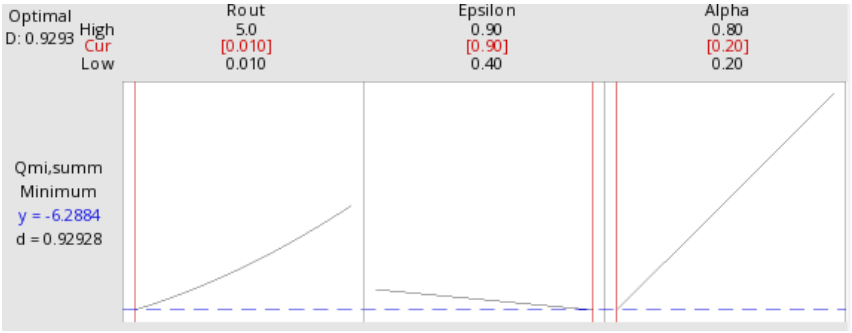

Figure 59. Optimal configuration of parameters for the summer optimization considering Epsilon.

If just summer months could be optimized (Figure 58 and Figure 59), an insulation with a low thermal resistance (no insulation if possible) would be preferable. Additionally, the coating would present low absorptivity, not to store heat coming from the Sun, and high emissivity.

Figure 60 shows in grey the values that the response Q_{mi} would take with the insulation coating obtained in the combined optimization. Above it, the response obtained during summer (in red) and the one obtained during winter (in blue) are presented, for the values of the individual optimizations. It can be seen how during summer months the red lines are somehow below the grey ones, whereas during winter months just the opposite occurs. However, this is just a theoretical configuration, because as said before, in real life the insulation and coating characteristics do not vary during winter and summer, so just the grey values would be obtained (as they are achieved with the combined optimization). It is important to remark that the values obtained in the optimization are just a compromise solution when reaching two opposing objectives as it is to maximize Q_{mi} during winter months and minimize it during summer months.

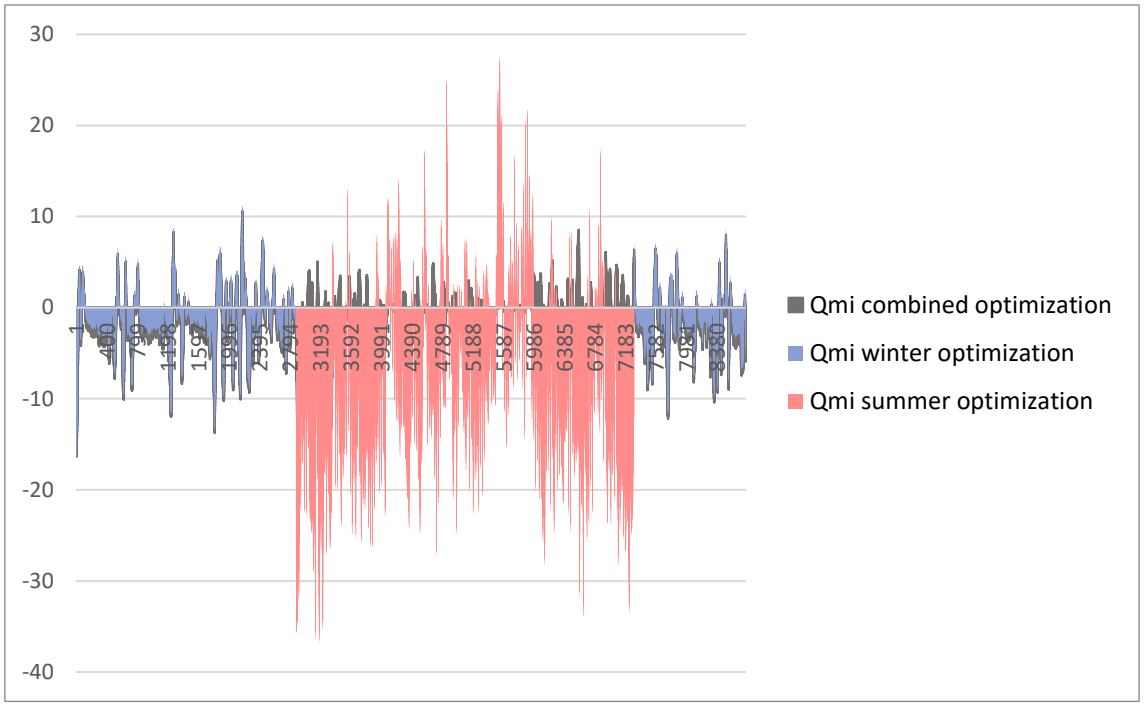

Figure 60. Q_{mi} $\left[\frac{W}{m2}\right]$ in the combined optimizations vs Q_{mi} $\left[\frac{W}{m2}\right]$ in the summer and winter optimizations.

3.2.3. Conclusions

After carrying out the parametric analysis of the dynamic RC model based on different DoE methods, the Box-Behnken Design (BBD) has been selected as the most appropriate one. The Faced-Centred Central Composite design (CCF) is also a possible alternative (in contrast to the Fractional Factorial ½, which does not estimate curvature, and is needed in this model) but it has been discarded as the BBD has been proved to be more accurate. The results obtained with both methods (for the case in which Epsilon is considered) show that the responses in *Matlab* and the predictions in *Minitab* are closer in the Box-Behnken method (see *Table 10*):

	Optimal Combination of Parameters			Difference between *Minitab's* prediction and *Matlab's* real response	
	Rout [m^2·K/W]	Epsilon	Alpha	$Q_{mi,summer,mean}$ [W/m^2]	$Q_{mi,winter,mean}$ [W/m^2]
CCF	3.4879	0.9	0.2	2.2046	0.3131
Box-Behnken	3.3366	0.9	0.2	1.40601	0.18947

Table 10. Differences between the CCF method and Box-Behnken Design.

The following sections (*Section 3.3* and 3.4) will therefore directly use the Box-Behnken method when doing the parametric analysis.

3.3. Response 2: $Q_{col,heating}$ and $Q_{col,cooling}$

It has been said there are two variables in this project that represent the energy efficiency of the building: Q_{mi} and Q_{col}. When analysing the respond Q_{mi}, two output variables

have been selected ($Q_{mi,summer.mean}$ and $Q_{mi,winter.mean}$). The same has been done with the variable Q_{col}.

Q_{col} (Solar collection at the external surface of the wall) ($Q_{col} = Q_{Cme} + Q_m$ (*2*)) [W/m^2] is the variable which has been obtained from the model constructed in *Matlab* in *Section 2.* As it has been said, this variable responds immediately to external changes. Therefore, it is a key parameter for controlling the heat demand. Note that Q_{col} is equal to Q_{me} in Figure 17. It represents the whole heat flow that is captured by the exterior surface of the wall. Some of this heat gets to the interior of the building (Q_{mi}) whereas another part is stored in the wall ($Q_{Cmi}\ and\ Q_{Cme}$).

The solar collection at the external surface has been calculated with *Matlab* for each time step (each hour). To be able to optimize the process, this Q_{col} vector has been divided into two vectors: $Q_{col,heating}$ and $Q_{col,cooling}$ which include the Q_{col} values of the time steps in which heating demand or cooling demand is foreseen, respectively. To make these demand predictions, the external temperature had to be estimated ($T_{e,pred}$). This has been done by a moving average (centred on 24 hours) of the external temperatures (T_e), which was an input data taken from the climatic file of Bilbao.

Therefore, each time step will have a predicted temperature which can be contrasted with HDD and CDD (reference external temperatures for heating and cooling demand, respectively). HDD has a value of 15 °C and CDD a value of 20 °C. If $T_{e,pred}$ is lower than HDD heating demand is foreseen while if it is greater than CDD cooling demand is foreseen. For temperature predictions between 15°C and 20°C, no demand is foreseen.

The following two output parameters have been selected for doing the Design of Experiments:

- $Q_{col,heating,mean}$ (Mean value of $Q_{col,heating}$) [W/m^2].
- $Q_{col,cooling,mean}$ (Mean value of $Q_{col,cooling}$) [W/m^2].

The input variables have been the same as when analysing the Q_{mi} responses (Rout, Alpha and Epsilon).

Once the input and output variables have been chosen, the next step is to apply the Design of Experiment technique in *Minitab* to perform parametric analysis and optimization. Box-Behnken has been selected as the method which best fits the model, so the same procedure followed when analysing Q_{mi} responses is followed:

3.3.1. Box-Behnken Design (BBD)

The first step has been to create the Box-Behnken design (Stat>DoE>Response Surface>Create Response Surface Design>Box Behnken with three continuous factors).

The same fifteen experiments given by Minitab for the Q_{mi} responses have been used, in which the centre point (Rout=2.505 m^2·K/W, Epsilon=0.65 and Alpha=0.5) is twice repeated.

The proposed experiments have been introduced in *Matlab*, giving the following responses (last two columns in Figure 61):

	C1	C2	C3	C4	C5	C6	C7	C8	C9
	StdOrder	RunOrder	PtType	Blocks	Rout	Epsilon	Alpha	Qcol,cooling,mean	Qcol,heating,mean
1	5	1	2	1	0.010	0.65	0.2	0.2915	-24.5166
2	9	2	2	1	2.505	0.40	0.2	0.0837	-2.9118
3	11	3	2	1	2.505	0.40	0.8	2.7932	-0.9029
4	1	4	2	1	0.010	0.40	0.5	11.7127	-15.3060
5	3	5	2	1	0.010	0.90	0.5	8.1233	-19.3407
6	8	6	2	1	5.000	0.65	0.8	1.1986	-0.6710
7	13	7	0	1	2.505	0.65	0.5	1.1176	-2.1232
8	10	8	2	1	2.505	0.90	0.2	-0.1590	-3.0929
9	2	9	2	1	5.000	0.40	0.5	0.7775	-1.0115
10	14	10	0	1	2.505	0.65	0.5	1.1176	-2.1232
11	6	11	2	1	5.000	0.65	0.2	-0.0323	-1.6069
12	12	12	2	1	2.505	0.90	0.8	1.8606	-1.5302
13	4	13	2	1	5.000	0.90	0.5	0.4589	-1.2230
14	7	14	2	1	0.010	0.65	0.8	19.0612	-10.5660
15	15	15	0	1	2.505	0.65	0.5	1.1176	-2.1232

Figure 61. The 15 experiments proposed by Minitab for the Box-Behnken Design method for the Q_{col} response, in columns C5-C7 the values of the input parameters provided by the design and in columns C8 and C9 the values of the outputs obtained from the model implemented in Matlab.

Once the table is completed, the Response Surface Analysis can be done.

Response Surface Regression

The same procedure followed when analysing the response Q_{mi} will be followed.

Pareto Chart of the Effects

Figure 62 shows the Pareto Charts of both responses.

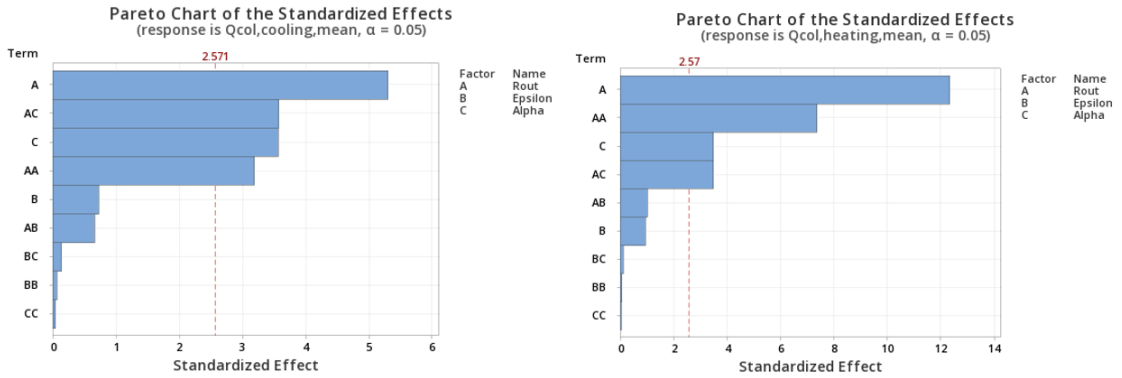

Figure 62. Pareto Chart of the Standardized Effects for response $Q_{col,cooling,mean}$ (left) and $Q_{col,heating,mean}$ (right).

As it happened with Q_{mi}, Epsilon is not statistically significant and can be omitted from the analysis. However, it will be considered to see how it influences the response, even if just in a short extent. Just the interactions CC, BB and BC will be omitted, resulting in the following Pareto Charts (Figure 63):

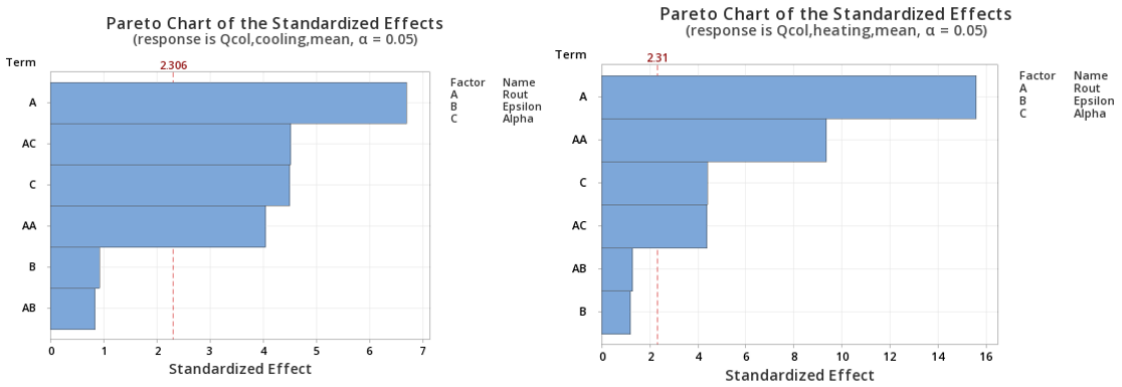

Figure 63. Pareto Chart of the Standardized Effects omitting some terms, for response $Q_{col,cooling,mean}$ (left) and $Q_{col,heating,mean}$ (right).

Regression Equation

The regression equations that relate the input parameters with the outputs are presented below (*Equations (76) and (77)*):

$$Qcol,cooling,mean = 1.15 - 3.04\ Rout - 5.83\ Epsilon + 24.98\ Alpha + 0.653\ Rout*Rout + 1.31\ Rout*Epsilon - 5.86\ Rout*Alpha \quad (76)$$

$$Qcol,heating,mean = -22.67 + 10.21\ Rout - 6.37\ Epsilon + 18.58\ Alpha - 1.151\ Rout*Rout + 1.53\ Rout*Epsilon - 4.347\ Rout*Alpha \quad (77)$$

To accept these equations, several things must be checked.

Analysis of Variance (ANOVA)

An analysis of variance has been carried out to determine whether a parameter is statistically significant or not. The p-value has been checked in Figure 64.

$Q_{col,cooling,mean}$

Analysis of Variance

Source	DF	Adj SS	Adj MS	F-Value	P-Value
Model	6	390.120	65.020	17.19	0.000
Linear	3	248.826	82.942	21.92	0.000
Rout	1	169.152	169.152	44.71	0.000
Epsilon	1	3.230	3.230	0.85	0.383
Alpha	1	76.445	76.445	20.21	0.002
Square	1	61.718	61.718	16.31	0.004
Rout*Rout	1	61.718	61.718	16.31	0.004
2-Way Interaction	2	79.576	39.788	10.52	0.006
Rout*Epsilon	1	2.675	2.675	0.71	0.425
Rout*Alpha	1	76.901	76.901	20.33	0.002
Error	8	30.266	3.783		
Lack-of-Fit	6	30.266	5.044	*	*
Pure Error	2	0.000	0.000		
Total	14	420.386			

$Q_{col,heating,mean}$

Analysis of Variance

Source	DF	Adj SS	Adj MS	F-Value	P-Value
Model	6	815.089	135.848	61.82	0.000
Linear	3	577.437	192.479	87.60	0.000
Rout	1	531.656	531.656	241.95	0.000
Epsilon	1	3.194	3.194	1.45	0.262
Alpha	1	42.588	42.588	19.38	0.002
Square	1	191.652	191.652	87.22	0.000
Rout*Rout	1	191.652	191.652	87.22	0.000
2-Way Interaction	2	46.000	23.000	10.47	0.006
Rout*Epsilon	1	3.654	3.654	1.66	0.233
Rout*Alpha	1	42.346	42.346	19.27	0.002
Error	8	17.579	2.197		
Lack-of-Fit	6	17.579	2.930	*	*
Pure Error	2	0.000	0.000		
Total	14	832.667			

Figure 64. Analysis of Variance for the response $Q_{col,cooling,mean}$ (left) and $Q_{col,heating,mean}$ (right).

The only p-values with a value higher than the significance level 0.05 are the ones of Epsilon and its interaction with Rout (what was expected after the results of the Pareto Charts) in both responses. The rest of the variables are statistically significant.

Some more things need to be checked to accept the regression equations.

R^2

The model fits well the data, as high values of R^2 are obtained (Figure 65).

$Q_{col,cooling,mean}$

S	R-sq	R-sq(adj)	R-sq(pred)
1.94506	92.80%	87.40%	64.67%

$Q_{col,heating,mean}$

S	R-sq	R-sq(adj)	R-sq(pred)
1.48235	97.89%	96.31%	89.63%

Figure 65. Model Summary for the response $Q_{col,cooling,mean}$ (left) and $Q_{col,heating,mean}$ (right).

Residual Plots

The Residual Plots below (Figure 66) show that the model meets the assumptions of the analysis (residuals are randomly distributed, with constant variance, independent and they are normally distributed).

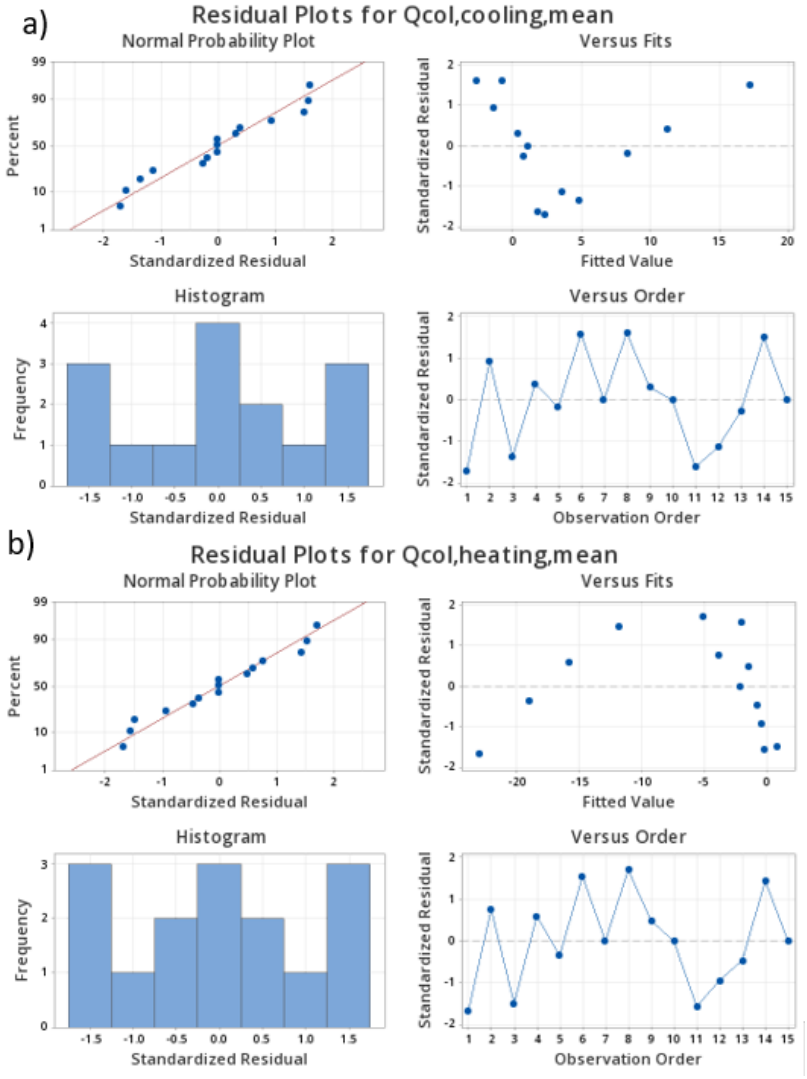

Figure 66. Residual Plots for response $Q_{col,cooling,mean}$ (a) and $Q_{col,heating,mean}$ (b).

Response Optimization

The reason of choosing as responses the solar collection at the external surface when heating demand is foreseen ($Q_{col,heating,mean}$) and cooling demand is foreseen ($Q_{col,cooling,mean}$) is that they can be used to reach energy efficiency in the building.

The objective of the DoE is to reach an estimation of the response of the model so that future predictions can be accurately made that allow optimizing processes.

It has been explained and it can be seen in Figure 17 that Q_{col} is the heat coming from the sun which is collected at the external surface of the building.

To reach energy efficiency, the objective of the project is to find out the combination of the input parameters (Rout, Epsilon and Alpha) that result in the best solution that maximizes the solar collection when heating demand is foreseen and minimizes it when cooling demand is foreseen.

Collecting large amounts of heat when heating is required in the building would lead to a heating reduction. In contrast, the less heat collected when cooling is demanded the better, as would result in a cooling demand reduction inside the building.

Before proceeding with the optimization analysis in *Minitab*, the interaction between the input variables can be graphically observed (Figure 67 and Figure 68).

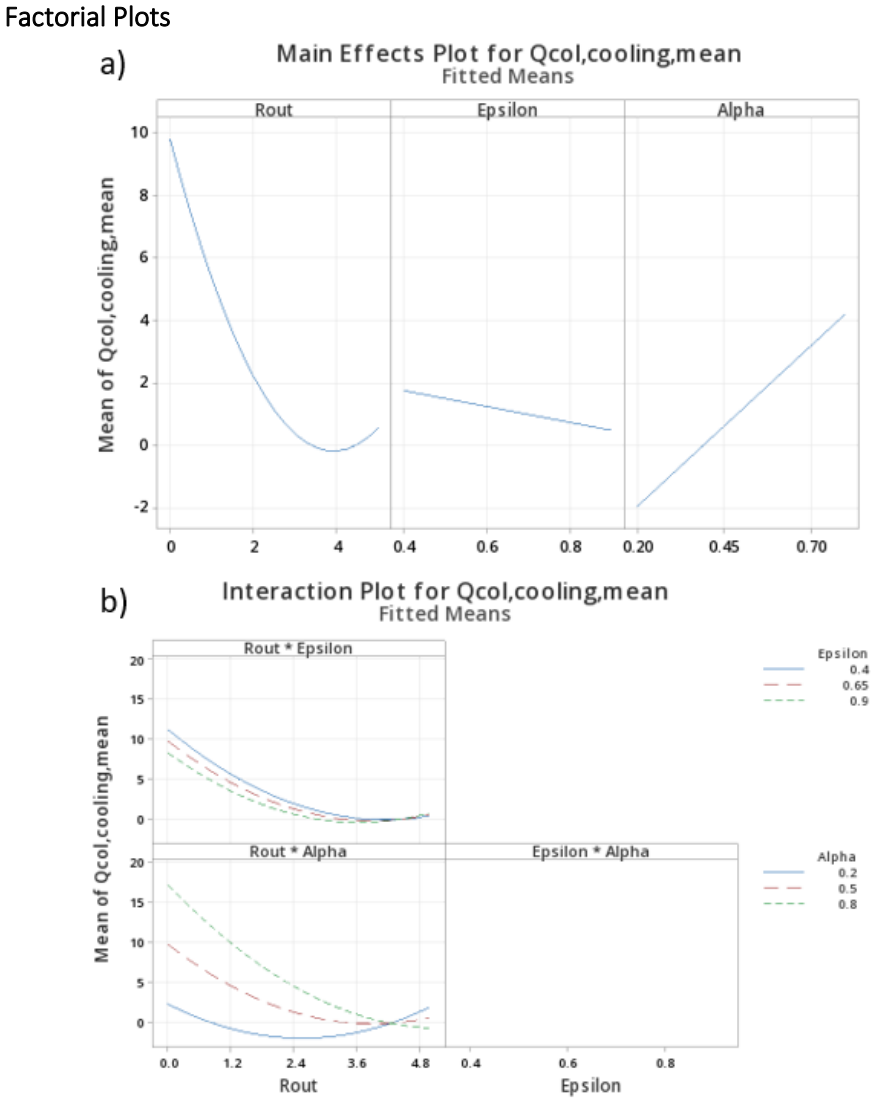

Figure 67. Factorial Plots for $Q_{col,cooling,mean}$ response. Main Effects Plot (a) and Interaction Plot (b).

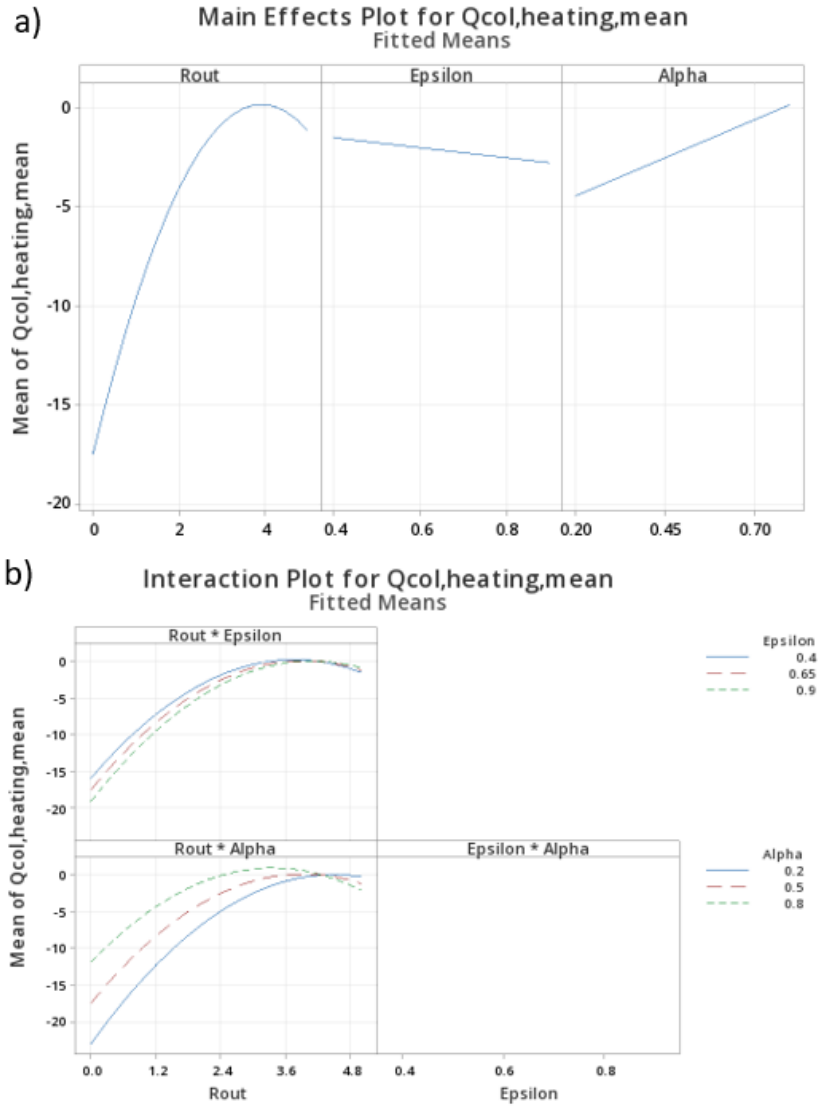

Figure 68. Factorial Plots for $Q_{col,heating,mean}$ response. Main Effects Plot (a) and Interaction Plot (b).

If the factorial plots are compared with the ones obtained for the Q_{mi} response (not omitting Epsilon) (Figure 50 and Figure 51) it is observed that the variables follow the same slopes for the Q_{col} during cooling demand and Q_{mi} during summer, and for Q_{col} during heating demand and Q_{mi} during winter months, respectively.

Combined Optimization

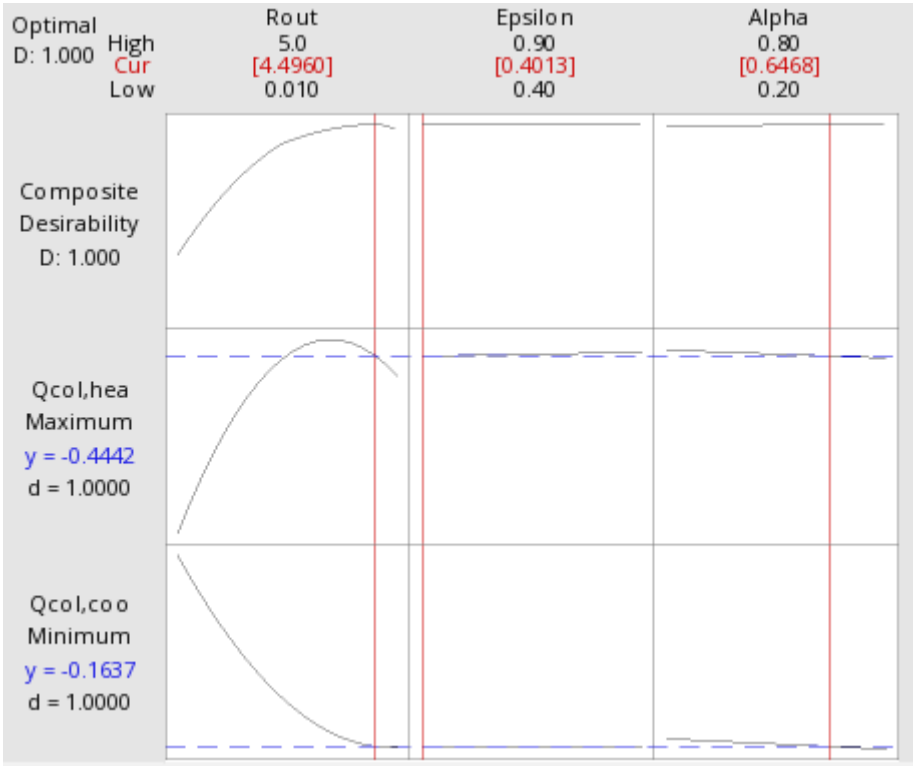

Figure 69. Optimal configuration of parameters for Combined Optimization in the Q_{col} response.

If the optimal configuration given by Minitab is introduced in *Matlab*, the mean Q_{col} values for cooling and heating can be obtained and compared to what *Minitab* predicted:

Optimal Combination of Parameters	
Rout [m²·K/W]	4.4960
Epsilon	0.4013
Alpha	0.6468

Table 11. Optimal Combination of parameters for the combined optimization in the response Q_{col}.

	MATLAB	MINITAB	Difference
$Q_{col,cooling,mean}$ [W/m²]	1.2451	-0.1637	1.4088
$Q_{col,heating,mean}$ [W/m²]	-0.8293	-0.4442	0.3851

Table 12. Minitab´s response predictions vs Matlab's responses for the optimal combination of parameters in the response Q_{col}.

The DoE method used fits good the model, as the difference between the predictions and the real values obtained in *Matlab* are almost the same (Table 12).

The physical meaning of the solutions given for the Q_{col} response in the combined optimizations (Table 11) will be analyzed the same way it has been done previously with Q_{mi}. The given Rout (around 4.5 m^2·K/W, the highest value obtained until now) means a strong insulation is desired to reach both objectives; maximizing the collected heat when heating is foreseen and minimizing the collection when cooling is foreseen. It seems obvious that this combined optimization result prioritizes maximizing heat collections when heating is foreseen to minimizing them when cooling is foreseen, as it has been said previously that a strong insulation would prevent the heat escaping from the interior (so more heat will be collected in the interior). The values of Alpha and Epsilon indicate low emissivity and quite high absorptivity is preferable, what once more, is more favourable for winter months, when higher portions of heat are desired to be collected.

The differences between the obtained responses in the $Q_{col}\ and\ Q_{mi}$ responses are explained and analyzed below in this section (*3.3.2. Conclusions*).

Maximizing $\boldsymbol{Q_{col}}$ when heating demand is foreseen

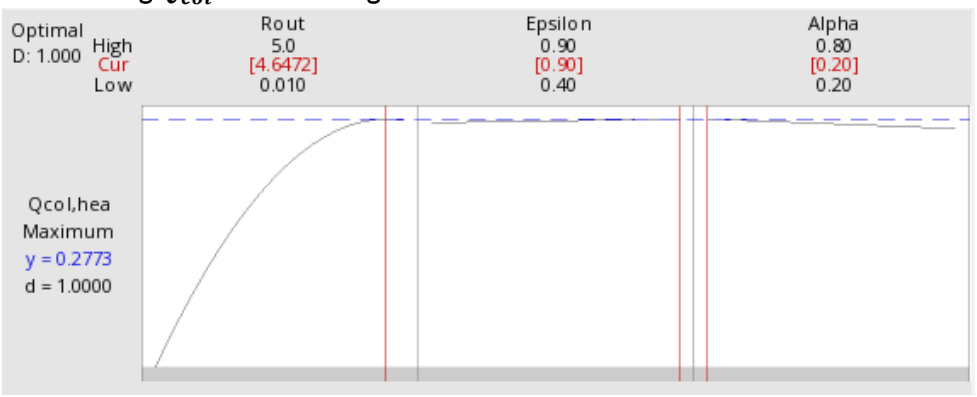

Figure 70. Optimal configuration of parameters for $Q_{col,heating,mean}$.

The high value of Rout, in Figure 70, makes sense with the goal of maximizing heat collections, as strong insulations store more heat in the interior. When it comes to Epsilon and Alpha, the given values are not the ones which are expected. If the heat is desired to be collected, high absorptivity and low emissivity seem to be the most rational solution, what it just the opposite to what is given. However, looking at the slopes of the curves of Epsilon and Alpha in Figure 70 it is observed that these to parameters hardly make any difference in the response (as the curves are almost flat). When it comes to these two variables, the optimization carried out by *Minitab* is insignificant.

Minimizing $\boldsymbol{Q_{col}}$ when cooling demand is foreseen

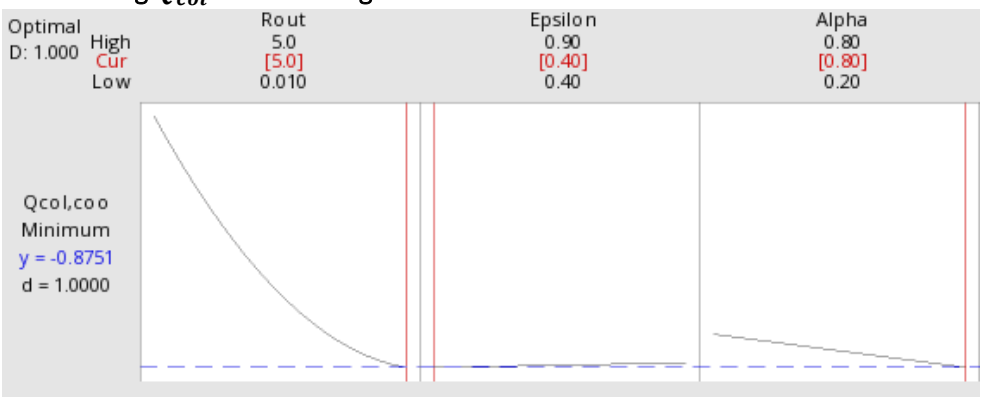

Figure 71. Optimal configuration of parameters for $Q_{col,cooling,mean}$.

The same that occurred when maximizing $Q_{col,heating,mean}$ when heating is foreseen happens when minimizing $Q_{col,cooling,mean}$. High values of Epsilon and low values of Alpha were expected, but the optimization gives just the opposite (see Figure 71). The slopes of these parameters are, as well, almost flat, so the obtained values are insignificant. The given Rout (the maximum allowed value) means that during warm months (when cooling is expected inside the building) a big insulation is preferable, to prevent the heat flux from entering the building (minimizing the collected heat).

3.3.2. Conclusions

The optimal combination of parameters obtained for the analysed two responses (Q_{mi} and Q_{col}) are not the same since they are not representing the same heat fluxes. In this project, thermal comfort is desired to be reached by energy efficiency. It has been said that in the response Q_{col}, part of the heat gets to the interior of the building (Q_{mi}) whereas another part is stored in the wall ($Q_{Cmi}\ and\ Q_{Cme}$), so it is not as direct as it is with Q_{mi} to guarantee that thermal comport is assured with just studying Q_{col}. Therefore, just the response Q_{mi} will be analysed in the remaining façades in *Section 3.4*, as it is the heat flux that gets the interior of the building.

3.4. Changes in the facade

Up to this point, the whole study has been done considering a solid concrete façade. The characteristics of the façade are included in the following three inputs which have been introduced in *Matlab* in *Section 2.*

- R_m: thermal resistance of the wall [$\frac{m^2K}{W}$] (*Equation (78*)) where e is the thickness of the wall [m] and λ is the thermal conductivity [W/mK].

$$R_m = \frac{e}{\lambda}\ [\frac{m^2K}{W}] \qquad (78)$$

- C_{me}: thermal capacitance lumped to the external surface of the wall [$\frac{J}{m^2K}$].

- C_{mi}: thermal capacitance lumped to the internal surface of the wall [$\frac{J}{m^2K}$].

C_{me} and C_{mi} are obtained from *Equations (79*) *and (80*), respectively, where $\{\gamma_e, \gamma_i\}$ are factors that relate those thermal capacitances with the total capacitance (c_p). These factors are not known at first, and they depend not only on the thermal conditions of the model but also on its boundary conditions (obtained from the previously mentioned weather file). For each type of façade studied, a different combination of $\{\gamma_e, \gamma_i\}$ has been selected, always fulfilling $\gamma_e + \gamma_i < 1$.

$$C_{me} = \gamma_e \sum e\rho c_p \qquad (79)$$

$$C_{mi} = \gamma_i \sum e\rho c_p \qquad (80)$$

The values for the specific heat capacity (c_p), density (ρ), thickness of the wall (e) and thermal conductivity (λ) in the equations above are characteristics that depend on the façade selected. A total of three different façades have been studied: the concrete wall, a brick wall with chamber and thermal insulation and a brick wall with chamber and no thermal insulation. These last two façades have nothing to do with the concrete one

studied. Therefore, almost the entire "spectrum" of existing façades is covered with these three façades. The values considered for each specific wall studied have been given by *Tecnalia* and obtained from the software *WUFI Pro* [*41]* (which determines the hygrothermal performance of building components under real climate conditions).

3.4.1. Solid concrete façade

For the solid concrete façade studied until now, the values have been 850 [J/kg·K] for the specific heat capacity, 2300 [kg/m3] for density, 0.2 [m] thickness and 1.6 [W/m·K] for thermal conductivity. The optimal combination of $\{\gamma_e, \gamma_i\}$ in this case is $\{\gamma_e = 0{,}40, \gamma_i = 0{,}60\}$. The specific characteristics of the selected concrete façade are presented in Figure 72:

	e [m]	λ [W/mK]	ρ [kg/m³]	c_p [J/kgK]
Solid Concrete façade	0,2	1,6	2300	850

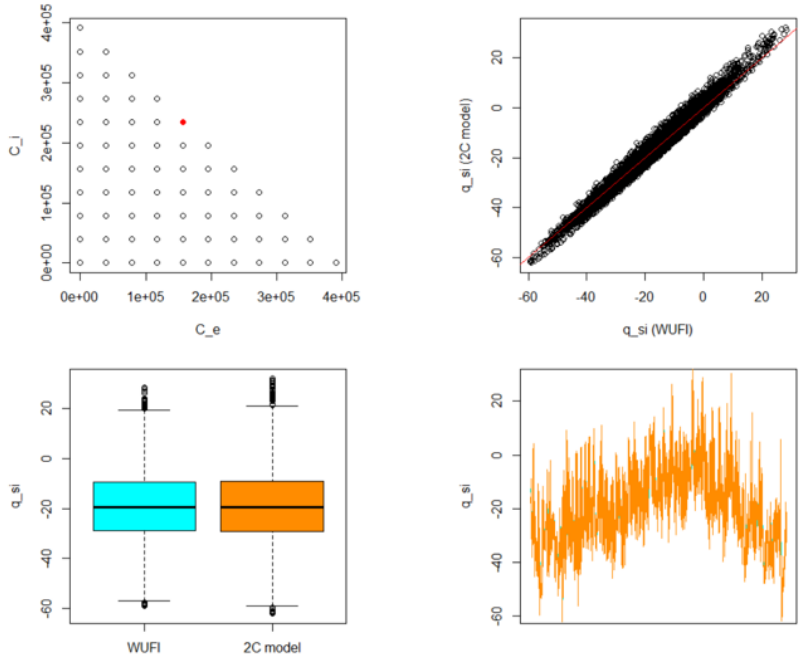

Figure 72. Characteristics of a solid concrete façade for specific climate conditions.

This results in the following inputs in the model implemented in *Matlab (Equations (81), (82) and (83))*.

$$R_m = 0{,}125 \frac{m^2 K}{W} \qquad (81)$$

$$C_{me} = \gamma_e e \rho c_p = 156400 \frac{J}{m^2 K} \qquad (82)$$

$$C_{mi} = \gamma_i e \rho c_p = 234600 \frac{J}{m^2 K} \qquad (83)$$

Response optimizations

The results obtained with the Box-Behnken method, when analysing a solid concrete wall (*Section* 3.2), are summarized below (*Table 13* and *Table 14*).

Optimal Combination of Parameters	
Rout [m^2·K/W]	3.33667
Epsilon	0.9
Alpha	0.2

Table 13. Optimal Combination of parameters in the combined optimization of the solid concrete wall.

	Optimal Combination of Parameters	
	For maximizing Q_{mi} [W/ m2] during winter	For minimizing Q_{mi} [W/ m2] during summer
Rout [m^2·K/W]	4.5968	0.01
Epsilon	0.4	0.9
Alpha	0.2	0.2

Table 14. Optimal combination of parameters in the individual optimizations of the solid concrete wall.

3.4.2. Brick wall with chamber and no thermal insulation

If a new façade is analysed, the above mentioned three inputs must be modified according to the characteristics of the selected façade.

The specific characteristics of the selected brick wall with chamber and no thermal insulation are presented in Figure 72:

	e [m]	λ [W/mK]	ρ [kg/m³]	c_p [J/kgK]
Cement mortar	0,02	1,2	2000	850
Brick	0,115	0,6	1900	850
Air chamber	0,1	0,59	1,3	1000
Brick	0,07	0,6	1900	850
Plaster	0,015	0,2	850	850

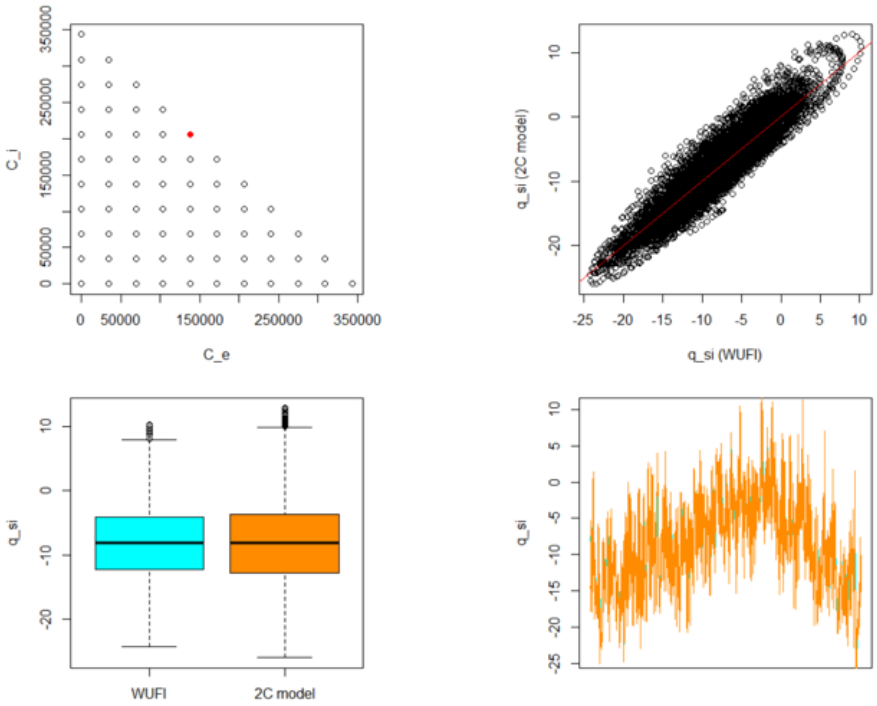

Figure 73. Characteristics of a Brick wall with chamber and no thermal insulation.

With the values from Figure 72 and considering $\{\gamma_e = 0.40,\ \gamma_i = 0.60\}$, the following inputs are introduced in the model implemented in Matlab, *Equations (84), (85) and (86)*.

$$R_m = 0.569 \frac{m^2 K}{W} \qquad (84)$$

$$C_{me} = \gamma_e e \rho c_p = 137500 \frac{J}{m^2 K} \qquad (85)$$

$$C_{mi} = \gamma_i e \rho c_p = 206200 \frac{J}{m^2 K} \qquad (86)$$

Response optimizations

As it has been done with the concrete façade, two situations will be analysed, with a total of three optimizations. The first situation (combined optimization) considers a unique configuration of the outer insulation building coating so that Q_{mi} is maximized during winter months and minimized during winter months. The second situation consists of evaluating both seasons independently, obtaining the optimal configuration in each period (knowing that in real life it is not possible to modify these properties once the envelope has been attached to the wall).

The same steps followed in *Section* 3.2. will be followed, Figure 74:

	C1	C2	C3	C4	C5	C6	C7	C8	C9
	StdOrder	RunOrder	PtType	Blocks	Rout	Epsilon	Alpha	Qmi,winter,...	Qmi,summe...
1	5	1	2	1	0.010	0.65	0.2	-10.2025	-3.37637
2	9	2	2	1	2.505	0.40	0.2	-2.3721	-0.72299
3	11	3	2	1	2.505	0.40	0.8	-0.6109	1.54419
4	1	4	2	1	0.010	0.40	0.5	-6.1666	1.72589
5	3	5	2	1	0.010	0.90	0.5	-7.6882	-0.14237
6	8	6	2	1	5.000	0.65	0.8	-0.5280	0.61816
7	13	7	0	1	2.505	0.65	0.5	-1.6795	0.14913
8	10	8	2	1	2.505	0.90	0.2	-2.5270	-0.92448
9	2	9	2	1	5.000	0.40	0.5	-0.8447	0.23284
10	14	10	0	1	2.505	0.65	0.5	-1.6795	0.14913
11	6	11	2	1	5.000	0.65	0.2	-1.4009	-0.48789
12	12	12	2	1	2.505	0.90	0.8	-1.1613	0.78331
13	4	13	2	1	5.000	0.90	0.5	-1.0427	-0.04304
14	7	14	2	1	0.010	0.65	0.8	-3.8726	4.65821
15	15	15	0	1	2.505	0.65	0.5	-1.6795	0.14913

Figure 74. The 15 experiments proposed by Minitab for the Brick wall with chamber and no thermal insulation, in columns C5-C7 the values of the input parameters provided by the design and in columns C8 and C9 the values of the outputs obtained from the model implemented in Matlab.

For this façade, the Pareto Charts show that the inputs follow the same statistical significance than when the concrete façade was being analysed (Epsilon and some other interactions can be omitted) (see Figure 75). However, as it has been seen in the concrete wall, if Epsilon is not omitted, the optimal results given by Minitab hardly change, so in this case, just the optimization not omitting Epsilon will be performed, in order to get more information. Therefore, the omitted terms from Figure 75 will be CC, BB, BC and AB, resulting on the Pareto Charts in Figure 76, which give the optimal configurations of Figure 76 and Figure 77.

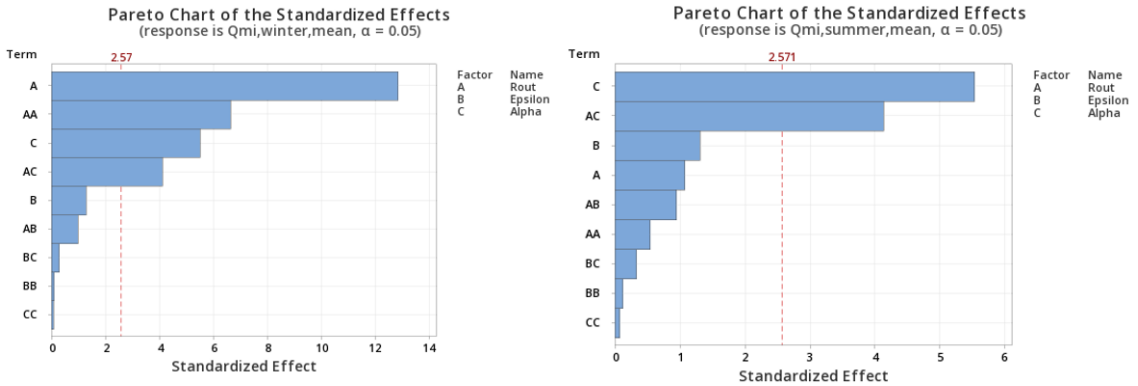

Figure 75. Pareto Chart of the Standardized Effects omitting some terms, for response $Q_{mi,winter,mean}$ (left) and $Q_{mi,summer,mean}$ (right) in the Brick wall with chamber and no thermal insulation.

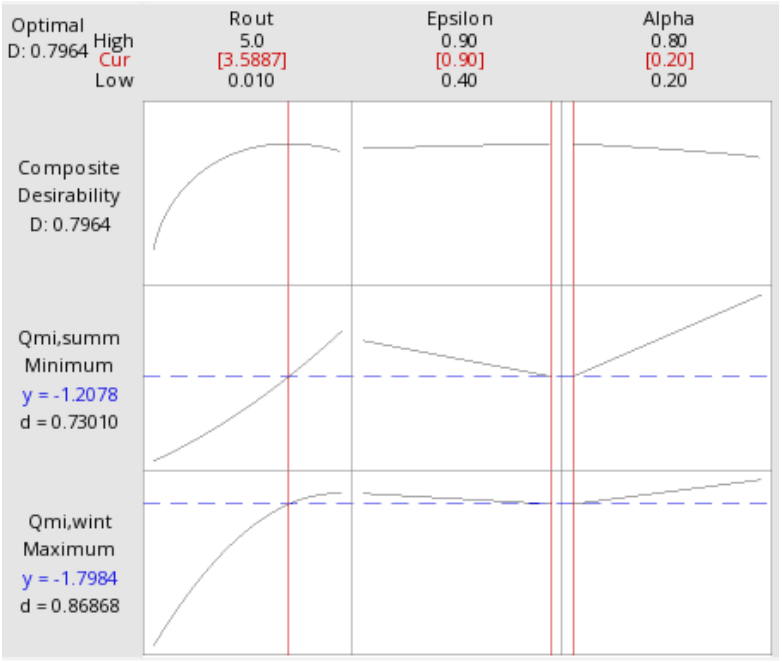

Figure 76. Optimal configuration of parameters for Combined Optimization in the Brick wall with chamber and no thermal insulation.

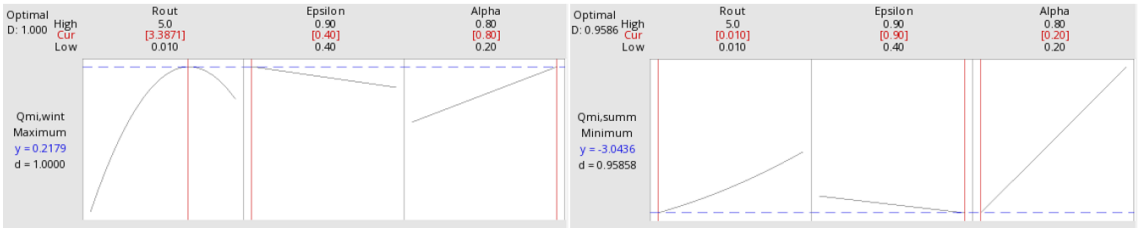

Figure 77. Optimal combination of parameters for maximizing Q_{mi} during winter (left) and minimizing Q_{mi} during summer (right) in the Brick wall with chamber and no thermal insulation.

Summarizing the obtained results, for each performed optimization (see *Table 15* and *Table 16):*

Optimal Combination of Parameters	
Rout $[\mathrm{m2 \cdot K/W}]$	3.5887
Epsilon	0.9
Alpha	0.2

Table 15. Optimal combination of parameters in the combined optimization of the brick wall with chamber and no thermal insulation.

	Optimal Combination of Parameters	
	For maximizing Q_{mi} [W/ m2] during winter	For minimizing Q_{mi} [W/ m2] during summer
Rout $[\mathrm{m2} \cdot \mathrm{K/W}]$	3.3871	0.01
Epsilon	0.4	0.9
Alpha	0.8	0.2

Table 16. Optimal combination of parameters in the individual optimizations of the brick wall with chamber and no thermal insulation.

3.4.3. Brick wall with chamber and thermal insulation

The specific characteristics of the selected brick wall with chamber and thermal insulation are presented in Figure 78.

	e [m]	λ [W/mK]	ρ [kg/m³]	c_p [J/kgK]
Cement mortar	0,02	1,2	2000	850
Brick	0,115	0,6	1900	850
Air chamber	0,05	0,28	1,3	1000
EPS isolation	0,05	0,04	15	1500
Brick	0,07	0,6	1900	850
Plaster	0,015	0,2	850	850

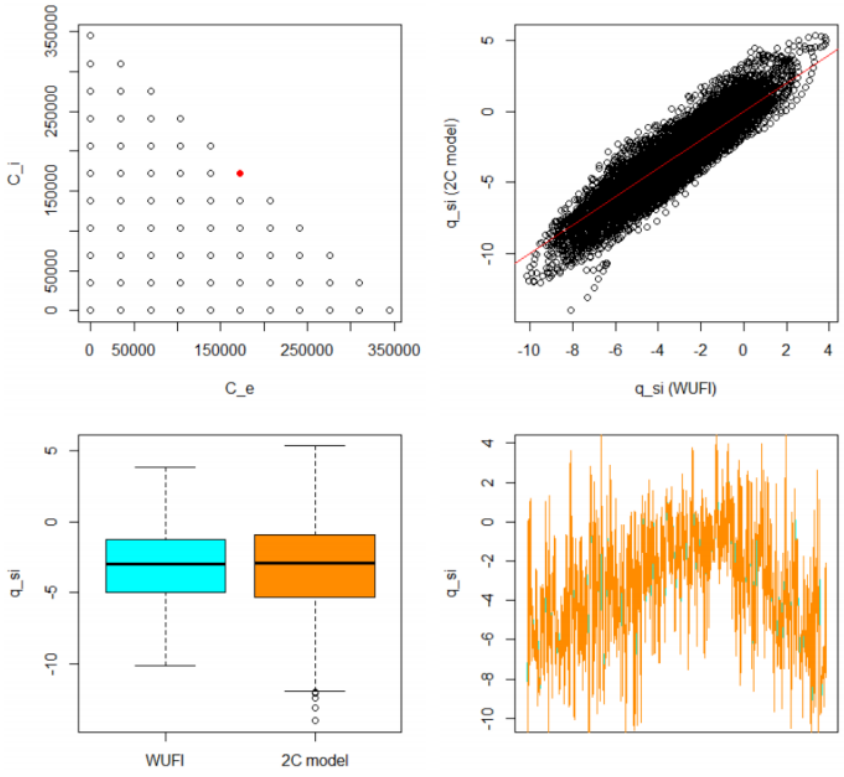

Figure 78. Characteristics of a Brick wall with chamber and thermal insulation.

With the values from Figure 78 and considering $\{\gamma_e = 0.50,\ \gamma_i = 0.50\}$, the following inputs are introduced in the model implemented in Matlab, *Equations (87), (88) and (89)*.

.

$$R_m = 1.829\frac{m^2K}{W} \qquad (87)$$

$$C_{me} = \gamma_e e\rho c_p = 172400\frac{J}{m^2K} \qquad (88)$$

$$C_{mi} = \gamma_i e\rho c_p = 172400\frac{J}{m^2K} \qquad (89)$$

Response optimizations

The same way as it has been done with the other façades, an optimization has been carried out in this new façade to determine which is the combination of the three input parameters of the adaptive layer (Rout, Alpha and Epsilon) that result in the best solution for energy efficiency. Figure 79-82 show different steps followed during the optimization of the parameters.

	C1	C2	C3	C4	C5	C6	C7	C8	C9
	StdOrder	RunOrder	PtType	Blocks	Rout	Epsilon	Alpha	Qmi,winter,...	Qmi,summe...
1	5	1	2	1	0.010	0.65	0.2	-3.97287	-1.32020
2	9	2	2	1	2.505	0.40	0.2	-1.70185	-0.52646
3	11	3	2	1	2.505	0.40	0.8	-0.43326	1.11913
4	1	4	2	1	0.010	0.40	0.5	-2.42906	0.67835
5	3	5	2	1	0.010	0.90	0.5	-2.97045	-0.05855
6	8	6	2	1	5.000	0.65	0.8	-0.42301	0.50862
7	13	7	0	1	2.505	0.65	0.5	-1.20165	0.10662
8	10	8	2	1	2.505	0.90	0.2	-1.80971	-0.67098
9	2	9	2	1	5.000	0.40	0.5	-0.68104	0.19134
10	14	10	0	1	2.505	0.65	0.5	-1.20165	0.10662
11	6	11	2	1	5.000	0.65	0.2	-1.13406	-0.40193
12	12	12	2	1	2.505	0.90	0.8	-0.82833	0.56587
13	4	13	2	1	5.000	0.90	0.5	-0.84205	-0.03557
14	7	14	2	1	0.010	0.65	0.8	-1.51207	1.81193
15	15	15	0	1	2.505	0.65	0.5	-1.20165	0.10662

Figure 79. The 15 experiments proposed by Minitab for the Brick wall with chamber and thermal insulation, in columns C5-C7 the values of the input parameters provided by the design and in columns C8 and C9 the values of the outputs obtained from the model implemented in Matlab.

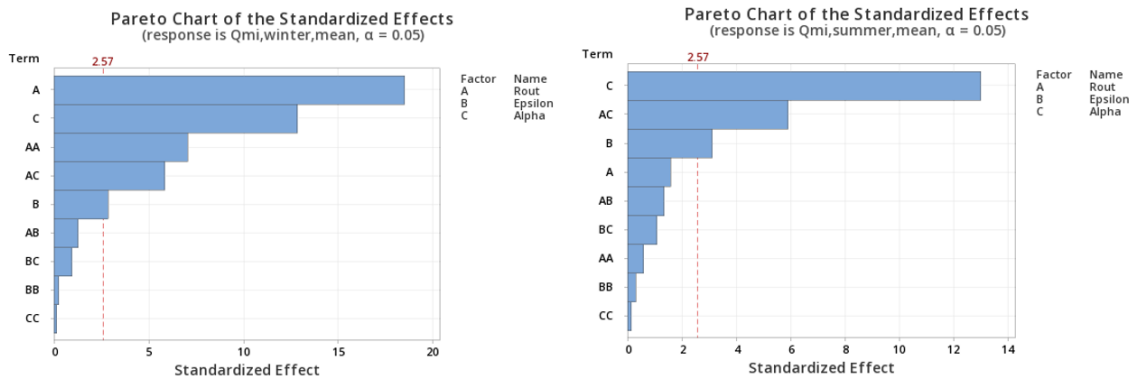

Figure 80. Pareto Chart of the Standardized Effects omitting some terms, for response $Q_{mi,winter,mean}$ (left) and $Q_{mi,summer,mean}$ (right) in the Brick wall with chamber and thermal insulation.

In this case, the Pareto Charts show that Epsilon is statistically significant in both responses. In contrast, Rout seems to be no significant for the summer response. The only terms that will be omitted are CC, BB, BC and AB (as they are not significant for neither answers).

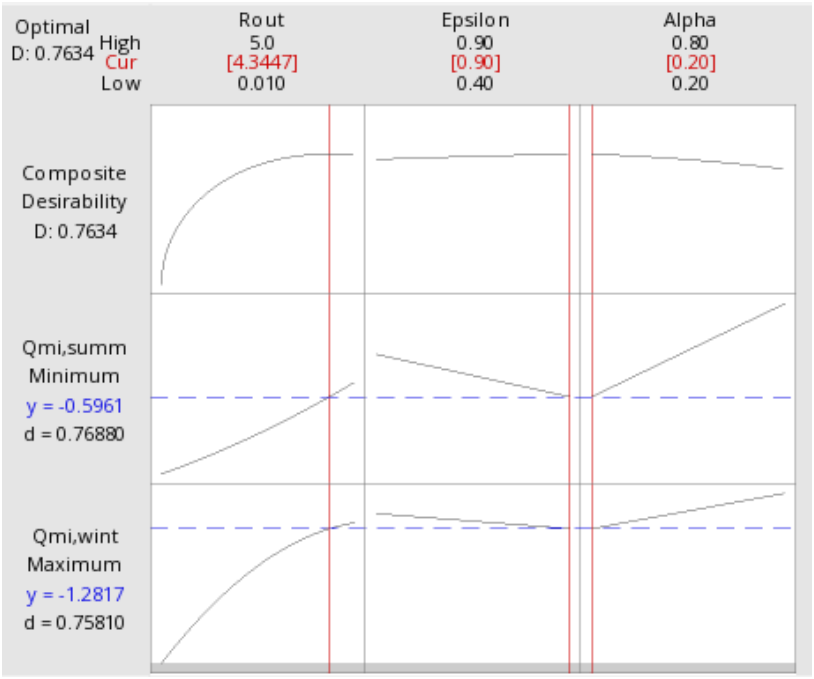

Figure 81. Optimal configuration of parameters for Combined Optimization in the Brick wall with chamber and thermal insulation.

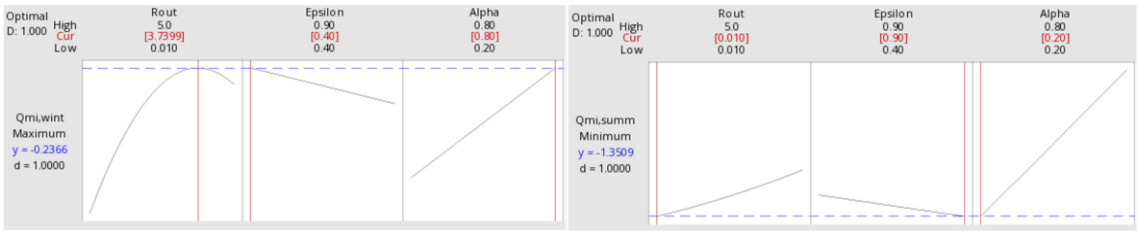

Figure 82. Optimal combination of parameters for maximizing Q_{mi} during winter (left) and minimizing Q_{mi} during summer (right) in the Brick wall with chamber and thermal insulation.

Summarizing the obtained results, for each performed optimization, (*Table 17 and Table 18)*:

Optimal Combination of Parameters	
Rout $[\mathrm{m2 \cdot K/W}]$	4.3447
Epsilon	0.9
Alpha	0.2

Table 17. Optimal combination of parameters in the combined optimization of the brick wall with chamber and thermal insulation.

	Optimal Combination of Parameters	
	For maximizing Q_{mi} [W/ m2] during winter	For minimizing Q_{mi} [W/ m2] during summer
Rout [m2 · K/W]	3.7399	0.01
Epsilon	0.4	0.9
Alpha	0.8	0.2

Table 18. Optimal combination of parameters in the individual optimizations of the brick wall with chamber and thermal insulation.

The results given in the studied three different façades will be analyzed and contrasted in the next section (*4. Conclusions*).

4. CONCLUSIONS

This project investigates the energy performance of an external building envelope in which a building coating is applied. The envelope has been characterized by three parameters: the thermal conductive resistance (Rout), the shortwave solar absorptivity (Alpha) and the longwave emissivity (Epsilon). Two different possibilities or scenarios have been considered when doing the optimizations: a combined optimization that finds out the optimal configuration of the building insulation coating so that heating and cooling systems are minimized all over the year; and a second situation, in which the optimizations have been performed independently for summer and winter months. The aim of the two individual optimizations performed is to find out what the optimal theoretical configurations in each case would be, but physically, it would not make sense to change the insulation coating's properties for different months of the year.

After performing several simulations of the dynamic RC model that represents the system, different optimal combinations of the above mentioned three parameters have been obtained for the three different studied façades. For doing these optimizations, a parametric analysis has been carried out by using the Box-Behnken Design of Experiments (DoE) method. The key parameter used as efficiency indicator has been the internal surface heat flux (Q_{mi}), which has a direct impact on the heating and cooling loads. The solar collection at the external surface of the wall (Q_{col}) is a parameter that has been discarded when analysing the efficiency of the building, as Q_{mi} gives a more accurate response for assuring thermal comfort inside the building. In Figure 83 the predicted internal temperature of the building all over a year is illustrated (in grey), which has been estimated from the external air temperature (explained in *Section 2*). The red lines represent the range of temperatures that guarantee internal thermal comfort during summer months, whereas the blue lines show the range for thermal comfort during winter months [*44*]. The optimization has therefore consisted in finding the optimal configuration of the external insulation coating so that the internal heat flux is maximized during winter months and minimized during summer months. The logic behind this is to keep the interior of the building in the just mentioned thermal comfort ranges minimizing the use of mechanical systems and making the most of the internal surface heat flux.

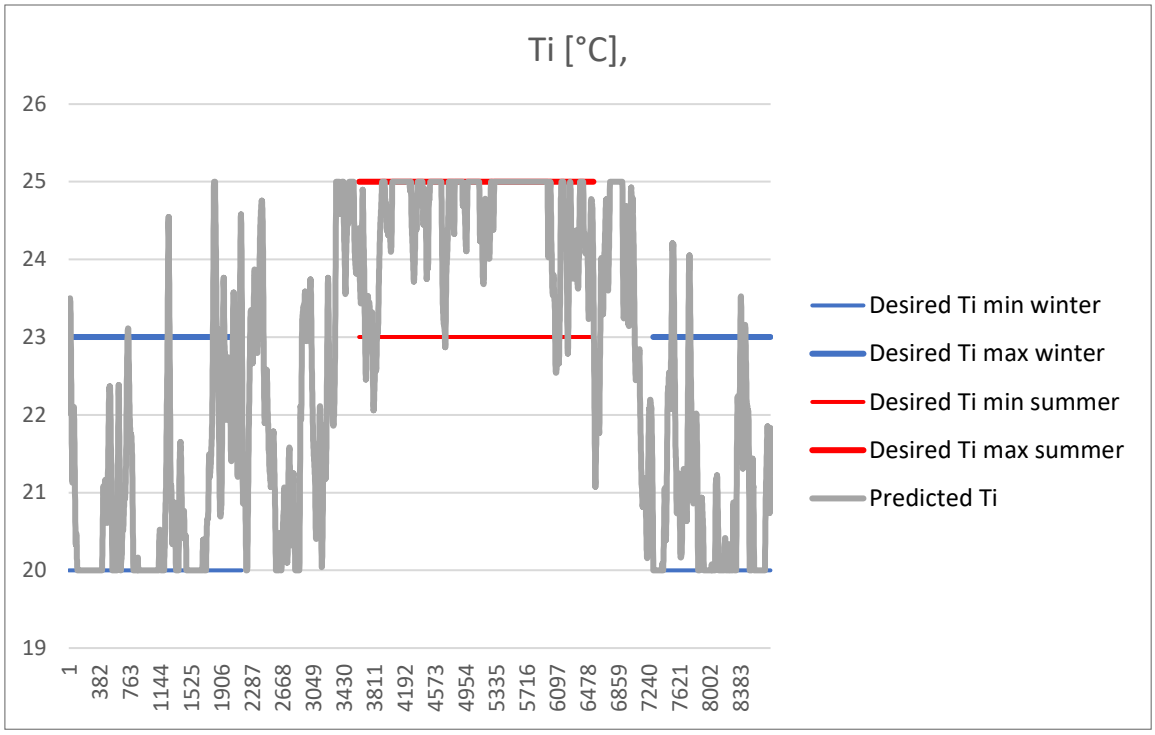

Figure 83. Predicted interior temperature during a year.

The optimal results obtained in the previous section (*Section 3.4)* when analysing the three different façades will be explained below.

As mentioned before, the analysis has been carried out under the weather conditions of Bilbao (north of Spain). The results would vary for other climatological conditions.

When analyzing the results given by the three different studied façades, quite similar optimal solutions have been reached.

When the combined optimization is performed, the three different analyzed façades coincide in the parameters that represent the external insulation coating, that is, in the emissivity and absorptivity values (0.9 and 0.2, respectively). When it comes to Rout, the optimal values for the thermal resistance go from around 3.3 $m^2 \cdot K/W$ (for the concrete wall) to 4.34 $m^2 \cdot K/W$ (for the brick wall with chamber and thermal insulation).

The obtained values in the parameters representing the external coating suggest that a reflective coating is preferable (which can be achieved, for instance, by painting the external layer of a light color). Reflective coatings are most effective in hot climates, when cooling has a big impact in energy consumption. However, they might have the opposite effect in cold climates, making the temperature difference between the exterior surface (which would remain cooler) and the interior surface (where the building is heated using mechanical heating) even bigger.

The most important conclusion taken out from the combined optimization results is how effective an insulation layer can be for energy savings, as it is a parameter that has a big impact in summer and winter responses (highlighting its effect during winter months) for the three analyzed façades. In this project, values between 0.01-5 [$m^2 \cdot K/W$] have been considered as possible thermal resistances for the insulation. It can be seen in Figure

15 that the thermal resistance depends, among others, in the insulation material and thickness selected.

The optimal results for the thermal resistance in the combined optimizations for the three different walls (3.34 m^2·K/W, 3.59 m^2·K/W and 4.34 m^2·K/W) affirm what has been said before; the more insulation does not necessarily mean the better. A thermal resistance of a value of 5 m^2·K/W (which was the highest value allowed in the optimization) has been rejected when finding the equilibrium between minimizing heat gains during summer and maximizing them in winter.

The predicted optimal values of the thermal resistances can be achieved by combining one of the many existing insulation materials from the market with a proper thickness.

If the individual optimizations are analyzed, during summer months, the optimal configuration of parameters (for the three façades) would be a light insulation, or none, if possible (Rout=0.01 m^2·K/W in this project), with a reflective coating (high emissivity and low absorptivity). This makes sense as the parameters have almost the same impact in the Q_{mi} response during summer for the three walls (Figure 84).

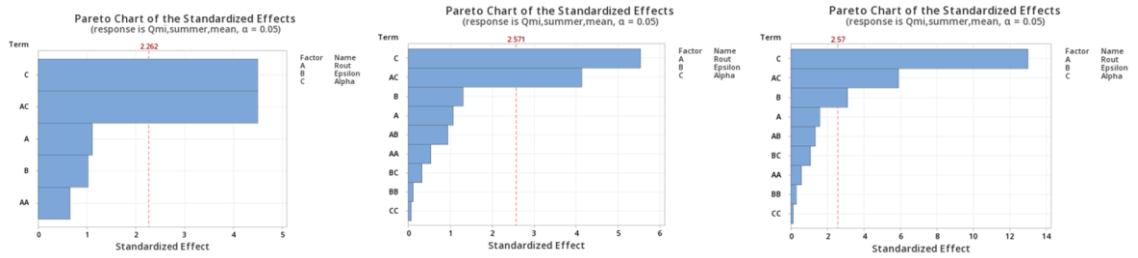

Figure 84. Pareto Chart of the Effects for summer response for concrete wall (left), brick wall with chamber and no thermal insulation (centre) and brick wall with chamber and thermal insulation (right).

Figure 84 shows that during summer, the absorptivity of the coating is the parameter that has the biggest impact on energy reduction (opting for the lowest value possible), followed by Rout (the lowest Rout gets the better). This result seems illogical, as an insulation layer would prevent the heat from entering the building (what is desired during summer). However, if Figure 20 is observed, during summer months (red lines in the figure) even though the value that the response Q_{mi} gets is mostly positive, there are certain moments where it becomes negative (reaching high negative values). One possible explanation to the low Rout given in the summer optimization could be that no insulation is desired so that the heat flux that enters the building (during these time steps when Q_{mi} is negative) can easily escape to the exterior.

However, if winter months are analyzed, the optimal configuration of the external insulation coating differs from one façade to other.

In the concrete façade, the external insulation would have an optimal thermal resistance of 4.6 m^2·K/W for winter months, preventing the heat to escape from the interior. The value of the resistance in the combined optimization of this façade was lower, what makes sense, as a combined goal was being followed. However, if the remaining two façades are observed, the given thermal resistance for winter months is lower than the one given for the combined optimization, meaning less insulation would be desired if just the coldest months were observed. This difference is more critical in the brick wall with thermal insulation, whose thermal resistance decreases from 4.34 m^2·K/W for the combined optimization to 3.74 m^2·K/W for winter optimization. The explanation of it can be found in the Pareto Charts of each response and façade (Figure 85).

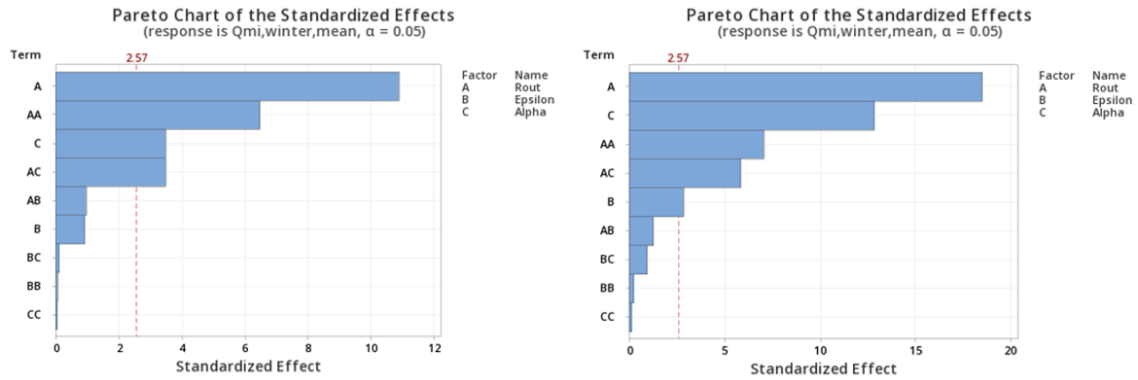

Figure 85. Pareto Chart of the Effects for $Q_{mi,winter,mean}$ response in concrete façades (left) and brick walls with chamber and thermal insulation (right).

If the Pareto Chart of the winter response of the concrete wall (Figure 85 left) is observed, it can be seen how Rout is the variable that has the biggest impact in the response, with much difference respect to the second most significant variable (Alpha). If the brick wall with chamber and thermal insulation is analyzed (Figure 85 right) results show that in this case, Rout and Alpha are closer to each other in what respects to significancy, being both the variables with highest impact in the response.

Therefore, it makes sense that when Q_{mi} is desired to be maximized during winter months, the concrete façade would rather opt for adding more insulation to the exterior (as altering the properties of the external coating hardly make a difference) whereas in the brick wall there is no need of adding that much insulation as the absorptivity attached to the coating does also influence Q_{mi} . An equilibrium of these two parameters has been given by *Minitab* to reach energy efficiency during winter months in the brick wall (instead of simply adding a thick insulation, as in the concrete wall).

The fact that the emissivity is almost insignificant in this project does not mean that coatings are not effective in energy consumption reductions. The thing is that in this project an insulation layer (with a high thermal resistance) has also been applied to the exterior, which is always a much more effective solution that simply applying a building coating to the exterior, even though it has been proved that Alpha (which is also a characteristic of the coating) does have a big impact on Q_{mi}. The insulation requires building renovation and bigger costs than simply altering the superficial part of the external layer. To really appreciate the effects that adding an external coating has, no insulation (or a thinner one with less thermal resistance), should be applied. Nevertheless, even if in small extent, it has been proved that reflective properties contribute positively on energy savings in this concrete climate and location.

5. FUTURE RESEARCH LINES

This project covers in a simplified way a topic that is now in the spotlight: reaching energy efficiency by building renovation. The actual model, which allows to estimate in a theoretical way the optimal configuration of a building insulation coating, could be an incentive and the basis for further research in the future.

The implementation of a model that in addition to being optimized for a single configuration offers the opportunity to adapt dynamically to the surroundings is a future research line in which this work has been inspired (see *8. ANNEX 1*). The wide variety of adaptive building envelopes that nowadays exist has been presented previously in this project (*1.2. State of the art*). In this context, it seems obvious that adaptive skins will become more and more popular, as further knowledge in this field is gained. The reason why they are not widely implemented yet is that they are a complex system with a high cost, so still more advances need to be made so that they become a practical solution in building renovation.

The complexity that this adaptivity involves is the reason why the initial idea of the project was discarded, as the model that was supposed to simulate the performance of adaptive layers was not correctly designed (*8. ANNEX 1*). The accurate implementation of this initial idea is a future research line of the actual project.

6. BUDGET

In this section the total cost of the project is presented. The total budget is divided into three main areas:

- Equipment: the cost due to the use of machines is included in this section. To calculate the expenses the average depreciation cost of the equipment as well as its time of use has been considered (*Table 19)*.
- Software: the cost attached to the software needed in the realization of the project is included in this section. The depreciation cost of the licenses has been considered (*Table 20*).
- Labour cost: human resources involved in the project are included in this section (*Table 21*).

6.1. Equipment Budget

Equipment	Acquisition fee (€)	Depreciation period (years)	Depreciation fee per month (€)	Use time (month)	Depreciation (€)
Laptop	1,200	4	25	4	100
					100

Table 19. Equipment budget.

6.2. Software Budget

Software	Acquisition fee (€)	Depreciation period (years)	Depreciation fee per month (€)	Use time (month)	Depreciation (€)
Matlab	2,000	1	166.67	4	666.67
Minitab	1,996.5	1	166.38	4	665.52
Windows 10	439	1	35.58	4	141.43
Office	126	1	10.5	4	42
					1,515.62

Table 20. Software budget.

6.3. Human resources Budget

Task	Duration (hours)	Cost (€)	
		Unit	Total
Project	300	50	15,000
			15,000

Table 21. Human resources budget.

6.4. Budget Summary

The total Budget of the project is presented below (*Table 22*), which has a total cost of 22,115.39 €.

	Cost (€)	
	Partial	Accumulated
Equipment	100	100
Software	1,515.62	1,615.62
Human Resources	15,000	16,615.62
Indirect costs (10%)		1,661.562
Total (VAT not included)		18,277.182
Total (VAT included)		22,115.39

Table 22. Total budget of the project.

7. REFERENCES

[1] Hanna Modin, Adaptive Building Envelopes. Master of Science Thesis in the Master´s Programme Architecture and Engineering, (2014), doi: 20.500.12380/214574

[2] R.C.G.M. Loonen, M.Trcka, D.Cóstola, J.L.M. Hensen, Climate adaptive building shells: State-of-the-art and future challenges, Renewable and Sustainable Energy Reviews 25 (2013) 483-493, doi: 10.1016/j.rser.2013.04.016

[3] Hadeer Samir MohamedShahin, Adaptive building envelopes of multistory buildings as an example of high performance building skins, Alexandria Engineering Journal 58 (2019) 345-352, doi: 10.1016/j.aej.2018.11.013

[4] Fabrizio Ascione, Nicola Bianco, Rosa Francesca De Masi, Giuseppe Peter Vanoli, Rehabilitation of the building envelope of hospitals: Achievable energy savings and microclimatic control on varying the HVAC systems in Mediterranean climates, Energy and Buildings 60 (2013) 125-138, doi: 10.1016/j.enbuild.2013.01.021

[5] Rita Andrade Santos, Ines Flores-Colen, Nuno Simões, José D. Silvestre, Auto-responsive technologies for thermal renovation of opaque facades, Energy and Buildings 217 (2020) 109968, doi: 10.1016/j.enbuild.2020.109968

[6] IEA (2020), Tracking Buildings 2020, IEA, Paris https://www.iea.org/reports/tracking-buildings-2020

[7] IEA (2020), Key World Energy Statistics 2020, IEA, Paris https://www.iea.org/reports/key-world-energy-statistics-2020

[8] RATURI, Atul K. Renewables 2019 global status report. 2019. https://www.worldgbc.org/sites/default/files/2019%20Global%20Status%20Report%20for%20Buildings%20and%20Construction.pdf

[9] Data from publications and website OECC (Oficina Española de Cambio Climático), HOJA DE RUTA DE LOS SECTORES DIFUSOS A 2.020. https://www.miteco.gob.es/images/es/Hoja%20de%20Ruta%202020_tcm30-178253.pdf (accessed 14/07/2021)

[10] Data from publications and website of the Official website of the European Union, European Commission. Long-term strategy for 2050. https://ec.europa.eu/clima/policies/strategies/2050_es#tab-0-0 (accessed 14/07/2021)

[11] BHANWARE, Prashant Kumar, et al. Development of RETV (Residential Envelope Transmittance Value) Formula for Cooling Dominated Climates of India for the Eco-Niwas Samhita 20181. En 16th International Building Simulation Conference, Rome, Italy. IBPSA. 2019. https://www.beepindia.org/wp-content/uploads/2020/04/MethodologyforRFormulaDevelopmentforENS2018.pdf

[12] Data from publications and website of the World Green Building Council. Green Building Minimum Compliance System in Rwanda (November 2016). https://www.worldgbc.org/member-directory/rwanda-green-building-organization (accessed 14/07/2021)

[13] Data from publications and website of the Global Environment Facility (GEF). Energy Efficiency and Renewable Energy in Social Housing. https://www.thegef.org/project/energy-efficiency-and-renewable-energy-social-housing (accessed 14/07/2021)

[14] Data from publications and website of the Official website of the European Union, European Commission. Energy performance of buildings directive. https://ec.europa.eu/energy/topics/energy-efficiency/energy-efficient-buildings/energy-performance-buildings-directive_en (accessed 14/07/2021)

[15] Data from publications and website of the Build Up (The European Portal for Energy Efficiency in Buildings). Build Upon project (December 2019). https://www.buildup.eu/en/explore/links/build-upon-2-project (accessed 14/07/2021)

[16] Data from publications and website of the iBroad (Individual Building Renovation Roadmaps). Horizon 2020 European programme. https://ibroad-project.eu/ (accessed 14/07/2021)

[17] IEA (2021), Net Zero by 2050, IEA, Paris https://www.iea.org/reports/net-zero-by-2050

[18] Data from publications and website of Meka. New Building renovation plan. https://www.meka3.com/plan-rehabilitacion-de-viviendas/ (accessed 14/07/2021)

[19] IEA (2020), Building Envelopes, IEA, Paris https://www.iea.org/reports/building-envelopes

[20] ZHANG, Yinping, et al. A new approach, based on the inverse problem and variation method, for solving building energy and environment problems: preliminary study and illustrative examples. Building and Environment, 2015, vol. 91, p. 204-218. https://doi.org/10.1016/j.buildenv.2015.02.016

[21] LEE, Kyoung-ho; BRAUN, James E. Model-based demand-limiting control of building thermal mass. Building and Environment, 2008, vol. 43, no 10, p. 1633-1646. https://doi.org/10.1016/j.buildenv.2007.10.009

[22] YANG, Liu; LAM, Joseph C.; LIU, Jiaping. Analysis of typical meteorological years in different climates of China. Energy Conversion and Management, 2007, vol. 48, no 2, p. 654-668. https://doi.org/10.1016/j.enconman.2006.05.016

[23] ASAN, H.; SANCAKTAR, Y. S. Effects of wall's thermophysical properties on time lag and decrement factor. energy and buildings, 1998, vol. 28, no 2, p. 159-166. https://doi.org/10.1016/S0378-7788(98)00007-3

[24] PÉREZ-LOMBARD, Luis; ORTIZ, José; POUT, Christine. A review on buildings energy consumption information. Energy and buildings, 2008, vol. 40, no 3, p. 394-398. https://doi.org/10.1016/j.enbuild.2007.03.007

[25] FIGASZEWSKI, Jarosław; SOKOLOWSKA-MOSKWIAK, Joanna. The concept of multifuncional wall—an energy system integrated in a single wall. Architecture Civil Engineering Environment, 2017, vol. 10, no 1, p. 5-10. https://www.exeley.com/exeley/journals/architecture_civil_engineering_environment/10/1/pdf/10.21307_acee-2017-001.pdf

[26] MARTIN-MALIKIAN, Elizabeth. High Octane: Eco-Adaptive Architecture. En 2012 ACSA Fall Conference. 2012. p. 163-167. https://www.acsa-arch.org/proceedings/Fall%20Conference%20Proceedings/ACSA.FALL.12/ACSA.FALL.12.25.pdf

[27] A Fuller Explanation: The Synergetic Geometry of R. Buckminster Fuller

[28] AHMED, Mostafa MS, et al. The thermal performance of residential building integrated with adaptive kinetic shading system. International Energy Journal, 2016, vol. 16, no 3. http://rericjournal.ait.ac.th/index.php/reric/article/download/1452/477

[29] BUMBARU, Dinu. Habitat 67 and Expo-Conserving the Young Monument and its Intentional Universality or the Mode de Vie?. ICOMOS–Hefte des Deutschen Nationalkomitees, 2017, vol. 63, p. 62-69. https://journals.ub.uni-heidelberg.de/index.php/icomoshefte/article/download/40703/34361

[30] SUNG, Doris. A new look at building facades as infrastructure. Engineering, 2016, vol. 2, no 1, p. 63-68. https://doi.org/10.1016/J.ENG.2016.01.008

[31] ALOTAIBI, Fahad. The role of kinetic envelopes to improve energy performance in buildings. J Archit Eng Tech, 2015, vol. 4, no 149, p. 2. http://dx.doi.org/10.4172/2168-9717.1000149

[32] ENRIC RUIZ GELI and HIS TEAM AT CLOUD 9. MEDIA-ICT. Fabricate 2011. https://www.jstor.org/stable/pdf/j.ctt1tp3c6d.33.pdf

[33] PREMIER, Alessandro. dynamic façades and smart technologies for building envelope requalification. Research Gate. https://www.academia.edu/download/39923654/premier_mediaenv_low.pdf DYNAMIC_FACADES_AND_SMART_TECHNOLOGIES_FOR_BUILDING_ENVELOPE_REQUALIFICATION, 2012.

[34] Data from publications and website of the Netherlands Enterprise Agency. Smart, energy-generating windows. https://english.rvo.nl/news/business-cases/physee-develops-smart-energy-generating-windows (accessed 14/07/2021)

[35] SHEN, Hui; TAN, Hongwei; TZEMPELIKOS, Athanasios. The effect of reflective coatings on building surface temperatures, indoor environment and energy consumption—An experimental study. Energy and Buildings, 2011, vol. 43, no 2-3, p. 573-580. https://doi.org/10.1016/j.enbuild.2010.10.024

[36] GUO, W., et al. Study on energy saving effect of heat-reflective insulation coating on envelopes in the hot summer and cold winter zone. Energy and Buildings, 2012, vol. 50, p. 196-203. https://doi.org/10.1016/j.enbuild.2012.03.035

[37] AL-HOMOUD, Mohammad S. Performance characteristics and practical applications of common building thermal insulation materials. Building and environment, 2005, vol. 40, no 3, p. 353-366. https://doi.org/10.1016/j.buildenv.2004.05.013

[38] José Mª de Juana et al., Energías Renovables para el Desarrollo, Paraninfo, Madrid, 2002. https://www.todostuslibros.com/libros/energias-renovables-para-el-desarrollo_978-84-283-2864-7

[39] Data from publications and website of the European Commission. Development of insulating concrete systems based on novel low CO2 binders for a new family of eco-innovative, durable and standardized energy efficient envelope components. Development of insulating concrete systems based on novel low CO2 binders for a new family of eco-innovative, durable and standardized energy efficient envelope components | ECO-Binder Project | H2020 | CORDIS | European Commission (europa.eu) (accessed 14/07/2021)

[40] REMUND, J., et al. The use of Meteonorm weather generator for climate change studies. En 10th EMS Annual Meeting. 2010. p. EMS2010-417. https://ui.adsabs.harvard.edu/abs/2010ems..confE.417R/abstract

[41] ZIRKELBACH, D., et al. Wufi® Pro–Manual. Fraunhofer Institute, 2007. https://wufi.de/download/WUFI-Pro-5_Manual.pdf

[42] Frank P.Incropera, David P.DEWITT, Fundamentos de Transferencia de Calor. https://www.u-cursos.cl/usuario/cfd91cf1d8924f74aa09d82a334726d1/mi_blog/r/INCROPERA_-_Transferencia_de_calor.pdf

[43] British Standards Document, BS EN 15026, Hygrothermal performance of building components and building elements. Assessment of moisture transfer by numerical simulation. https://doi.org/10.3403/30124008U

[44] RINCÓN MARAVILLA, Carlos del, et al. Caracterización térmica de muros y simulación energética de un edificio histórico. 2012. Tesis Doctoral. Universitat Politècnica de València. https://riunet.upv.es/bitstream/handle/10251/17724/Caracterizacion%20t%E9rmica%20de%20muros%20y%20simulaci%F3n%20energ%E9tica%20de%20un%20edificio%20hist%F3rico.pdf?sequence=1

[45] Data from publications and website of the Official website of the European Environment Agency. Heating and cooling degree days. https://www.eea.europa.eu/data-and-maps/indicators/heating-degree-days-2 (accessed 14/07/2021)

[46] MONTGOMERY, Douglas C. Design and analysis of experiments. John Wiley & sons, 2017. http://citeseerx.ist.psu.edu/viewdoc/download?doi=10.1.1.459.8273&rep=rep1&type=pdf

[47] MATHEWS, Paul G. Design of Experiments with MINITAB. Milwaukee, WI, USA: ASQ Quality Press, 2005. https://www.academia.edu/download/44283092/Mathews__Paul_G.-Design_of_Experiments_with_MINITAB-American_Society_for_Quality_ASQ_2005.pdf

[48] FERREIRA, SL Costa, et al. Box-Behnken design: an alternative for the optimization of analytical methods. Analytica chimica acta, 2007, vol. 597, no 2, p. 179-186. https://doi.org/10.1016/j.aca.2007.07.011

8. ANNEX 1

The initial idea of this project consisted of assessing the energetic performance of an adaptive building envelope (with macro-level adaptivity) for façade renovation. The initial RC model studied was the one presented in Figure 86:

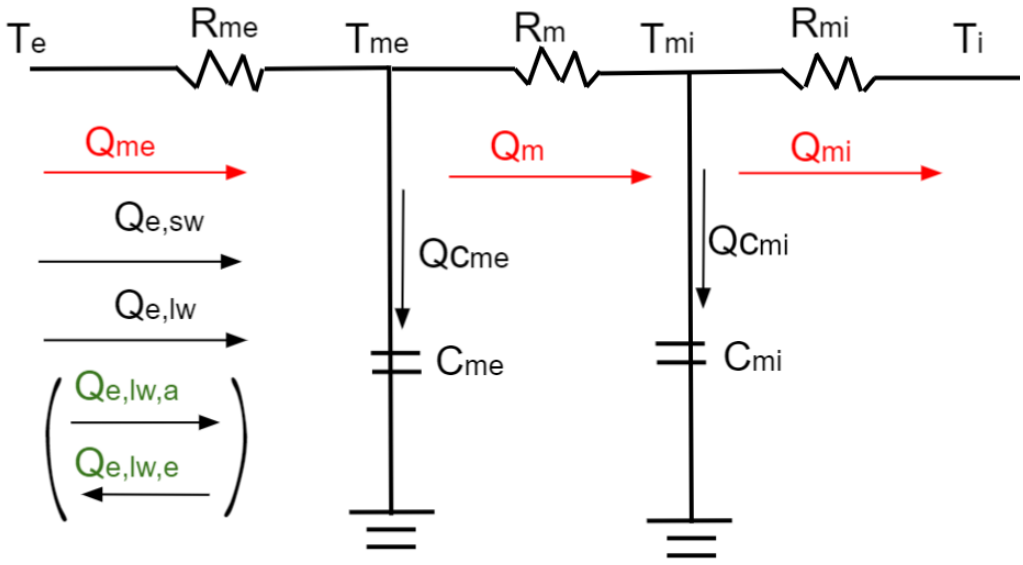

Figure 86. RC model of the initial idea of the project.

R_{me} was obtained as $R_{me} = R_{se} + R_{out}$, where R_{se} was a function of the wind velocity and direction (as it is in the final project), and R_{out} was the thermal resistance of outer insulation layers (the adaptive envelope). The objective of this model was to determine the best combination of the parameters that represented the external adaptive envelope that resulted in a energy consumption reduction of the building. In other words, find the optimal configuration of the external adaptive layer so that the internal heat flux was maximized during winter months and minimized during summer months.

When doing the Design of Experiments, R_{out}, the thermal resistance of outer insulation layer, could take a value in the range of 0 m^2·K/W and 1 m^2·K/W, pretending that a value of 0 m^2·K/W meant the position of the layers were such that no effect of layers could be considered and 1 m^2·K/W if they were completely covering the building. The intermediate values would represent the other configurations, or inclination angles, of the layers covering the building.

The problem with this model was that R_{out} was included in R_{me}, and looking at Figure 86 it can be seen that the radiation coming from the sun would directly hit the external face of the wall (as if no envelopes were being considered). This model would just work if no external envelopes were applied (R_{out} =0 m^2·K/W). If R_{out} got higher values Figure 86 would not change and the heat fluxes would still impact on the same wall (not on the external surface of the adaptive layers, as it was pretended). The emissivity and absorptivity would also be properties of the exterior of the wall and not of the adaptive envelope, which does not make sense.

Therefore, the model was modified, and the adaptive layers were replaced by an insulation layer whose thickness and material (thermal resistance) as well as the exterior coating properties (emissivity and absorptivity) are optimized.

9. ANNEX 2

The code implemented in *Matlab* is attached in this section. The equations have been already explained in *Section 2*, when describing the model.

```
%Collect values from the climatic file Bilbao
fid=fopen('datos1año.txt','r');
datos=fscanf(fid,'%f %f %f %f %f %f %f %f %f\n');
%for each time step, 9 inputs are collected
fclose(fid);

%-------------INPUTS--------------------
Rout=4.4960; %Thermal resistance of outer insulation layer
(0.01-5)
epsilon_lwe=0.4013; %long-wave emissivity of external surface
(0.4-0.9)
alpha_sw=0.6468; %short-wave absorptivity of external surface
(0.2-0.8)

%-------------CALENDAR-------------
%WINTER (from november to april)
january_days=31;
february_days=28;
march_days=31;
april_days=30;
november_days=30;
december_days=31;
winter_hours1=(january_days+february_days+march_days+april_days)
*24;
winter_hours2=(november_days+december_days)*24;

%SUMMER (from may to october)
%-----------------------------------------
s=90;
s= (s*pi)/180;%radayns
f_dif=(1+cos(s))/2; %vision factor for the diffuse component of
radaytion
f_ground=(1-cos(s))/2;
%-----------------------------------------------
orientation=180;
azimuth=(orientation-180)*pi/180;
n_dat=length(datos);
num_datos=9; %for each time step, 9 inputs
num_tsteps=n_dat/num_datos;
tstep=3600; %[s]
rho.ground=0.2; %SW reflectivity of ground (0.2 assumed as
default value)
epsilon.ground=0.9; %LW emissivity of ground (0.9 assumed as
default value)
f.ground=0.5;
glw.ground=0.5;%view factor from wall to ground
f.sky=0.5;
glw.sky=0.5; %view factor from wall to sky
timezone=1; %for Bilbo
latitude=43.3;
latitude= (latitude*pi)/180;% to radayns
```

```
HDD = 15; % #Reference external temperature for heating demand
CDD = 20; % #Reference external temperature for cooling demand

f_sw=1;%(Short Wave)
Stefan.Boltz=5.67*10^[-8]; %[W/m2K4]

%CHARACTERICTIS OF DIFFERENT FACADES:
%-------------------------------------------------------------
-------------
% %Concrete facade:
Cme=156400; %thermal capacitance lumped to external surface of
wall [J/m2K]
Cmi=234600; %thermal capacitance lumped to internal surface of
wall [J/m2K]
Rm=0.2/1.6; %0.1 thermal resistance of wall (excl. surfaces)
[m2K/W]
% %-------------------------------------------------------------
---------------
% % %Brick wall with chamber and NO thermal insulation:
% Cme=137500;
% Cmi=206200;
% Rm=0.569;
%-------------------------------------------------------------
-------------
% %Brick wall with chamber and thermal insulation:
% Cme=172400;
% Cmi=172400;
% Rm=1.829;
%-------------------------------------------------------------
-------------
%Rmi: internal surface resistance of wall (convection and
radaytion) [m2K/W]
Rmi = 0.125; %value from WUFI Pro (convection and radaytion)
Cmout=0;%insignificant compared to Cme and Cmi

%The data has been collected in a vector. To move it to a
matrix:
A=zeros(num_tsteps,num_datos);
k=1;
a=1;
while k<=n_dat
    for j=1:num_datos
    A(a,j)=datos(k);
    k=k+1;
    end
    a=a+1;
end
%--------NOT CTE VARIABLES--------------
v_wind=zeros(num_tsteps,1);
f_wind=zeros(num_tsteps,1);
Te=zeros(num_tsteps,1);
Rse=zeros(num_tsteps,1);
Rme=zeros(num_tsteps,1);
ILAH=zeros(num_tsteps,1);
ISGH=zeros(num_tsteps,1);
ISD=zeros(num_tsteps,1); %Idif
```

```
Ibeam=zeros(num_tsteps,1); %ISDH=ISGH-ISD
Idif=zeros(num_tsteps,1);
Iref=zeros(num_tsteps,1);
Idir=zeros(num_tsteps,1);
Isw=zeros(num_tsteps,1);
Ilwa_sky=zeros(num_tsteps,1);
Ilwa_ground=zeros(num_tsteps,1);
Ilwa_ref=zeros(num_tsteps,1);
Ilwa=zeros(num_tsteps,1);
f_lwe=zeros(num_tsteps,1); %LW emission factor f_lwe
f_lwe_sky=zeros(num_tsteps,1);
f_lwe_ground=zeros(num_tsteps,1);
f_lwe_sky_ground=zeros(num_tsteps,1);
epsilon_sky=zeros(num_tsteps,1);
Rb=zeros(num_tsteps,1);
delta=zeros(num_tsteps,1);
omega=zeros(num_tsteps,1);
omega_grad=zeros(num_tsteps,1);
cos_inc=zeros(num_tsteps,1);
sen_alfa=zeros(num_tsteps,1);
alfa=zeros(num_tsteps,1);
Qe_sw=zeros(num_tsteps,1);
Qe_lw=zeros(num_tsteps,1);
Qe_lwa=zeros(num_tsteps,1);
k=1;
n=1; % day
hour=1;
for i=1:num_tsteps
    v_wind(i)=A(i,8); %WS
    num=(A(i,7)-orientation+450)/360;
    decim=num-fix(num);
    if (decim<0.5)
        f_wind(i)=1.6;
    else
        f_wind(i)=0.33;
    end
    Rse(i)=(1/(4.5+f_wind(i)*v_wind(i)));
    Rme(i)=Rse(i);
    ILAH(i)=A(i,5);
    ISGH(i)=A(i,3);
    ISD(i)=A(i,4);
    Te(i)=A(i,1)+273.15; %TA in Kelvin
    Ibeam(i)=ISGH(i)-ISD(i);
    Idif(i)=ISD(i)*f_dif;
    Iref(i)=ISGH(i)*rho.ground*f_ground;

    Ilwa_sky(i)=ILAH(i)*f.sky;

Ilwa_ground(i)=epsilon.ground*Stefan.Boltz*((Te(i))^4)*f.ground;
    Ilwa_ref(i)=(1-epsilon.ground)*ILAH(i)*f.ground;
    Ilwa(i)=Ilwa_sky(i)+Ilwa_ground(i)+Ilwa_ref(i);

    epsilon_sky(i)=ILAH(i)/(Stefan.Boltz*((Te(i))^4));
    f_lwe_sky(i)=epsilon_sky(i)*glw.sky;
    f_lwe_ground(i)=epsilon.ground*glw.ground;
```

```
    f_lwe_sky_ground(i)=epsilon_sky(i)*(1-
epsilon.ground)*glw.ground;
    f_lwe(i)=f_lwe_sky(i)+f_lwe_ground(i)+f_lwe_sky_ground(i);

    delta(i)=23.45*(sin((360/365)*(284+n)*(pi/180))); %delta:
angle of the solar declination

    if k<24 %to know which day is it
        k=k+1;
    else %when k=24
        n=n+1;
        k=1;
    end
    delta(i)= (delta(i)*pi)/180;%to radayns
    omega_grad(i)=((hour-2*timezone)-12)*15; %solar hour angle
    if hour<24
        hour=hour+1;
    elseif hour==24
        hour=1;
    end

    omega(i)= (omega_grad(i)*pi)/180;%to radayns

sen_alfa(i)=sin(delta(i))*sin(latitude)+cos(delta(i))*cos(latitu
de)*cos(omega(i));
    alfa(i)=asin(sen_alfa(i));%in radayns

cos_inc(i)=sin(s)*sin(azimuth)*cos(delta(i))*sin(omega(i))+sin(d
elta(i))*(cos(s)*sin(latitude)-
sin(s)*cos(azimuth)*cos(latitude))+cos(delta(i))*cos(omega(i))*(
(cos(s)*cos(latitude))+(sin(s)*cos(azimuth)*sin(latitude)));

    Rb(i)=cos_inc(i)/sen_alfa(i);
    if sen_alfa(i)<0.1 %assumption
        Rb(i)=0;
    end
    if Rb(i)<0
        Rb(i)=0;
    end

    Idir(i)=Ibeam(i)*Rb(i);
    Isw(i)=Idir(i)+Idif(i)+Iref(i);

    Qe_sw(i)=Isw(i)*f_sw*alpha_sw;%short wave solar irradaytion
    Qe_lwa(i)=Ilwa(i)*epsilon_lwe; %absorbed radaytion

end
Te_long=zeros(num_tsteps+24,1);%to calculate the moving average
Te_long2=zeros(num_tsteps+24,1);%to calculate the predicted Te
for i=1:12
    Te_long(i)=Te(num_tsteps-i+1);
    Te_long(num_tsteps+12+i)=Te(i);
end
for j=1:num_tsteps
   Te_long(12+j)=Te(j);
   Te_long2(j)=Te(j);
```

```
end
for h=1:24
    Te_long2(num_tsteps+h)=Te(h);
end

%We calculate the 24-hour centered moving average over Te:
(Te_meday_mov)
%We calculate the prediction of Te mean to find out Cdem
(heating demand)
Te_meday_mov=zeros(num_tsteps,1);
Tint=zeros(num_tsteps,1);
Te_pred=zeros(num_tsteps,1);%predicted Te mean
for i=1:num_tsteps
    Te_pred(i)=0;
    Te_meday_mov(i)=Te_long((i+12)-12)+Te_long((i+12)+12);
    for j=1:11

Te_meday_mov(i)=Te_meday_mov(i)+2*Te_long((i+12)+j)++2*Te_long((
i+12)-j);
    end
    Te_meday_mov(i)=(Te_meday_mov(i)+2*Te_long(i+12))/48;
        if ((Te_meday_mov(i)-273.15)*0.5+15)<20 %the maximum is
taken
            temp=20;
        else
            temp=(Te_meday_mov(i)-273.15)*0.5+15;
        end
        if temp>25
            temp=25;
        end
        Tint(i)=temp+273.15; %kelvin
    for k=1:24
        Te_pred(i)=Te_long2(i+k)+Te_pred(i);
    end
    Te_pred(i)=Te_pred(i)/24;
end

% Cdem (heating demand)from the predicted Te mean for the next
24h (Te_pred)
Cdem=zeros(num_tsteps,1);%una por cada hour
for i=1:num_tsteps
    if Te_pred(i)<(HDD+273.15)
        Cdem(i)=1; %heating demand foreseen
    elseif Te_pred(i)>(CDD+273.15)
        Cdem(i)=-1; %cooling demand foreseen
    else
        Cdem(i)=0; %no demand foreseen
    end
end
%initilize the previous temperatures for 20°
Tme=zeros(num_tsteps,1);
Tme_prev=zeros(num_tsteps,1);
Tme_prev(1)=20+273.15;
Tmi=zeros(num_tsteps,1);
Tmi_prev=zeros(num_tsteps,1);
Tmi_prev(1)=20+273.15;
```

```
Tenv=zeros(num_tsteps,1);
Tenv_prev=zeros(num_tsteps,1);
Tenv_prev(1)=20+273.15;

A1=zeros(num_tsteps,1);
B1=zeros(num_tsteps,1);
C1=zeros(num_tsteps,1);
D1=zeros(num_tsteps,1);
A2=zeros(num_tsteps,1);
B2=zeros(num_tsteps,1);
C2=zeros(num_tsteps,1);
D2=zeros(num_tsteps,1);
A3=zeros(num_tsteps,1);
B3=zeros(num_tsteps,1);
C3=zeros(num_tsteps,1);
D3=zeros(num_tsteps,1);

Q_mi=zeros(num_tsteps,1);
Q_me=zeros(num_tsteps,1);
Q_m=zeros(num_tsteps,1);
Q_ext=zeros(num_tsteps,1);
Qe_lwe=zeros(num_tsteps,1);
Qe_lwe2=zeros(num_tsteps,1);
Q_Cme=zeros(num_tsteps,1);
Q_Cmi=zeros(num_tsteps,1);
Q_Cmout=zeros(num_tsteps,1);
Balance1=zeros(num_tsteps,1);
Balance2=zeros(num_tsteps,1);
Qcol=zeros(num_tsteps,1);
opt=zeros(num_tsteps/24,1);%one for each day
day=1;
hour=1;
%solve the system:
for i=1:num_tsteps

A1(i)=(Cmout/tstep)+(1/Rse(i))+(1/Rout)+(f_lwe(i)*4*epsilon_lwe*
Stefan.Boltz*(Tenv_prev(i))^3);
    B1(i)=-1/Rout;
    C1(i)=0;

D1(i)=(Cmout*Tenv_prev(i)/tstep)+(Te(i)/Rse(i))+Qe_sw(i)+Qe_lwa(
i)-
(f_lwe(i)*epsilon_lwe*Stefan.Boltz*((Tenv_prev(i))^4))+f_lwe(i)*
epsilon_lwe*Stefan.Boltz*4*((Tenv_prev(i))^4);
    A2(i)=1/Rout;
    B2(i)=-((Cme/tstep)+(1/Rout)+(1/Rm));
    C2(i)=1/Rm;
    D2(i)=-(Cme*Tme_prev(i)/tstep);
    A3(i)=0;
    B3(i)=1/Rm;
    C3(i)=-((1/Rm)+(Cmi/tstep)+(1/Rmi));
    D3(i)=-((Cmi*Tmi_prev(i)/tstep)+(Tint(i)/Rmi));
    %Solve the matritial system for each time step
    Mat=[A1(i) B1(i) C1(i);A2(i) B2(i) C2(i);A3(i) B3(i) C3(i)];
    b=[D1(i); D2(i); D3(i)];
    solucion=linsolve(Mat,b);
```

```
    Tenv(i)=solucion(1);
    Tme(i)=solucion(2);
    Tmi(i)=solucion(3);
    Q_mi(i)=((Tmi(i)-Tint(i))/Rmi);
    Q_me(i)=((Tenv(i)-Tme(i))/Rout);
    Q_m(i)=((Tme(i)-Tmi(i))/Rm);
    Q_ext(i)=((Te(i)-Tenv(i))/Rse(i)); %Rse=Rme de antes

Qe_lwe(i)=f_lwe(i)*epsilon_lwe*Stefan.Boltz*((Tenv_prev(i))^4)+f
_lwe(i)*epsilon_lwe*Stefan.Boltz*4*((Tenv_prev(i))^3)*(Tenv(i)-
Tenv_prev(i));
    Qe_lwe2(i)=f_lwe(i)*epsilon_lwe*Stefan.Boltz*((Tenv(i))^4);
    Qe_lw(i)=Qe_lwa(i)-Qe_lwe(i);
    Q_Cme(i)=(Cme*(Tme(i)-Tme_prev(i)))/tstep;
    Q_Cmi(i)=(Cmi*(Tmi(i)-Tmi_prev(i)))/tstep;
    Q_Cmout(i)=(Cmout*(Tenv(i)-Tenv_prev(i)))/tstep;

    % Energetic balance
    Balance1(i)=Q_ext(i)+Qe_lw(i)+Qe_sw(i)-Q_me(i)-Q_Cmout(i);
    Balance2(i)=Q_me(i)-Q_Cme(i)-Q_m(i);
    Balance3(i)=Q_m(i)-Q_Cmi(i)-Q_mi(i);

    Qcol(i) = Q_Cme(i) + Q_m(i);%solar collection at external
surface (key parameter)

    Tme_prev(i+1)=Tme(i);
    Tmi_prev(i+1)=Tmi(i);
    Tenv_prev(i+1)=Tenv(i);
end

%divide Qcol in heating, cooling y and no-demand
heat=1;
cool=1;
nodemand=1;
for i=1:num_tsteps
    if Cdem(i)==1 %heating demand foreseen
        Qcol_heating(heat)=Qcol(i); %collects Qcol during
heating
        heat=heat+1;
    elseif Cdem(i)==-1 %cooling demand
        Qcol_cooling(cool)=Qcol(i);%collects Qcol during cooling
        cool=cool+1;
    else
        Qcol_nodemand(nodemand)=Qcol(i); %no demand foreseen
        nodemand=nodemand+1;
    end

end
max_Qcol_heat=max(Qcol_heating);
Qcol_heat_meday=mean(Qcol_heating);
min_Qcol_cool=min(Qcol_cooling);
Qcol_cool_meday=mean(Qcol_cooling);
Qcol_heating=Qcol_heating';
Qcol_cooling=Qcol_cooling';

%in degrees:
```

```
Te_degrees=zeros(num_tsteps,1);
Ti_degrees=zeros(num_tsteps,1);
for i=1:num_tsteps
    Te_degrees(i)=Te(i)-273.15;
    Ti_degrees(i)=Tint(i)-273.15;
end

%Divide Qmi in summer and winter:
winter=1;
summer=1;
for i=1:num_tsteps
    %WINTER
    if i<=winter_hours1 || i>(num_tsteps-winter_hours2) %winter
       Te_winter(winter)= Te_degrees(i);
       Q_mi_winter(winter)=Q_mi(i);
       winter=winter+1;
    %SUMMER
    else
       Te_summer(summer)= Te_degrees(i);
       Q_mi_summer(summer)=Q_mi(i);
       summer=summer+1;
    end
end

Q_mi_winter_mean=mean(Q_mi_winter);
Q_mi_summer_mean=mean(Q_mi_summer);

for i=1:(winter-1)
    Q_mi_winter_mean_vector(i)=Q_mi_winter_mean;
end
for j=1:(summer-1)
    Q_mi_summer_mean_vector(j)=Q_mi_summer_mean;
end
Q_mi_winter=Q_mi_winter';
Q_mi_summer=Q_mi_summer';

%export data to EXCEL:
Vector_datos=[Q_mi_winter_mean;Q_mi_summer_mean;Qcol_cool_meday;
Qcol_heat_meday];
filename='datos(Qmi_winter_summer_Qcol_cool_heat.xlsx';
xlswrite(filename,Vector_datos);
```